

## ABSTRACT

ABDULLAH, SAIF-AL-DIN MOHD. Numerical Study of a Reactivity Controlled Compression Ignition (RCCI) Engine using iso-octane and n-heptane. (Under the direction of Dr. Tarek Echehki).

In the modern world, the higher fuel costs and strict environmental restrictions demand cleaner and more efficient internal combustion engines. The need for higher efficiency has put compression ignition engines ahead of spark ignition engines. But, the higher NO<sub>x</sub> and soot emission from CI engines requires us to look at certain in cylinder solutions that might mitigate the problem. Reactivity Controlled Compression Ignition (RCCI) is a variant of Homogeneous Charge compression ignition (HCCI) that provides more control over the combustion process which promises to achieve higher fuel efficiency and lower emissions. RCCI involves the introduction of a low reactivity fuel in the cylinder to form a well formed mixture of fuel and air and a high reactivity fuel is injected during the compression stroke to form a stratified charge. In this numerical study, an ODT model is used to investigate the RCCI process using iso-octane and n-heptane as port fuel and directly injected fuel respectively. For this numerical study, a 171-species PRF skeletal mechanism with 861 elementary reactions has been employed.

In the first part of the study, a single injection strategy is used to study RCCI combustion process. The later injection timings showed more uniform heat release than the earlier injection timings. The injection timing change showed great potential in controlling combustion phasing at both equivalence ratios  $\phi=0.3$  and  $\phi=0.5$ , however, ignition was delayed at the higher equivalence ratios. The effect of premixed ratio (PR) showed that at higher ratios, the ignition delay is significantly increased due to the higher proportion of the low reactivity fuel, iso-octane.

In the second part of the study, the direct injection of n-heptane is split into two injections at different timings into the compression stroke as termed here onwards as double injection

strategy. The effects of first and second injection timings and the n-heptane mass split between the two injections is studied. The earlier timings for both first and second injection showed more uniform heat release and pressure rise, however showed no control over ignition and combustion phasing for a mass split of 50/50 between injections. As 75% of the n-heptane mass is injected during the first injection, a higher cylinder pressure is observed compared to the other cases. Also for 75/25 mass split, the ignition timings could be controlled by both first and second injection timings respectively.

© Copyright 2018 by Saif-al-din Mohd Abdullah

All Rights Reserved

Numerical Study of a Reactivity Controlled Compression Ignition (RCCI) Engine using iso-octane and n-heptane.

by  
Saif-al-din Mohd Abdullah

A thesis submitted to the Graduate Faculty of  
North Carolina State University  
in partial fulfillment of the  
requirements for the degree of  
Master of Science

Mechanical Engineering

Raleigh, North Carolina

2018

APPROVED BY:

---

Dr. Tiegang Fang

---

Dr. Alexei Saveliev

---

Dr. Tarek Echehki  
Chair of Advisory Committee

## **DEDICATION**

To

Mom, *Regina Khatun* and Dad, *Baqi Khalily*

## **BIOGRAPHY**

Saif-al-din Mohd Abdullah was born on 7 September, 1990 in Ohio, USA. Soon after that, he moved with his family to Dhaka, Bangladesh. He completed his O level and A level certificate examination from Sunnydale School, Dhaka in 2007 and 2009 respectively. He then went to Bangladesh University of Engineering and Technology (BUET) for his undergraduate studies and earned his Bachelor of Science degree in Mechanical Engineering in November, 2015.

Saif developed an interest in combustion and engines rooting from his childhood passion for automobiles. His undergraduate project and research work regarding an experimental study of a diesel engine concreted his interests in engine research.

In Fall 2016, Saif enrolled as a graduate student for Master of Science in Mechanical Engineering in North Carolina State University, Raleigh, NC. His interests in modelling combustion in engines led him to seek Dr. Tarek Echehki as his mentor, under whose supervision, he has been working from Spring 2017.

## **ACKNOWLEDGMENTS**

I would like to thank my advisor and mentor, Dr. Tarek Echehki, his help and guidance have led to the successful completion of this thesis. I am grateful to Dr. Tiegang Fang and Dr. Alexei Saveliev for serving as members on my advisory committee and providing their valuable insights and suggestions.

I thank my best friends Ayaan, Saurabh, Ayaz, Richi, Pinaki, Shayan and Krystal for everything. Also, all other friends and family for all the love and support without which completing this thesis would have been difficult.

## TABLE OF CONTENTS

|  |      |
|--|------|
| LIST OF TABLES .....   | vii  |
| LIST OF FIGURES .....  | viii |
| <b>Chapter 1: Introduction</b> .....                                   | 1    |
| 1.1 Reactivity Controlled Compression Ignition (RCCI) Combustion.....  | 2    |
| 1.1.1 Advantages of RCCI operation.....                                | 3    |
| 1.2 Review of Literature on RCCI combustion .....                      | 4    |
| 1.3 The One-dimensional Turbulence (ODT) Model .....                   | 11   |
| 1.4 Objective.....   | 12   |
| 1.5 Overview.....  | 13   |
| <b>Chapter 2: Numerical Setup</b> .....                                | 14   |
| 2.1 Domain Specification.....  | 15   |
| 2.2 Assumptions.....   | 16   |
| 2.3 Species Conservation .....   | 18   |
| 2.4 Momentum Conservation.....   | 18   |
| 2.5 Energy Conservation.....   | 18   |
| 2.6 Constitutive Relations.....  | 19   |
| 2.6.1 In-cylinder Pressure Model.....                                  | 19   |
| 2.6.2 Piston Speed.....  | 19   |
| 2.7 Summary of ODT Equations .....                                     | 21   |
| 2.8 Numerical Implementation .....                                     | 22   |
| <b>Chapter 3: Single Injection Strategy</b> .....                      | 25   |
| 3.1 Motivation.....  | 25   |
| 3.2 Run Conditions .....   | 25   |
| 3.3 Results and Discussion .....                                       | 26   |
| 3.3.1 Effects of Injection Timing.....                                 | 26   |
| 3.3.2 Effects of Equivalence Ratio .....                               | 34   |
| 3.3.3 Effects of Premixed Ratio.....                                   | 38   |
| 3.4 Conclusion .....   | 43   |
| <b>Chapter 4: Double Injection Strategy</b> .....                      | 45   |
| 4.1 Motivation.....  | 45   |
| 4.2 Run Conditions .....   | 45   |
| 4.3 Results and Discussion .....                                       | 46   |
| 4.3.1 Second Injection Timing.....                                     | 46   |
| 4.3.2 First Injection Timing.....                                      | 57   |
| 4.3.3 Effect of second injection timing for different mass splits..... | 62   |
| 4.3.4 Effect of first injection timing for different mass splits.....  | 71   |
| 4.4 Conclusion .....   | 78   |

|   |    |
|---|----|
| <b>Chapter 5: Summary and Future Work</b> ..... | 81 |
| 5.1 Summary.....                                | 81 |
| 5.2 Future Work.....                            | 82 |
| <b>References</b> .....                         | 84 |

## LIST OF TABLES

|           |   |    |
|-----------|---|----|
| Table 2.1 | The ODT RCCI Engine Model .....                                 | 21 |
| Table 2.2 | List of the common parameters used in the numerical study ..... | 24 |
| Table 3.1 | Run conditions used for the single injection strategy.....      | 26 |
| Table 4.1 | Run conditions used for the double injection strategy .....     | 46 |

## LIST OF FIGURES

|             |  |    |
|-------------|--|----|
| Figure 2.1  | Schematic showing 1-D spatial domain along the bore of the engine cylinder .....   | 16 |
| Figure 3.1  | Heat Release plots at different Injection timings .....                            | 28 |
| Figure 3.2  | Area heat release plots for SOI-40 and SOI-120.....                                | 30 |
| Figure 3.3  | Pressure plots for the different injection timings .....                           | 30 |
| Figure 3.4  | Temperature plots at different crank angles for SOI-40.....                        | 32 |
| Figure 3.5  | Temperature plots at different crank angles for SOI-120.....                       | 33 |
| Figure 3.6  | Ignition timings for different injection timings.....                              | 34 |
| Figure 3.7  | Pressure plots for the different injection timings at $\phi=0.5$ .....             | 35 |
| Figure 3.8  | Maximum pressure at different injection timings for different equivalence ratios.. | 36 |
| Figure 3.9  | Heat Release plots at different injection timings for $\phi=0.5$ .....             | 37 |
| Figure 3.10 | Ignition timings at different injection timing for $\phi=0.5$ .....                | 38 |
| Figure 3.11 | Pressure plots for the different premixed ratios .....                             | 39 |
| Figure 3.12 | Heat release plots for the different premixed ratios .....                         | 42 |
| Figure 3.13 | Ignition delay for the different premixed ratios .....                             | 43 |
| Figure 4.1  | Heat release plots for different second injection timings.....                     | 48 |
| Figure 4.2  | Heat release area plots for SOI-125 CA and SOI-140 CA.....                         | 50 |
| Figure 4.3  | Pressure plots for the different second injection timings .....                    | 52 |
| Figure 4.4  | Maximum pressure for the different second injection timings.....                   | 52 |
| Figure 4.5  | Ignition timings for the different second injection timings.....                   | 54 |
| Figure 4.6  | Temperature plots for different crank angles for SOI-125 CA .....                  | 55 |
| Figure 4.7  | Temperature plots for different crank angles for SOI-130 CA .....                  | 56 |
| Figure 4.8  | Heat release plots for different first injection timings.....                      | 60 |
| Figure 4.9  | Pressure plots for the different first injection timings.....                      | 61 |
| Figure 4.10 | Ignition timings for the different first injection timings.....                    | 62 |
| Figure 4.11 | Pressure plots for different mass splits for SOI-120 CA.....                       | 64 |
| Figure 4.12 | Pressure plots for different mass splits for SOI-125 CA.....                       | 64 |
| Figure 4.13 | Pressure plots for different mass splits for SOI-135 CA.....                       | 65 |
| Figure 4.14 | Maximum pressure for different n-heptane mass percentages in first injection ..... | 66 |
| Figure 4.15 | Heat release plots for different mass splits for SOI-120 CA.....                   | 68 |
| Figure 4.16 | Heat release plots for different mass splits for SOI-125 CA.....                   | 68 |
| Figure 4.17 | Heat release plots for different mass splits for SOI-135 CA.....                   | 69 |
| Figure 4.18 | Ignition timings for the different injection timings .....                         | 70 |
| Figure 4.19 | Pressure plots for different mass splits for SOI-40 .....                          | 72 |
| Figure 4.20 | Pressure plots for different mass splits for SOI-60 .....                          | 72 |
| Figure 4.21 | Pressure plots for different mass splits for SOI-80 .....                          | 73 |
| Figure 4.22 | Maximum pressure for different first injection mass percentage.....                | 74 |
| Figure 4.23 | Heat release plots for different mass splits for SOI-40 .....                      | 75 |
| Figure 4.24 | Heat release plots for different mass splits for SOI-60 .....                      | 76 |
| Figure 4.25 | Heat release plots for different mass splits for SOI-80 .....                      | 77 |
| Figure 4.26 | Ignition timing for different injection timings for different mass splits.....     | 78 |

# CHAPTER 1

## INTRODUCTION

In the modern world, the higher fuel costs and strict environmental mandates demand cleaner and more efficient internal combustion engines. The need for higher efficiency has put compression ignition engines in the forefront ahead of spark ignition engines. Conventional diesel engines are known for their higher thermal efficiency but their major disadvantage is the production off high levels of NO<sub>x</sub> and soot which have adverse effect on humans and nature [1]. To combat this problem, many after treatment methods have been used [2] but it results in significant increase in cost. The ideal solution would be to achieve high thermal efficiencies while maintaining low emissions.

To investigate such grounds, researchers have looked into premixed low temperature combustion (LTC) processes like Homogeneous Charge Compression Ignition (HCCI). Since they operate with premixed mixtures, the lower temperature of combustion results in lower levels of NO<sub>x</sub> and longer ignition delays prevent the formation of fuel rich zones thus reducing the soot production. However, HCCI combustion has controllability issues since it is a near constant volume process, which limits the control over combustion phasing and, thus, results in very high pressures and heat release rates that are undesirable for an engine. This issues prompted the researchers to look into premixed charge compression ignition (PCCI), where the fuel is injection in the early stages of the compression stroke thus avoiding the fuel rich zones resulting in higher efficiencies and lower emissions [3,4]. Issues with PCCI combustion included the lack of controllability, limited load range and combustion phasing [5,6].

Investigations concluded the need for fuel reactivity to be controlled on a per cycle basis. Further studies were conducted on a dual fuel process called Reactivity controlled Compression Ignition (RCCI) combustion. This dual fuel technique involves at least two fuels of different reactivity. The purpose is to control the cycle-to-cycle mixture reactivity and to optimize combustion phasing. The process involves early injection of the lower reactivity fuel into the cylinder forming a premixed mixture while the high reactivity fuel is injected before the ignition of the high reactivity fuel in single or multiple injections resulting in a variation of fuel reactivity across the cylinder. This concept resulted in higher fuel and thermal efficiencies than HCCI and PCCI, in certain cases reaching almost 60%, and extremely low levels of NO<sub>x</sub> and soot emissions.

### **1.1 Reactivity Controlled Compression Ignition (RCCI) Combustion**

Reactivity Controlled Compression Ignition (RCCI) combustion technology was first developed in the Engine Research Center, University of Wisconsin-Madison. This concept is a variant of Homogeneous Charge Compression Ignition (HCCI) combustion process. The HCCI technology is highly attractive thermodynamically, however, it lacked control over the combustion phasing, operating range and the rapid rise in pressure and temperature [7].

The basic concept of RCCI combustion process is that it controls the in-cylinder mixture reactivity by injecting at least two fuels of different reactivity. The process results in better control of the combustion process, smoother heat release and extremely low emissions. A low reactivity fuel is injected as port fuel forming a pre-mixed charge of fuel, air with/without EGR. A high reactivity fuel is injected into the cylinder later in the compression stroke using single or multiple injection strategies. Kokjohn et al. [8] showed that compared to a conventional diesel engine, the

RCCI process reduced the NO<sub>x</sub> production by a factor of six, soot by a factor of three and increased the gross efficiency by 16.4%.

### **1.1.1 Advantages of RCCI combustion operation-**

The advantages of RCCI operation has been well documented [9, 10, 11]-

1. High Efficiency: The RCCI process promises high thermal efficiency due the ability to run on high compression ratios. This is beneficial for fuel consumption and economy.
2. Low emission: RCCI has the potential to produce extremely low NO<sub>x</sub> and soot emissions which is a problem for conventional compression ignition engines. It complies with the EPA 2010 emissions guidelines without the need for after treatment.
3. Combustion phasing control: Controlling the overall reactivity of the mixture by the injection timing, amount of each fuel, type of fuel, the combustion phasing can be controlled.
4. Flexibility of fuel: Investigations can be made with a lot of different combinations of fuel that would help increase the operational range and provide more control over the combustion process.

## 1.2 Review of Literature on RCCI combustion

A concept called Premixed Compression Ignition (PCI) was investigated by Inagaki et al. [12] to achieve extremely low NO<sub>x</sub> and smoke emissions, also reported by authors [3,4]. Iso-octane was injected as the port fuel while diesel was used as the high cetane fuel to trigger the combustion process. The results showed that the ignition timings could be controlled by varying the ratios of the two fuels. It can be inferred from the work that different fuel blends could be required for different operating conditions of the engine that is running on high cetane number fuel at low loads to lower cetane number fuel at higher loads.

In 2009, this dual fuel RCCI combustion process was suggested by Kokjohn et al. [9]. The study investigated the potential of controlling the partial premixed charge compression ignition method by injecting gasoline through the port while early direct injection of diesel to control the combustion phasing. By using in cylinder fuel blending, the fuel reactivity can be varied cycle to cycle in accordance to the engine load and speed. From the study, it was observed as the fuel reactivity was decreased, the optimal combustion phasing was achieved with less EGR. As the engine load was increased, a higher PRF was required to maintain appropriate phasing of combustion. Though fuel reactivity could control the combustion phasing but a rapid pressure rise was still observed, thus concluding that stratification fuel reactivity is required to control the heat release. Combustion phasing can be controlled by fuel mixture stratification has also been observed by Reitz et al. [10] and Mikulski et al. [11].

Benajes et al. [13] used a 1-D spray model, DICOM [14,15], and observed that RCCI combustion is a staged process controlled by mixture fuel stratification also observed by authors [16]. The first stage consists of the ignition of the high reactivity zone that is the premixed mixture of diesel, gasoline and air and then successive auto ignitions of lower reactivity zones which leads

to multiple propagation flames. Splitter et al. [16] concluded that the gross efficiency of RCCI combustion can be increased by optimizing in cylinder mixture stratification of two fuels of large reactivity differences.

Referring to the need for fuel stratification in RCCI combustion by authors [9,13], investigations were conducted to determine the effect of charge preparation, fuel stratification on RCCI combustion. In 2013, Eguz et al. [17] investigated the effect of ignition timings and charge composition using a multi zone approach with detailed kinetics. Experimental and numerical studies showed that the ignition delay increases with earlier injections of the diesel fuel, this is mainly because of the cooler lean zones create due to better mixing of air and fuel. Also, the greater the proportion of gasoline fuel, the greater the ignition delay was as octane is more resistant to auto ignition. Delvescovo et al. [18] also used ignition timings and injection pressure to control the charge stratification and combustion phasing. The results were similar to the findings of [17] showing that the combustion phasing advanced between SOI of -140 to -35 degrees but retarded beyond that. While the peak gross efficiency was found to be between -60 to -45 degrees, the NO<sub>x</sub> was seen to increase if the SOI was retarded beyond -40 degrees.

Contrary to the work by authors [17,18], Reitz et al. [19] split the direct injections into two with 62% of the diesel mass in the first injection. By changing SOI-1 and SOI-2 in separate cases, the effect on the cylinder pressure and combustion phasing was shown. As the first injection was advanced, the combustion phasing is observed to retard, NO<sub>x</sub> and peak pressure reduced and CO is seen to have increased. By retarding SOI-2 while keeping SOI-1 constant, the combustion phasing and peak pressure is both seen to have advanced and the NO<sub>x</sub> and PM increases due to the formation of richer regions due to later injection timings. Kokjohn et al. [9] investigated the effect of the change of quantity of diesel in the first injection while keeping the overall ratio of

gasoline/diesel constant. It was observed that as the SOI-1 mass percentage was increased from 36% to 62%, the CO and HC remains same while NO<sub>x</sub> and PM seem to increase. Also, it can be seen, with lower percentage, the heat release advances and shows two distinct heat release regions while combustion phasing is seen to retard with higher mass percentage.

Besides the already proven advantage of RCCI with low emissions and heat losses, the RCCI process has shown great potential in achieving high thermal efficiency as much as almost 60%. Splitter et al. [16] tried to observe the maximum practical cycle efficiency for RCCI combustion process. A zero dimensional computational study was conducted and engine experiments on a single cylinder heavy duty engine without piston oil gallery cooling was conducted. The investigation at a constant engine load of 6.5 IMEP shows results that demonstrates that the gross thermal efficiency can be increased by not cooling the piston, using high dilution and in cylinder fuel dilution of combination of fuel of high reactivity differences. The optimum result was nearly about 60% obtained in the study.

In compression ignition engines, natural gas as a fuel having a low carbon to hydrogen ratio has been identified as a viable fuel source due to its cleaner combustion, low particle matter and other emissions. Liss et al. [20] showed that natural gas has a cleaner combustion compared to gasoline/diesel. In the past couple of years, a lot of studies has shown the usage of natural gas as the low reactivity fuel in a RCCI engine. Numerous researchers [19, 21, 22, 23, 24] used natural gas as the low reactivity fuel for RCCI combustion mode. Results showed clean, quiet and efficient combustion in the testing range, the reduction in smoke and CO<sub>2</sub> emissions while running a dual fuel combustion system with natural gas and diesel. Reitz et al. [19] suggested that different injector configurations could be investigated to further improve the natural gas/diesel RCCI operation.

Kim et al. [25] showed the effect of natural gas composition on the combustion process in an engine. Investigating RCCI combustion process, Kakaee et al. [26] concluded that the natural gas composition with the higher Wobbe Number has a higher peak pressure, temperature and NO<sub>x</sub> emission and considerably lower hydrocarbon and CO emissions.

Researchers [27, 28] compared two dual fuel systems, RCCI combustion to DPI combustion process using natural gas and diesel. The study showed that RCCI has better fuel efficiency, lower HC, CO, NO<sub>x</sub> emissions. Also, it was found that RCCI combustion is better controlled by parameters like injection timing, intake temperature, intake pressure and EGR.

Other studies have been made using the RCCI concept using other promising alternate fuels like alcohols, bio-diesel etc. Qian et al. [29] suggested that at higher loads, ethanol is a good replacement for gasoline with a higher indicated thermal efficiency. Qian et al. [30] conducted further RCCI combustion studies using diesel and different alcohols like ethanol, n-butanol and n-amyl alcohol. The results showed that when the overall lower heating value per cycle is constant, the NO<sub>x</sub> and soot emissions decrease with higher premixed ratio. Loaiza et al. [31] investigated using hydrous ethanol as the lower reactivity fuel while using diesel as the high reactivity fuel both injected directly into the combustion chamber of a rapid compression machine (RCM). RCM allows studies to be made in different modes where the ethanol can be injected before/during/after the diesel injections. For different loading conditions, injection timings and compression ratios of 16:1 and 20:1, it can be observed from the results that as the diesel fuel is being replaced, the compression ratio has to be increased. Thus, for the increasing compression ratio, higher pressure ratios have been observed.

Zerrakki et al. [33] also studied the ethanol RCCI process but for the high reactivity fuel, a blend of bio diesel and diesel was used (10% biodiesel/90% diesel, 20% biodiesel/80% diesel,

50% biodiesel/50% diesel). The bio diesel primarily increases the reactivity of the diesel and assists in combustion initiation. Results found from the investigation shows that the peak pressure and the heat release rate have increased for all the test blends. The brake specific fuel consumption (bsfc) value has shown an increase of about 30% mostly due to the higher mass fuel consumption value for biodiesel. As for emissions, the NO<sub>x</sub> was seen to decrease considerably but a slight increase in emissions for CO and HC was observed compared to a single fuel system. Li et al. [32] also conducted a study where biodiesel was used instead of diesel fuel. The effects of gasoline fuel ratio and injection timings were investigated. The results showed that the combustion characteristics are less sensitive to a change in gasoline ratio at conventional injection timing (-7 aTDC) than in advanced timings (-35 aTDC).

Besides, having its advantages, methanol has a lower cetane number which means it is more difficult to achieve auto ignition compared to diesel. Chao et al. [34] and Huang et al. [35] used up to 18% of methanol by weigh which achieved a decrease in NO<sub>x</sub> but CO and HC increased with methanol proportions. Li et al. [36] used RNG K- $\epsilon$  turbulent model coupled with CHEMKIN solver for methanol and diesel RCCI combustion mode. Results show that methanol mass fraction and injection timings control the fuel reactivity distribution in the cylinder. It was concluded that advancing SOI results in reduction in HC and soot emissions while improving fuel economy and avoiding engine knock. Li et al. [37] studied the effects of methanol fraction, initial temperature, initial pressure, EGR and SOI on RCCI combustion system run on methanol and diesel. The results concluded that the initial temperature and EGR effect the overall performance and emissions of the engine since they have a considerable impact on the temperature.

Zhou et al. [38] used KIVA-CHEMKIN code to study the RCCI combustion process using methanol as the port fuel and bio diesel as the direct injected fuel. The results showed a decrease

in NO<sub>x</sub> emission under medium and high loads, also, soot emissions reduced with increased port injection of methanol.

In 2017, Pan et al. [39] studied multi cylinder RCCI combustion using 2-butanol and diesel in a turbocharged diesel engine. The investigation showed RCCI combustion had a higher heat release rate and almost a 7% higher brake thermal efficiency compared to conventional combustion mode. Also, lower NO<sub>x</sub> and particulate emissions can be achieved relative to conventional diesel combustion process.

For almost a decade, the concept of RCCI has been tried out using different combinations of fuel; however, a single fuel strategy using gasoline has been carried out by authors [19, 40, 41]. Reitz et al. [19] used gasoline as the low reactivity fuel and a combination of gasoline and DTBP for higher reactivity. It was observed that the emission results were similar to that of gasoline/diesel. It was also observed that a decreased low temperature heat release magnitude reduced the need of compression work thus resulting in an approximate increase of 1% in gross indicated thermal efficiency. Gross et al. [40] investigated the “single fuel” strategy by using gasoline and EHN and comparing it to gasoline-diesel RCCI combustion. The results show that the operating conditions need to be significantly altered for single fuel operation also the NO<sub>x</sub> emissions are much higher than conventional gasoline-diesel RCCI operation.

Wang et al. [42] observed comparable results to gasoline/diesel RCCI emissions when using iso-butanol/iso-butanol+DTBP as the low reactivity and high reactivity fuels respectively. However, due to the lower reactivity of iso-butanol, a larger proportion of DTBP had to be added to achieve the required reactivity for the direct injection. The simulations were extended to compare with a model of HCCI, where HCCI demonstrated similar results in the lower and medium loads, RCCI holds a clear advantage in the higher spectrum of loads. Delvesco et al. [43]

conducted a similar study which found that a very high percentage of DTBP is required to be compared to the results of gasoline.

Most of the studies on the RCCI concept revolved around the usage of different fuel combinations and their impact on emissions and the efficiency, investigations have been also conducted to find the effect of the geometry of different engine components on RCCI combustion. Dempsey et al. [44] studied the effect of piston bowl geometry in a light duty single cylinder engine using gasoline/diesel and methanol/diesel. The investigation was carried out in the operating range of 1500 to 2300 rpm and IMEP of 3.5 to 17 bar. At first, the stock re-entrant piston bowl geometry was studied showing low levels of NO<sub>x</sub> and PM emissions and obtaining a peak efficiency of about 48%. However, at light load conditions both the fuels showed poorer combustion efficiency. Previous studies showed that much piston induced mixing is not required as it causes further heat losses. Thus, the authors [44] made further studies using a shallow, flat piston bowl with no squish land. It showed better light load performances and a peak gross indicated efficiency of about 51%. Li et al. [45] used KIVA4 and CHEMKIN to model the effect of different piston geometries on the combustion process.

Salahi et al. [46] studied the natural gas/diesel RCCI combustion process to investigate the introduction of the active fuel in a pre-chamber instead of the main chamber. This meant the combustion would start at the pre chamber and the flame would then propagate to the main chamber resulting in a secondary heat release. Due to the high temperatures in the pre chamber, the NO<sub>x</sub> concentration was found to be relatively high. Also, complete combustion was only achieved with higher equivalence ratios. But introducing the secondary fuel in the pre chamber allowed the increase in the operating range of the engine in both low and high loads at lower intake temperatures.

Though RCCI combustion can achieve high efficiency and low emissions over a wide range of operating conditions, however, it is observed that as we want to extend the load range, there is excessive pressure rise and soot emissions. For this reason, Wang et al. [47] investigated the RCCI combustion strategy using gasoline as the low reactivity fuel and Polyoxymethylene dimethyl ethers as the higher reactivity fuel. The experiment was conducted on a single cylinder diesel engine using the late intake valve closing strategy and intake boosting. Results showed that the RCCI strategy helped extend the load range to up to 23 bar IMEP while maintaining low levels of NOx/soot emissions. Also, the stoichiometric combustion allows the use of a three-way catalytic converter to further reduce the HC and CO emissions.

### **1.3 The One-dimensional Turbulence (ODT) Model**

Turbulent combustion is a complex phenomenon which comprises of two distinct scenarios occurring over the same time period, which are chemical reactions and fluid mixing. While some of the earlier traditional models in turbulent combustion relied on the separation of scales between mixing and chemistry, this assumption is not valid for a wide range of combustion processes [48]. Another challenges of capturing the coupling between turbulent mixing and chemistry is the inherent multi-dimensionality of turbulent flows.

In 1991, Kerstein [49] developed the linear eddy model (LEM) which could resolve in 1D, advection, scalar, momentum transport, chemistry in both length and time scales while successfully predicting the coupling of turbulent mixing and chemical kinetics. A stochastic method was used in the model to determine the turbulent advection part which meant using a “triplet map” i.e. stirring events to randomly selected eddies of different lengths in the domain

[50]. The model also used deterministic processes for solving the diffusive and reactive parts of the governing equations.

Kerstein [51] extended LEM to formulate the One Dimensional Turbulence (ODT) Model. The ODT Model is capable of solving for velocity vectors, which provides crucial details about the shear fields which drives the turbulence. The ODT is a turbulence model which can on its own solve for simple flow problems making it ideal for its application in problems like RCCI.

The One-dimensional Turbulence (ODT) Model is a stand-alone model which can resolve all time and length scale in one dimension. It has been used in numerous works as a stand-alone ODT model [52, 53, 54]. In 2012, authors [56, 57] investigated hydrogen-fueled HCCI operation using an ODT model formulated for engine operations.

The ODT model being a stand-alone model can effectively study the turbulent flows in a RCCI engine. This would provide us with significant insight into the turbulence-chemistry interactions in a RCCI engine and compare the cases for different operational parameters.

#### **1.4 Objective**

A One-Dimensional Turbulence (ODT) model is used to model the turbulent-reacting mixture in a RCCI engine using iso-octane and n-heptane as fuels. The purpose of this investigation is to study the single and double injection strategies for the direct injection and understand how the different engine operating parameters effect the combustion process and characteristics.

## **1.5 Overview**

This thesis is presented in five chapters. The first chapter introduces the RCCI technology and literature review for the process, then provides a brief description of the One-Dimensional Turbulence (ODT) model and how it is suitable for simulation of the RCCI combustion process. The second chapter provides the mathematical model that is used to simulate the RCCI engine operation. It also provides a description of how the model was numerically implemented for the process. The third chapter investigates the single injection strategy for the RCCI process for the different run conditions presenting the results, discussion and conclusions. The fourth chapter studies the double injection strategy for the diesel fuel for the different operating conditions and how it effects the combustion characteristics which is presented in the results and discussion. The important conclusions from this study and the scope for future works has been presented in chapter five.

## CHAPTER-2

### NUMERICAL SETUP

In this chapter, the model formulated for the simulation of the one dimensional turbulence in the engine cylinder working under the Reactivity controlled compression ignition (RCCI) conditions is discussed. Echekki et al. [57] and Ashurst et al. [58] have provided many fundamental formulations for the ODT model; however, for this study, to correctly account for the varying spatial domain with time, a re-formulation is required. This is accounted for in the study of HCCI engines by Gowda et al [55, 56]. While the ODT formulation for the turbulent-reacting flow developed by Echekki et al. [57] was used as the standard for the model, a few variations are made by the authors. Firstly, due to the compression and expansion of the domain, the mixture density is allowed to change in a pseudo-steady manner. Secondly, to account for the boundary work, another term is added to the energy equation.

In the model developed by Gowda and Echekki [55, 56] which is used as the basis for this study, it has been assumed that the flow is a low-Mach number, variable density flow. In this formulation, the density is allowed to vary with compression and expansion, however, the Mach number is kept low enough to be consider the flow incompressible (i.e. not requiring a separate continuity equation or an account for the pressure waves). Another important assumption for this model is that there is no axial variation of the velocity, species concentrations and temperature while attempting to capture the direction of most variations (at least statistically) for these quantities.

The thermo-physical parameters, the density and velocity changes with the temperature, pressure, the domain length and evolving composition as time progresses. The overall energy conservation is used to calculate the temperature. The mass conservation equation is used to

calculate the species concentrations. The momentum equation is used to calculate the velocity. The ideal gas equation of state and the mass conservation equation is used to update the density and thermodynamic pressure. This chapter discusses the assumptions used for the model, the derivation of the governing reaction-diffusion equations, the simplification of the model and finally the implementation of the ODT model for the RCCI combustion process.

## 2.1 Domain Specification

The 1-D domain as shown in Fig. 1 is chosen in the lateral direction perpendicular to the motion of the piston. The domain is divided in to smaller differential elements  $dx$  of uniform cross-sectional area. The length of the domain  $dx$  is kept constant for all the realizations. It is assumed that each differential elements have uniform properties in the axial direction. For the purpose of modelling the varying volume due to the compression and expansion stroke, a variable  $\ell$  is defined in the axial direction which is updated to realize this variation. The choice of a domain like this helps simplify the flows and a reasonably realistic method to implement the other engine operations like injections and a moving boundary. To model the fuel injection, the fuel composition associated with each differential element ( $dx$ ) is adjusted at the position where the injection is desired. The size of the injector nozzle is assumed to be the same size as the length of each differential element ( $dx$ ). The desired fuel to air mass ratio defines the length of time the fuel is injected for.

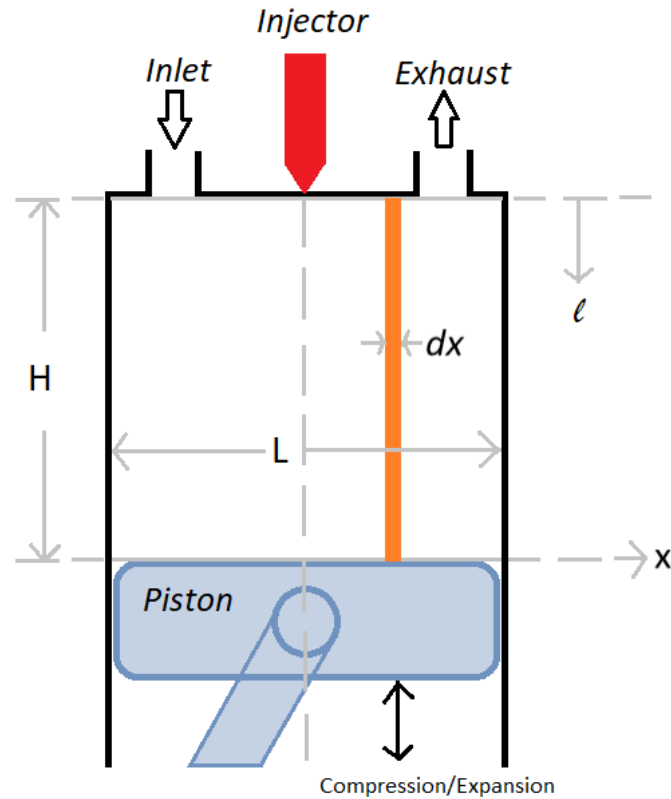


**Figure 2.1** Schematic showing 1-D spatial domain along the bore of the engine cylinder

## 2.2 Assumptions

The following assumptions are made for the derivation of the governing equations:

1. The total mass remains constant for the compression and expansion strokes of the engine. This is based on the assumption that for modelling purposes, the intake occurs before the start of the compression stroke and the exhaust occurs after the completion of the expansion stroke.
2. It is assumed that the cylinder charge is completely gaseous and contains no particulate matter (PM).

3. The gaseous mixture in the cylinder is assumed to be an ideal gas since the range of pressure and volume encountered in the cylinder does not cause much deviation from the ideal gas behavior.
4. The piston head is considered to be completely flat for all the runs.
5. The cross-sectional area for the cylinder is taken to be uniform and fixed for all the runs.
6. A variable density incompressible flow condition is assumed and no spatial pressure gradients exists.
7. It is assumed that there is no net mass transport due to diffusion. The diffusion for each species is such that, when summed over all the species, it is zero.
8. Since the 1-D domain is chosen in the lateral direction and perpendicular to the line of action of gravity. And since all properties in the axial direction is considered uniform, it is also assumed there is no effect of gravity.
9. The gas mixture is modelled as a Newtonian fluid.
10. The heat flux due to the Dufour effect is neglected.
11. It is assumed that there is no heat transfer in the axial direction through the cylinder head and piston and are considered adiabatic. The cylinder wall is assumed to be at constant temperatures and works as heat sinks.
12. The model has been derived from reaction and diffusion components and thus the advection terms have been neglected. The advection terms are implemented independently using stochastic methods.

### 2.3 Species Conservation

In the mixture, for each species, the component mass balance is obtained by equating the accumulation of species 'k' to the mass flow rate due to bulk flow, the mass flow rate due to diffusion and the mass flow rate due to reaction. This is applicable to all species including reactants, intermediates and products.

$$\frac{\partial Y_k}{\partial t} = -\frac{1}{\rho} \frac{\partial}{\partial x} (\rho Y_k V_k) + \frac{1}{\rho} \dot{\omega}_k$$

### 2.4 Momentum Equation

The conservation of momentum is applied over each differential length (dx) to characterize the fluid velocity. Newton's 2<sup>nd</sup> law of motion is used to find the rate of change of momentum represented as  $\dot{v}$ . The rate of generation of momentum for each element is calculated by the forces acting on the material in each element. The forces include local pressure forces, viscous forces and the gravitational forces.

The simplified differential equation for the velocity field (u) for the cylinder,

$$\frac{\partial u}{\partial t} = \frac{1}{\rho} \frac{\partial}{\partial x} \left( \mu \frac{\partial u}{\partial x} \right)$$

### 2.5 Energy Conservation

According to the 1<sup>st</sup> Law of thermodynamics, the rate of change of energy is equal to the sum of all the factors that add or remove energy from the system. In a gaseous mixture, energy transport occurs through heat transfer due to diffusion, conduction, chemical reaction and boundary work due to motion of piston.

$$\frac{\partial T}{\partial t} = \frac{1}{\rho C_p} \frac{\partial}{\partial x} \left( \lambda \frac{\partial T}{\partial x} \right) - \frac{1}{\rho C_p} \sum_{k=1}^N \frac{\partial}{\partial x} (\rho_k V_k C_{p,k} T) - \frac{1}{\rho C_p} \sum_{k=1}^N h_k \dot{\omega}_k - \frac{\bar{P}_T}{\rho C_p} \left[ \frac{dl}{dt} \right]_{\text{bdry}}$$

Initial conditions:  $T(0, x) = T_0(x) \quad \forall x \in [-\frac{L}{2}, \frac{L}{2}]$

The boundary conditions are depended on the kind of walls being modelled. For a constant temperature wall, a Dirichlet boundary conditions is used.

Dirichlet boundary conditions:  $T(t, -\frac{L}{2}) = T_{wall}$  and  $T(t, \frac{L}{2}) = T_{wall}$  for  $t > 0$

## 2.6 Constitutive Relations

### 2.6.1 In-Cylinder Pressure Model

The cylinder pressure is characterized by the following equation,

$$P_T = \langle \frac{\rho R_u T}{\bar{M}} \rangle = \frac{\int A_{cs} \left( \frac{\rho R_u T}{\bar{M}} \right) dx}{V_{total}}$$

As per the assumption that the overall mass of the system remains constant since the intake happens before the compression stroke and the exhaust occurs after the expansion stroke, the overall density of the mixture can be calculated as,

$$\rho = \frac{m_{total}}{V_{total}}$$

where  $m_{total}$  is a function of the initial density and the initial volume.

$$m_{total} = \rho_o V_o$$

### 2.6.2 Piston Speed

For this model, the Top Dead Center (TDC) is considered as a reference point and the cylinder head as the origin, then the total instantaneous volume inside the cylinder is,

$$V_{total} = V_c + A_{cs}(l_{rod} + a - l_{bdry})$$

where,  $l_{rod}$  is the length of the connecting rod,  $a$  is the crank radius,  $l_{bdry}$  is the instantaneous distance between the crank axis and the piston pin axis,  $A_{cs}$  is the surface area of the piston head and  $V_c$  is the clearance volume.

If the system is considered a slider-crank mechanism, the instantaneous distance between the crank and piston pin can be expressed as:

$$l_{bdry} = a \cos(vt) + (l_{rod}^2 - a^2 \sin^2(vt))^{\frac{1}{2}}$$

where  $v$  is the angular speed of the crank,  $v=2\pi N$  ( $N$ = Engine RPS)

The piston speed can be obtained by differentiating with time,

$$\frac{dl_{bdry}}{dt} = -a v \sin(vt) - \frac{a^2 v \sin(vt) \cos(vt)}{(l_{rod}^2 - a^2 \sin^2(vt))^{\frac{1}{2}}}$$

Defining stroke length ( $H_{stroke}$ ), mean piston speed ( $\bar{S}_p$ ) and the ratio of connecting rod length to the crank radius ( $R$ ) as:

$$H_{stroke} = 2a$$

$$\bar{S}_p = 2NH_{stroke}$$

$$R = \frac{l_{rod}}{a}$$

Therefore, the piston speed as a function of time,

$$\left[\frac{dl}{dt}\right]_{bdry} = -\frac{\pi}{2} \bar{S}_p \sin(vt) \left[1 + \frac{\cos(vt)}{(R^2 - \sin^2(vt))^{\frac{1}{2}}}\right]$$

The negative sign on the right hand side of the equation is there because the simulation starts with the compression stroke at bottom dead center (BDC).

## 2.7 Summary of ODT Equations

The ODT equations used for this model has been summarized in Table 2.1. A stochastic term ( $\Omega$ ) has been added to the equations to account for the turbulent advection which has been further discussed in Section 2.8.

Table-2.1 The ODT RCCI Engine Model

|                           |   |
|---------------------------|---|
| <b>Species</b>            | $\frac{\partial Y_k}{\partial t} = -\frac{1}{\rho} \frac{\partial}{\partial x} (\rho Y_k V_k) + \frac{1}{\rho} \dot{\omega}_k + \dot{\Omega}_k$   |
| <b>Momentum</b>           | $\frac{\partial u}{\partial t} = \frac{1}{\rho} \frac{\partial}{\partial x} \left( \mu \frac{\partial u}{\partial x} \right) + \Omega_u$  |
| <b>Energy</b>             | $\frac{\partial T}{\partial t} = \frac{1}{\rho \bar{c}_p} \frac{\partial}{\partial x} \left( \lambda \frac{\partial T}{\partial x} \right) - \frac{1}{\rho \bar{c}_p} \sum_{k=1}^N \frac{\partial}{\partial x} (\rho_k V_k C_{p,k} T) - \frac{1}{\rho \bar{c}_p} \sum_{k=1}^N h_k \dot{\omega}_k -$<br>$\frac{\bar{P}_T}{\rho \bar{c}_p} \left[ \frac{dl}{dt} \right]_{\text{bdry}} + \Omega_T$ |
| Initial<br>Boundary       | $T(0, x) = T_0(x) \quad \forall x \in \left[ -\frac{L}{2}, \frac{L}{2} \right]$<br>Dirichlet boundary conditions (constant temp.):<br>$T\left(t, -\frac{L}{2}\right) = T_{\text{wall}} \text{ and } T\left(t, \frac{L}{2}\right) = T_{\text{wall}} \quad \forall$<br>$t > 0$  |
| Constitutive<br>Relations | $P_T = \left\langle \frac{\rho R_u T}{M} \right\rangle = \frac{\int A_{cs} \left( \frac{\rho R_u T}{M} \right) dx}{V_{\text{total}}}$<br>$\left[ \frac{dl}{dt} \right]_{\text{bdry}} = -\frac{\pi}{2} \bar{S}_p \sin(vt) \left[ 1 + \frac{\cos(vt)}{(R^2 - \sin^2(vt))^{\frac{1}{2}}} \right]$<br>$\rho = \frac{\rho_0 (V_c + A_{cs} H)}{\int A_{cs} dx}$                                       |

## 2.8 Numerical Implementation

The One-dimensional Turbulence (ODT) model numerically implements the governing equations provided in Section 2.7. Solving the governing equations requires splitting them into two parts. The temporal section requires complete separation of the diffusion and reaction. The diffusive section is solved by using the central diffusive scheme to update the 1-D spatial domain. First-order forward Euler method is used to advance the diffusion while the reaction source term is directly integrated by using stiff-integrator, DVODE [59]. The CHEMKIN II suite [61] includes the transport libraries [60] to compute the mixture-averaged transport properties for heat and mass transfer.

A ‘triplet map’ for each stirring event is used to stochastic implementation of turbulent advection. These ‘triplet maps’ are capable of replicating the compressive strain and rotational folding effects which are characteristic to eddy events. The segments are randomly selected of length  $\hat{\mathbf{l}}$  and the left boundary at  $\hat{\mathbf{x}}$ . Therefore, in the 1-D scalar field, the triplet map is applied to the eddy span of range  $[\hat{\mathbf{x}}, \hat{\mathbf{x}} + \hat{\mathbf{l}}]$ .

The rearrangement of the selected 1-D profile is achieved by the replacement of the length  $\hat{\mathbf{l}}$ , with three identical copies compressed to one-third its original length. To maintain continuity of the values in the new profile, the copy is placed in the middle and inverted.

To modulate the location and frequency of stirring events, the shear rate is calculated using the velocity component of the scalar field in the 1-D domain. An ‘eddy rate distribution’ is calculated by assigning a time scale to every possible transport event at a given instant. This is used to find the frequency. The model consists of two adjustable parameters  $A$  and  $\beta$  of order unity. The parameter,  $A$ , associated the eddy characteristic time with the inverse of rate of shear.

On the other hand,  $\beta$ , forms a relationship between the eddy characteristic time to the elapsed temporal evolution of the domain.

Blends of hydrocarbons e.g. primary reference fuel (PRF) is often used to represent different commercial fuels. In this study, iso-octane and n-heptane has been used as surrogates for gasoline and diesel respectively. Many numerical investigations have been conducted on RCCI combustion process using PRF [29, 30, 70]. For this numerical study on RCCI, a 171-species PRF skeletal mechanism with 861 elementary reactions has been employed developed by authors [62]. This skeletal mechanism was developed from a detailed Lawrence Livermore National Laboratory (LNL) mechanism with 874 species and 3796 elementary reactions [63, 64]. The skeletal mechanism was developed by employing DRG with expert knowledge [67, 68] and isomer lumping method [69]. The laminar flame speed results have been compared and validated with experimental studies [65, 66].

Table-2.2 List of the common parameters used in the numerical study

| <b>Parameter</b>                       | <b>Value/Range</b> | <b>Units</b> |
|--|--------------------|--------------|
| Equivalence Ratio ( $\phi$ )           | 0.3-0.5            | -            |
| Compression Ratio (CR)                 | 16                 | -            |
| Engine RPM                             | 1300               | rev/min      |
| Cylinder bore                          | 8.2                | cm           |
| Cylinder stroke                        | 8.2                | cm           |
| Connecting rod length/Crank Radius (R) | 2                  | -            |
| Manifold Pressure                      | 1                  | atm          |
| Gasoline Fuel Temperature              | 650 (376.85)       | K (°C)       |
| Diesel Fuel Temperature                | 850 (576.85)       | K (°C)       |
| Injection Velocity                     | 1000               | cm/s         |
| Oxidizer Temperature                   | 650 (376.85)       | K (°C)       |
| No. of fuel injectors                  | 1-3                | -            |
| Wall type                              | Isothermal         | -            |
| Wall temperature                       | 350 (76.85)        | K (°C)       |

A list of the common engine operating parameters have been presented in Table 2.2. A change in a one or a combination of the parameters effects the mixing and combustion process. The problem setup and the run conditions for each case studied have been presented in their respective chapters. All simulation has been conducted on Intel Core i7 CPU with @3.2 GHz workstations. Computation time for one realization of 360 CA took between 20-24 hours.

## CHAPTER 3

### SINGLE INJECTION STRATEGY

#### 3.1 Motivation

In this study, an ODT model is used to understand the combustion process of RCCI technology and how the combustion characteristics vary with different engine parametrical changes using the single injection strategy. Also, comparisons are provided between the different cases studied in this section. The major parameters that have investigated in the present study, are the effects of change in injection timing, equivalence ratio and premixed ratio.

#### 3.2 Run Conditions

In order to study the effects on the combustion characteristics of a RCCI engine using iso-octane and n-heptane as the port fuel and the direct injected fuel respectively, in the first section, the injection timings for the single injection is varied while keeping all other operating parameters constant. In the second section, the same injection timings are used to study the effects of different equivalence ratio. And in the final section, the premixed ratio is changed and runs are made for the same injection timings used in the previous sections. The common run conditions have been provided in Table 3.1 and Table 3.2.

Table-3.1 Run conditions used for the single injection strategy

| Parameter                              | Value/Range | Units   |
|--|-------------|---------|
| Equivalence Ratio ( $\phi$ )           | 0.3-0.5     | -       |
| Compression Ratio (CR)                 | 16          | -       |
| Engine RPM                             | 1300        | rev/min |
| Direct Injection Timing                | 40-120      | CA      |
| Total injection time                   | 5           | CA      |
| Premixed Ratio (%)                     | 50-90       |         |
| Cylinder bore                          | 8.2         | cm      |
| Cylinder stroke                        | 8.2         | cm      |
| Connecting rod length/Crank Radius (R) | 2           | -       |
| Manifold Pressure                      | 1           | atm     |
| Fuel (iso-octane) Temperature          | 650         | K       |
| Fuel (n-heptane) Temperature           | 850         | K       |
| Injection Velocity                     | 1000        | cm/s    |
| Oxidizer Temperature                   | 650         | K       |
| Wall type                              | Isothermal  | -       |
| Wall temperature                       | 350         | K       |

### 3.3 Results and Discussion

#### 3.3.1 Effects of Injection Timing

In this section, the mixing and combustion process for a RCCI engine using single injection strategy is studied. A single injection method is used for the directly injected fuel and a sweep of the injection timings is made from 40 CA to 120 CA into the compression stroke, keeping other parameters constant as presented in Table 3.1. The equivalence ratio for all the cases studied is kept constant at  $\phi=0.3$ . When the n-heptane is injected into the cylinder, it vaporizes and is entrained with the air and iso-octane. This was observed in investigations by Benajes et al. [13]. The mixing time is significantly dependent on the time of injection of the n-heptane during the

compression stroke [11,18]. From Fig. 3.1, it is observed that when the n-heptane is being injected at an earlier timing i.e. 40 CA in the compression stroke, the mixing time is significantly higher forming an almost homogeneous mixture similar to HCCI combustion with a lower equivalence ratio than the other cases i.e. the resulting mixture is leaner and has a lower reactivity. The heat release curve for the case shows due to the less reactive mixture, the initial heat release is much lower. Also, the different pockets of almost homogeneous mixture ignite almost simultaneously in peaks of similar magnitude which results in the heat release occurring in a much shorter interval when compared to the other cases. Since, the mixture formed is near HCCI-like, the disadvantage is the rapid heat release and the lack of control in combustion phasing.

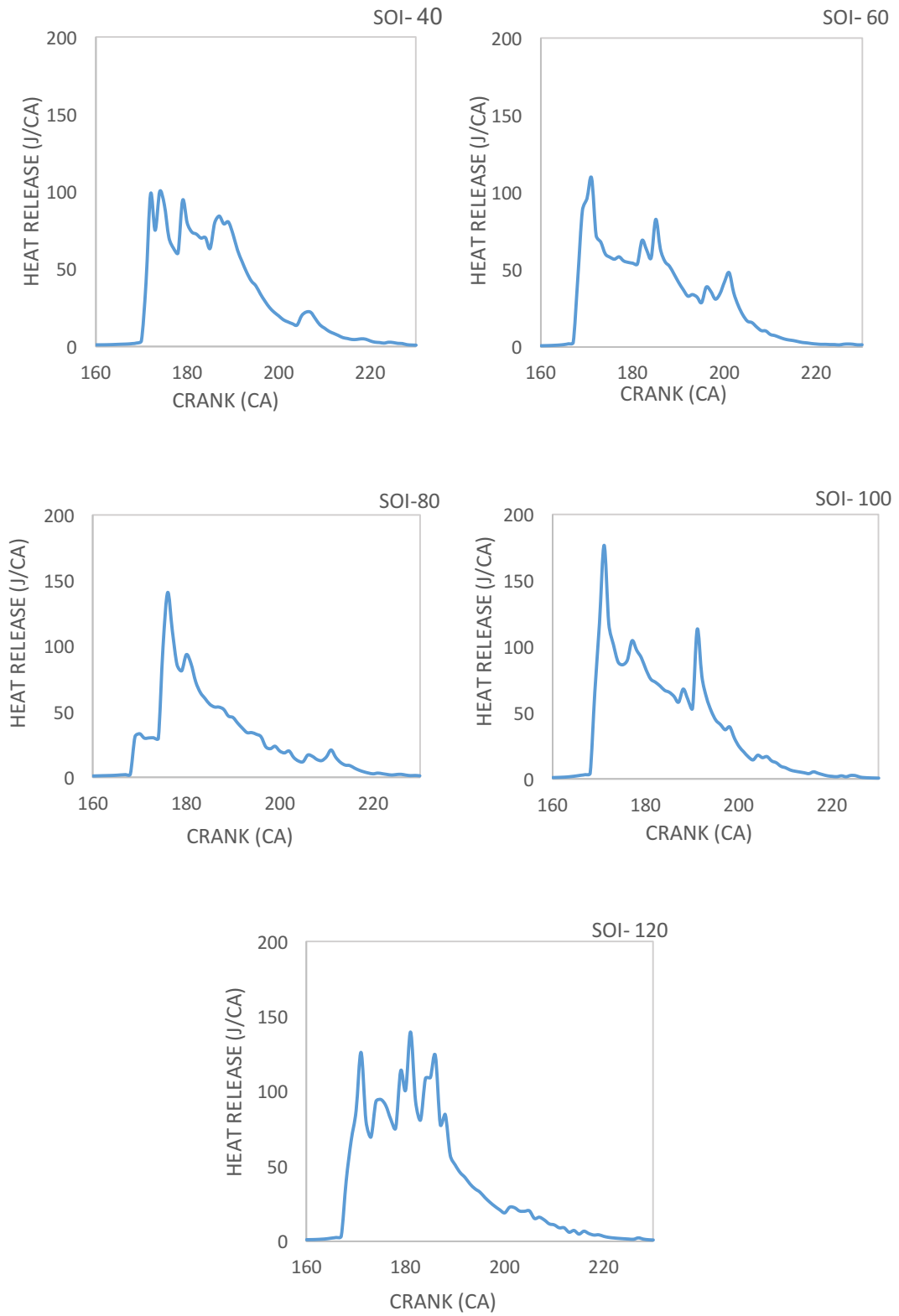


**Figure 3.1** Heat release plots at different Injection timings

As the injection timing is delayed, a staged combustion process is evident, which is more characteristic of a RCCI combustion process. The later injection means lower mixing time for the n-heptane; therefore, a highly reactive zone with high local equivalence ratio is produced where the proportion of the high reactivity fuel is much higher. Also, in the other parts of the cylinder, zones with lower local equivalence ratios are produced with the diesel entrained in gasoline and air. Therefore, the result is a stratified charge with varying reactivity across the cylinder. The heat release curve for SOI-80, shows an initial peak for the combustion of the high reactivity zone with the ignition of the diesel fuel. This ignites the leaner zones designated by the higher heat release curve since the fuel mass is much higher. And finally, small peaks can be observed afterwards which are results of flame propagation and the ignition of different pockets of lean zones. Similar results were shown by Nazemi et al. [71].

However, when the injection timing is further retarded to SOI-100, a much higher initial peak is observed. This is because the late injection timing means a small mixing time for the diesel fuel and a higher mass of the fuel in the richer zone resulting in the higher heat release. The higher heating value for diesel also contributes to the higher initial heat release.

It can be concluded that as compared to rapid heat release for HCCI combustion process, the heat release for RCCI combustion is much more uniform as it is a staged combustion process which is beneficial for the engine. This is further observed by comparing the area curve (Figure 3.2) for the heat release for the cases of SOI-40 and SOI-120. The case for SOI-120 shows multiple peaks for heat release over a wide range of crank angle rotations while for SOI-40 which almost produces an almost homogeneous mixture due to the early injection timing shows that most of the heat is produced in a shorter time interval with simultaneous ignitions of multiple zones.

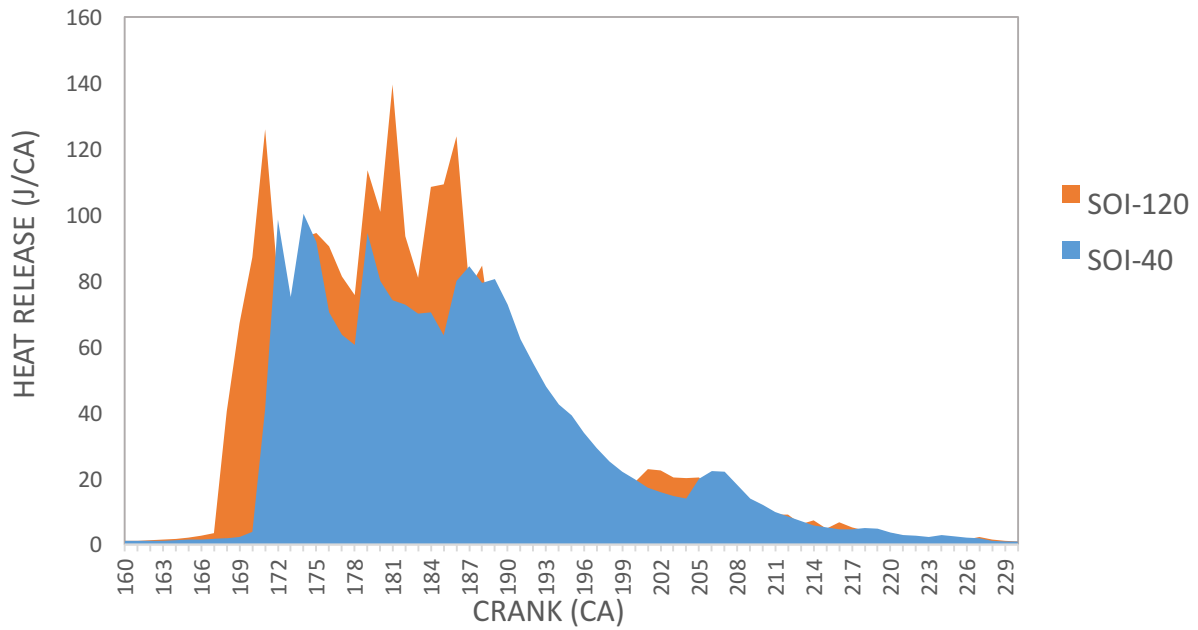


**Figure 3.2** Area heat release plots for SOI-40 and SOI-120

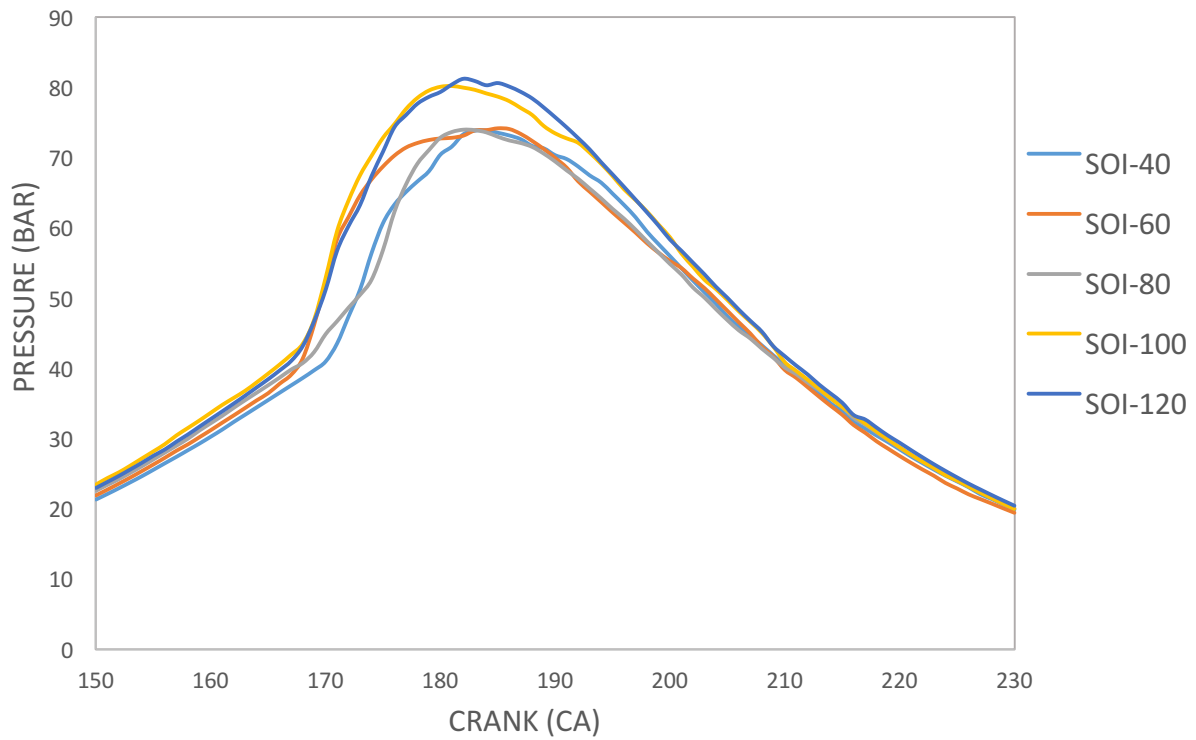


**Figure 3.3** Pressure plots for the different injection timings

In figure 3.3, it can be observed that as the injection timing is retarded from 40 CA to 120 CA, the maximum pressure is seen to increase correspondingly. This is because, with the late injection time, the mixing time is much lower and this results in a high reactivity mixture which leads to rapid heat release when ignition takes place and results in the higher pressure rise. For earlier injections, a lower equivalence ratio is achieved and the heat release is more uniformly distributed resulting in a lower maximum pressure rise.

Also, the ignition timings for the different start of injection (SOI) cases can be observed from figure 3.3. The ignition timings have been identified by the observation of the first rapid rise in pressure in the figure. Also, the exact crank angle for the ignition can be identified by studying the temperature profiles at each crank angle. The cases for SOI-40 and SOI-120 has been presented in the figures 3.4 and 3.5 where the temperature profiles have been provided for crank angles representing before ignition, during ignition and after ignition. It can be observed from the temperature profiles that a rapid rise in temperature occurs when ignition takes place, unlike the uniform rise in temperature which is observed before due to compression. Further simulation runs have been made including cases for other injection timings between 40 CA and 120 CA and an ignition map has been presented in figure 3.6. Eguz et al. [17] found similar results when the injection timing was delayed from 90 CA to 120 CA, the ignition timing advanced correspondingly.

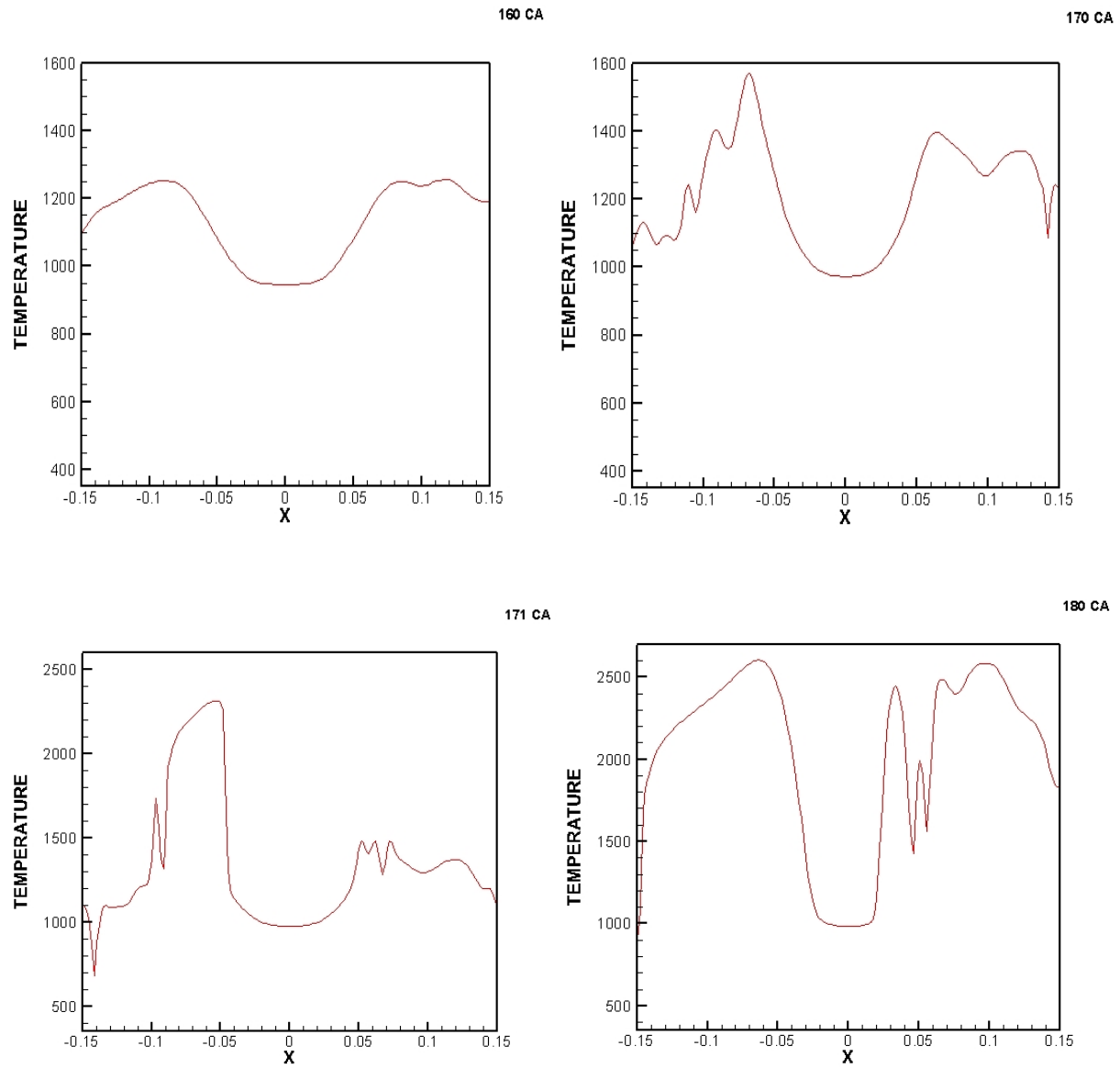


Figure 3.4 Temperature plots at different crank angles for SOI-40

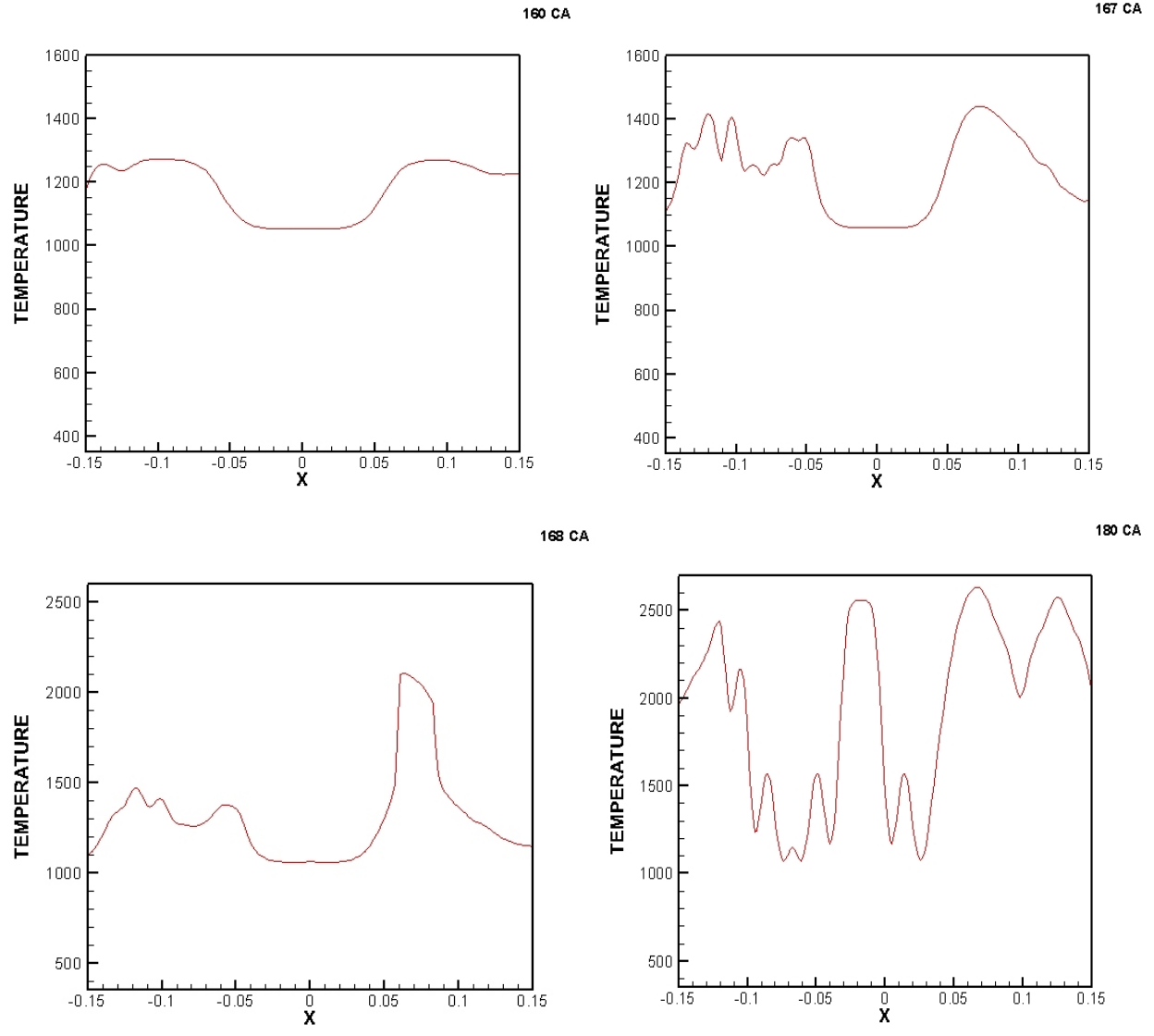
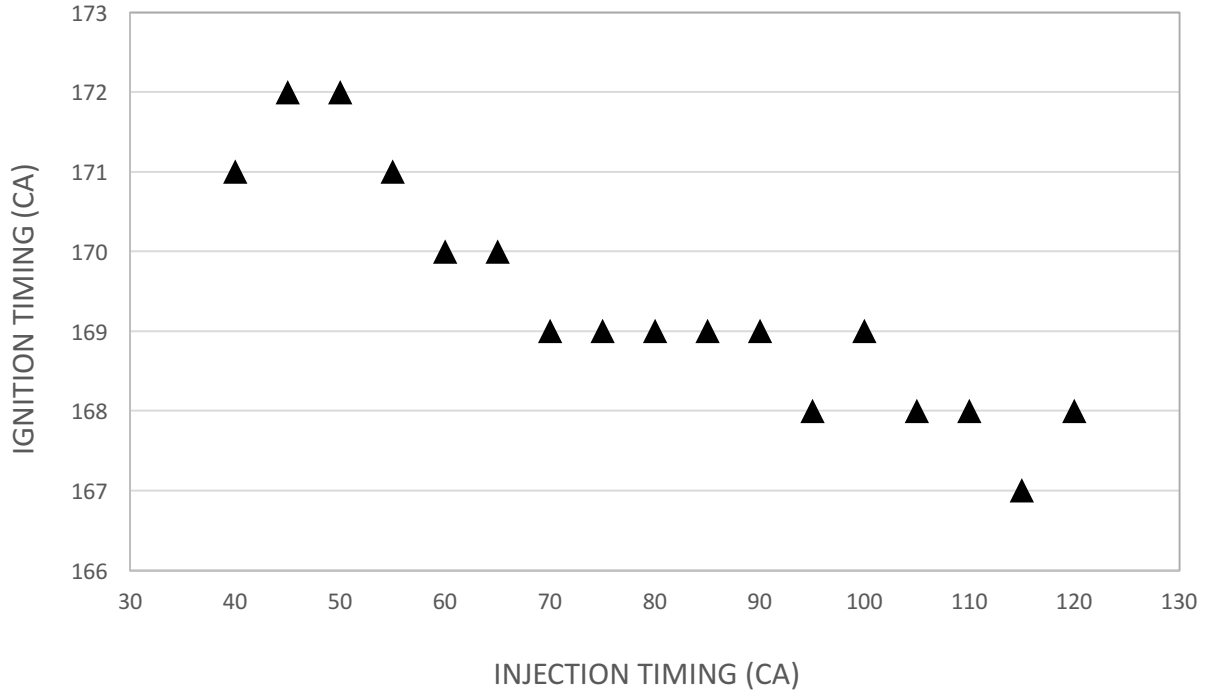


Figure 3.5 Temperature plots at different crank angles for SOI-120



**Figure 3.6** Ignition timings for the different injection timings

### 3.3.2 Effects of equivalence Ratio

In this section, the effects of the equivalence ratio on the combustion characteristics is presented. The two cases for equivalence ratios that are studied are  $\phi=0.3$  and  $\phi=0.5$ . All other engine operating parameters are kept constant as presented in Table 3.1.

Figure 3.7 shows the pressure plots for the different injection timings for an equivalence ratio of  $\phi=0.5$ . It is observed that with a delay in the injection timing, the maximum cylinder pressure rises. This is similar to the trend observed for an equivalence ratio of 0.3. With the delay of injection, the overall reactivity of the mixture would be higher because of lower mixing time and thus a higher pressure is achieved. However, if the pressure plots for  $\phi=0.3$  in Fig. 3.3 is compared to the pressure plots for  $\phi=0.5$  in Fig. 3.7, it can be observed that the maximum pressure is reached at a later crank angle for all the cases studied. The reason behind this is the higher

amount of fuel for  $\phi=0.5$  requires higher mixing time with air and iso-octane. Thus, the maximum pressure achieved is at a much later timing for  $\phi=0.5$ .

Figure 3.8 shows the sensitivity of maximum cylinder pressure to the change in injection timing differs between the cases presented for  $\phi=0.3$  and  $\phi=0.5$ . It can be inferred that the cylinder pressure for the equivalence ratio of 0.5 is more sensitive. This is because, at a higher equivalence ratio, the proportion of fuel to air is higher than the other cases presented. Therefore, a small change in the injection timings causes a significant change in the maximum cylinder pressure achieved. Also, in Fig. 3.8, it is observed that for the injection timings of 60 CA, 80 CA and 100 CA, the maximum pressure for  $\phi=0.5$  is much higher than  $\phi=0.3$ . This is the result of the higher amount of fuel that is being injected due to the higher equivalence ratio.

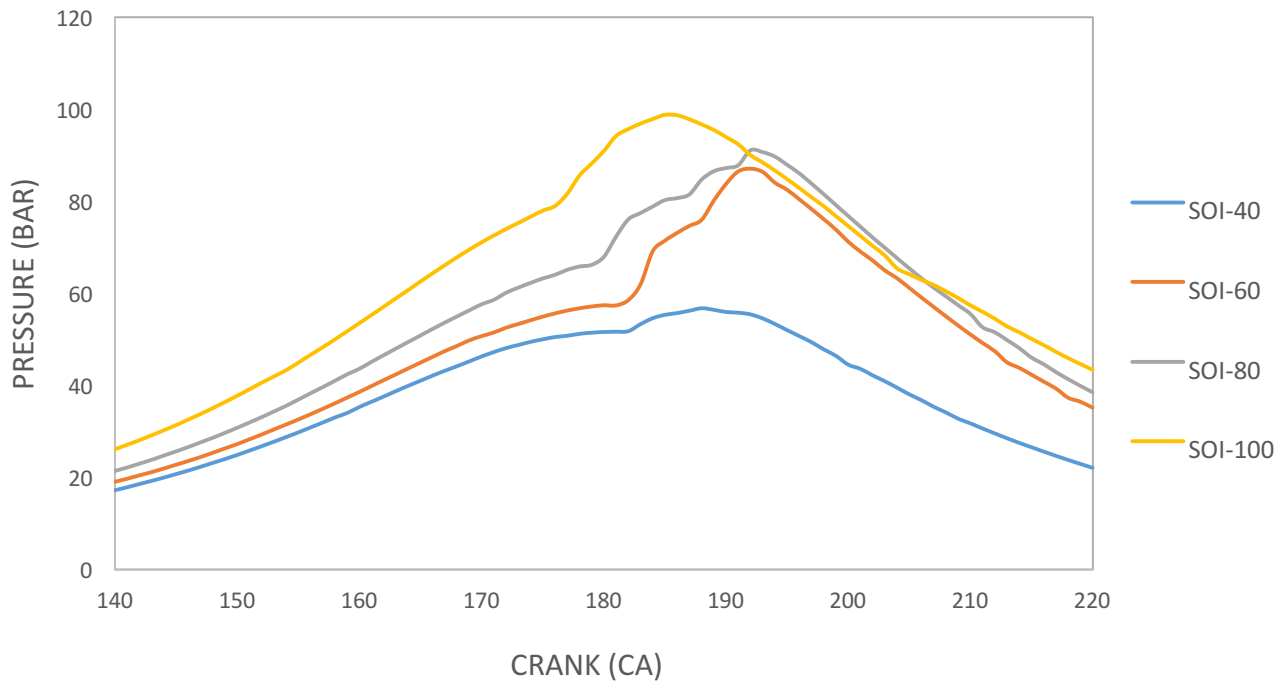


**Figure 3.7** Pressure plots for the different injection timings at  $\phi=0.5$ .

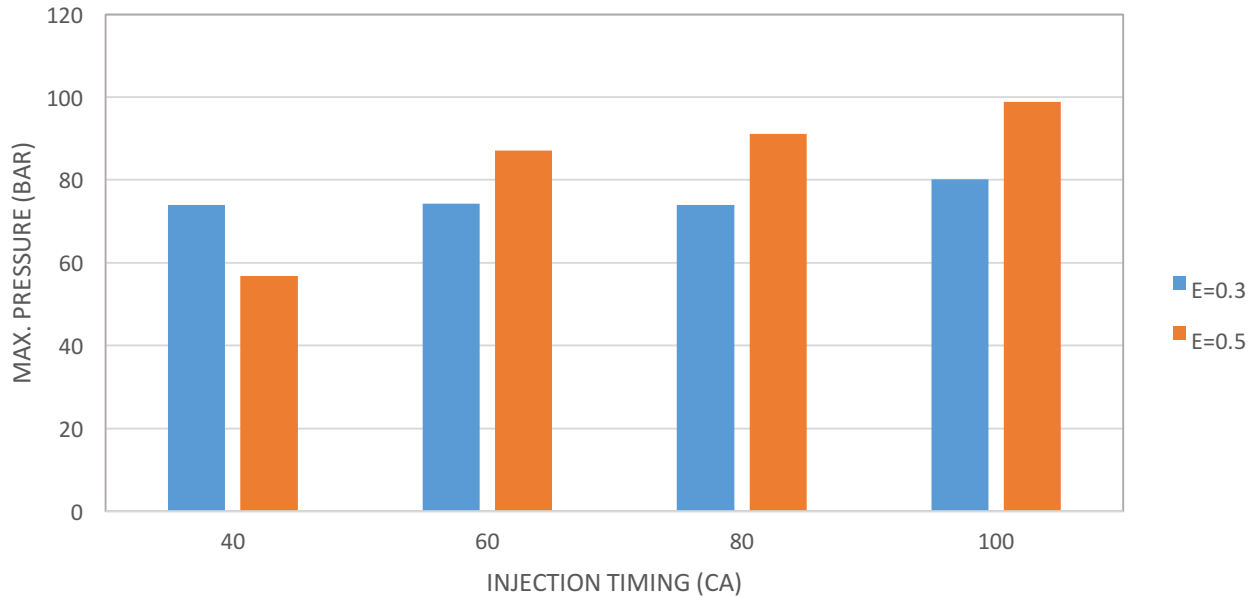


**Figure 3.8** Maximum pressure at different injection timings for different equivalence ratios

Figure 3.9 shows the heat release plots for the different injection timings for an equivalence ratio of  $\phi=0.5$ . It can be observed that the initial heat release for the cases of  $\phi=0.5$  has much higher value compared to the cases for  $\phi=0.3$  presented in Fig. 3.1. Also, the peaks of the heat release are much higher for  $\phi=0.5$  than for  $\phi=0.3$ . The reason for both of this observation is that with a higher equivalence ratio, a larger amount of fuel is being injected. Therefore, the overall heat release increases.

For an equivalence ratio of  $\phi=0.5$ , the ignition timings for the different injection timings is presented in Fig. 3.10. The ignition timings have been identified in a similar manner as observed in Figs. 3.4 and 3.5. It is evident from Fig. 3.10 that, with the delay of the injection timing, the ignition timing advances. This is because with the delay in injection timing, the mixing time decreases. Thus, the n-heptane does not get enough time to mix with the air and iso-octane. Since, n-heptane is the higher reactivity fuel used for this study, the overall reactivity increases with lower mixing time. Therefore, the mixture is more prone to ignition at an earlier timing with later

injection. Similar results were observed for an equivalence ratio of  $\phi=0.3$  presented in Section 3.3.1. However, compared to the case for  $\phi=0.3$ , the ignition seems to occur at a much later timing for the same injection timings. This is because due to the higher proportion of fuel for  $\phi=0.5$ , it takes more time for the fuel to mix with the air and ignite.

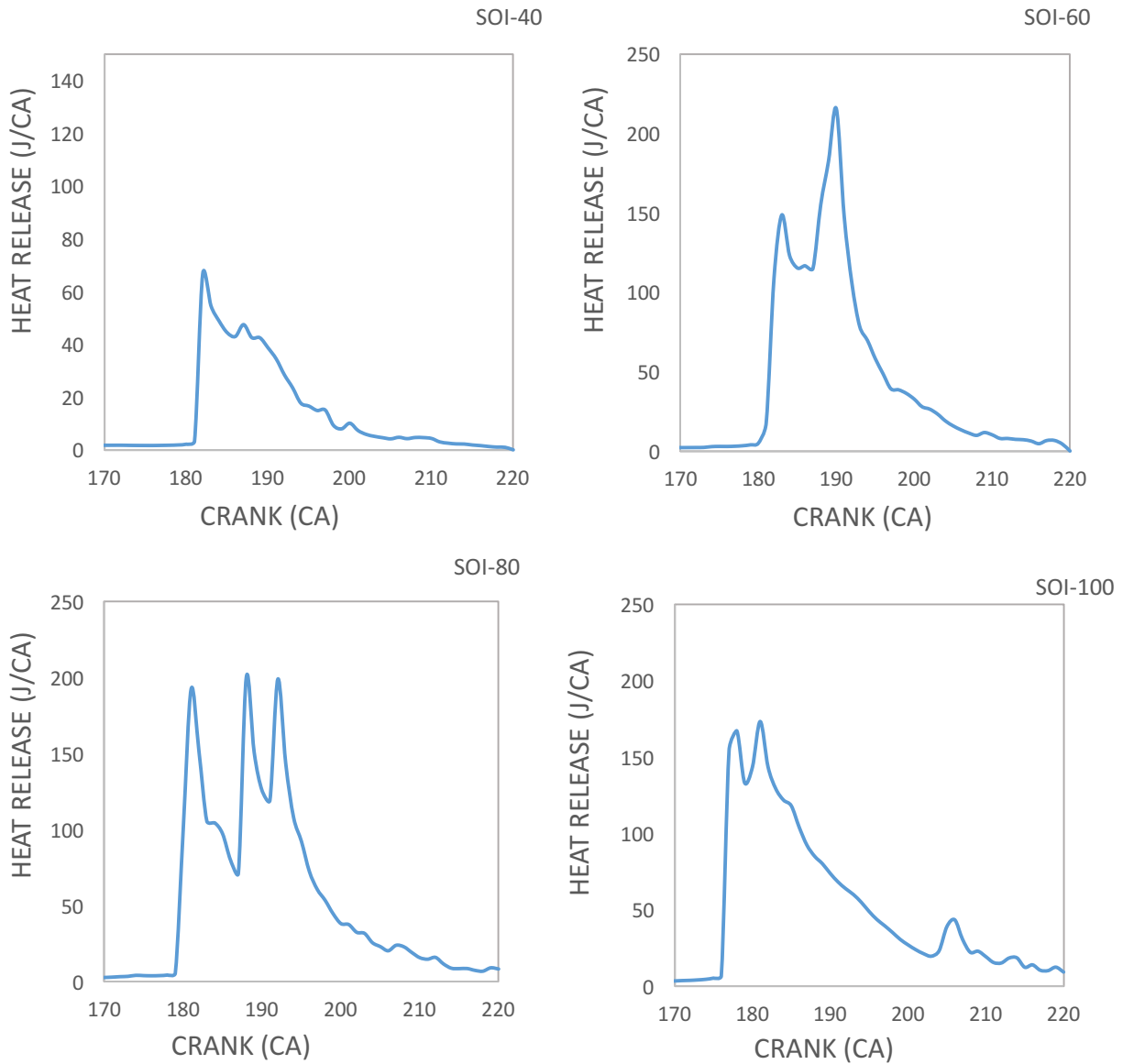


**Figure 3.9** Heat Release plots at different injection timings for  $\phi=0.5$ .

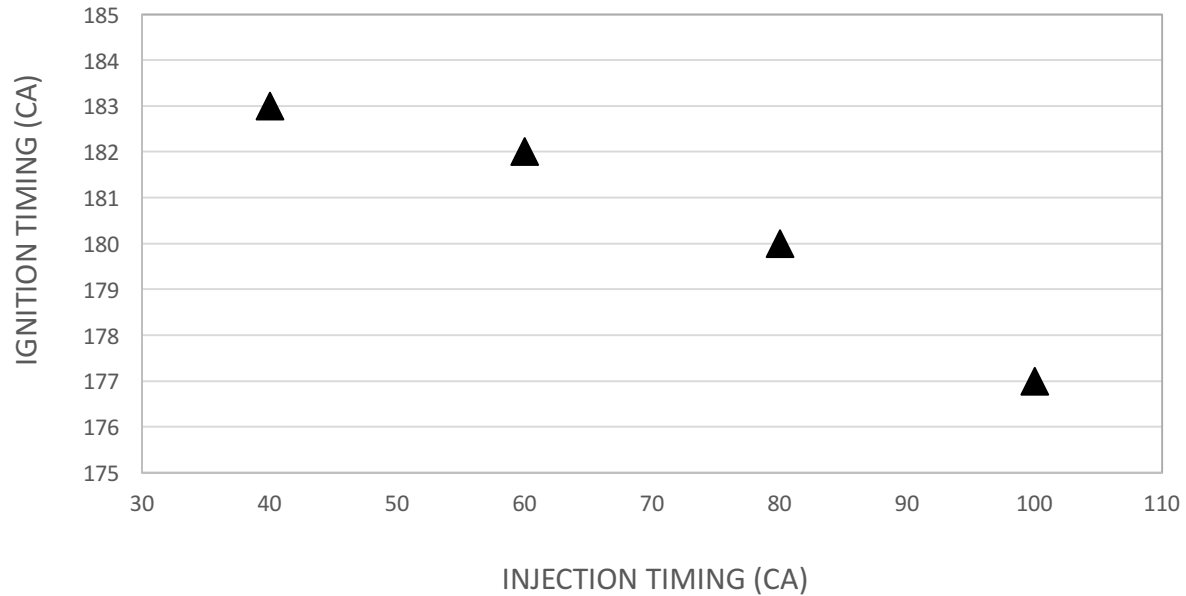


**Figure 3.10** Ignition timings at different injection timing for  $\phi=0.5$ .

### 3.3.3 Effects of Premixed Ratio

In a RCCI combustion process, the iso-octane is injected as port fuel and forms a premixed mixture with air. The n-heptane is injected through direct injection at a specified crank angle during the compression stroke to mix with the already premixed iso-octane and air and forms a stratified mixture [8,11]. In this section, the timing of injection for the direct injected fuel is at 80 CA and using an equivalence ratio of  $\phi=0.3$  for all the cases studied, the premixed ratio is changed and its effect on the combustion characteristics of RCCI combustion process has been studied. Premixed ratio can be defined as the ratio of the iso-octane in the total fuel injected both as port fuel and directly injected.

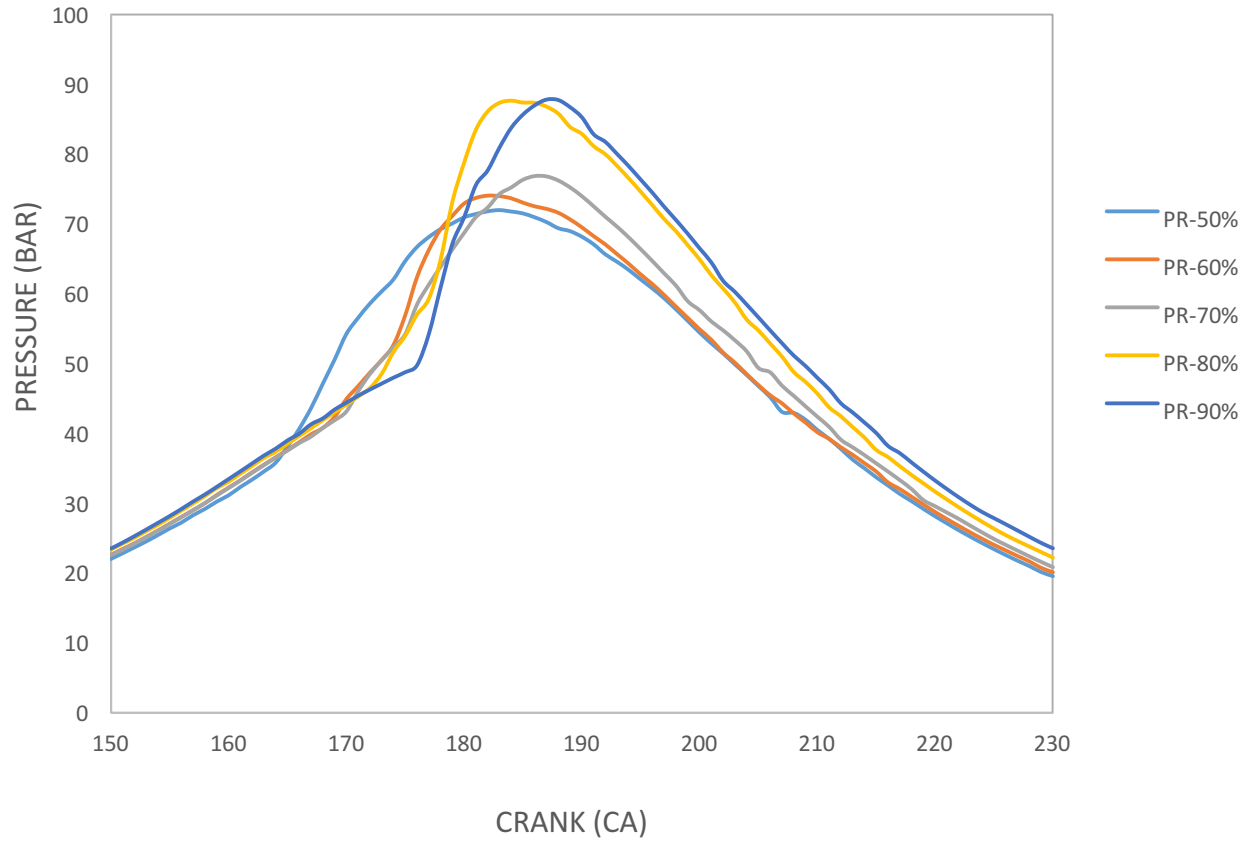


**Figure 3.11** Pressure plots for the different premixed ratios

In Figure 3.11, the pressure curves for the different premixed ratios have been plotted against the crank angle. It can be observed that as the premixed ratio is increased from 50% to 90%, the start of ignition is retarded. The start of ignition can be identified by the point of rapid rise in pressure in the pressure curves, also by identifying the first rapid rise in heat release on the curves presented in Fig. 3.12. To further study the case, the ignition delay for each case can be calculated by the difference in crank angles between the injection of n-heptane which is constant for every case at 80 CA and the point of ignition. The results are presented in Fig. 3.13 where the ignition delay is plotted against the premixed ratio. It can be observed from the plot that as the premixed ratio is increased, the ignition delay increases correspondingly. This is mainly because iso-octane has a comparatively higher auto ignition temperature compared to n-heptane, so it is

more resistant to ignition. Therefore, the increase in premixed ratio means that the amount of iso-octane in the mixture compared to n-heptane is much higher. As a result, the overall mixture becomes more resistant to ignition as the premixed ratio increases and the result is observed on the heat release curve with the premixed ratio of 90% ignites the latest.

In Fig. 3.12, it is observed for the curve of PR-50% that the heat release starts at an earlier timing than the other ratios, also the peaks are not that high comparatively and the heat is released over a uniform time towards the end of the compression stroke and the start of the expansion stroke. The early start to heat release is due to the higher percentage of n-heptane which have a much lower auto ignition temperature thus the overall mixture has a higher reactivity. Therefore, the mixture combusts at an earlier time. Then, a series of heat release peaks is observed which is due to the flame propagation and the ignition of the other pockets of iso-octane, n-heptane and air.

However, for the cases of PR-60% and PR-70%, the staged combustion process is more evident which is more typical of RCCI combustion process. A low initial heat release peak is observed which infers the ignition of the high reactivity zone of the stratified mixture and then a series of higher magnitude peaks is produced for the combustion of the other pockets of leaner mixture.

The heat release curves for PR-80% and PR-90%, are unlike the other ratios as they have a much higher initial heat release. In both the cases, the characteristic staged combustion of RCCI combustion process is not evident. The heat release is much higher and the rate of release is extremely high. This corresponds to the rapid rise in pressure and the higher maximum pressure for both the case observed on the pressure plots. Also. The peaks for the maximum pressure are reached at a later crank angle than the other ratios, this is because of the late ignition of the mixture due to the higher percentage of iso-octane. The high rate of heat release for these cases is

characteristic for engine knocking where pockets of fuel and air mixture explodes instead of combustion occurring through flame propagation. So, here the low reactivity mixture produced due to higher percentage of iso-octane resists ignition to the stage where the rise in pressure and temperature due to compression causes the different pockets of the stratified mixture to explode. This also explains the absence of an initial low peak for heat release due to the ignition of the fuel air mixture. This phenomenon of knocking is undesirable for the engine as it produces unwanted noise and vibration.

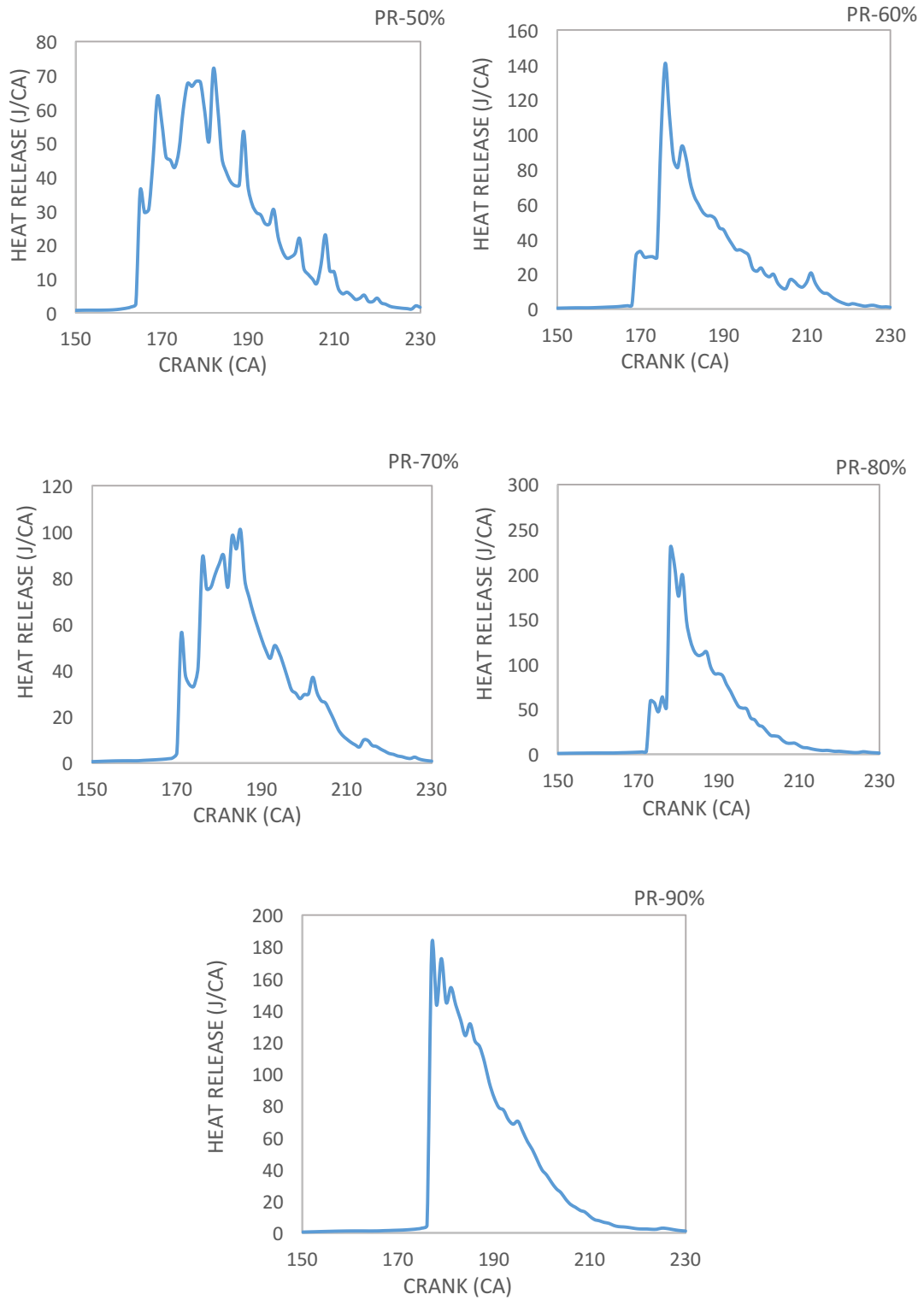


**Figure 3.12** Heat release plots for the different premixed ratios

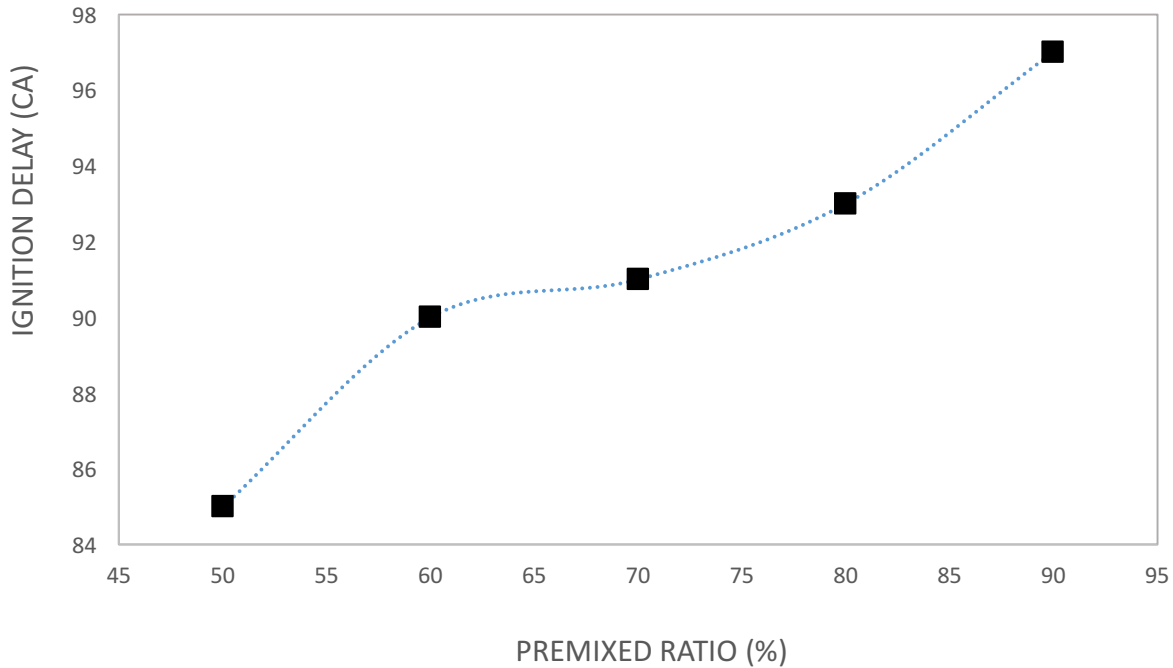


**Figure 3.13** Ignition delay for the different premixed ratios

### 3.4 Conclusions

The following conclusions can be drawn from the study of the single injection strategy for RCCI combustion process-

1. With the single injection strategy, a later injection timing resulted in a more uniform heat release compared to an earlier timing. This is important in keeping the cylinder temperatures lower which is a deterrent to NO<sub>x</sub> production.
2. Investigations into both equivalence ratios  $\phi=0.3$  and  $\phi=0.5$ , showed that the single injection timing is a key factor in controlling ignition timing and combustion phasing. With a delay in the injection timing, the ignition timing significantly advances for both the cases.
3. For the different equivalence ratios  $\phi=0.3$  and  $\phi=0.5$ , the ignition timings and maximum pressure peak is observed to occur at a delayed timing for the higher equivalence ratio. Also, for the case of  $\phi=0.5$ , a higher overall cylinder pressure is observed. It can be

concluded that equivalence ratio provides some control over the combustion phasing besides the injection timings.

4. In the study of the effect of premixed ratio on the single injection strategy, high premixed ratio above 80% resulted in very high heat release compared to the other cases, this may result in high cylinder temperature and act as a precursor to NO<sub>x</sub> production.
5. Also, apart from the use of equivalence ratio and injection timing for combustion phasing control, premixed ratio is observed to effect the ignition delay for the combustion process. The higher the premixed ratio, the longer is the ignition delay.

## CHAPTER-4

### DOUBLE INJECTION STRATEGY

#### 4.1 Motivation

The authors [9,19] conducted experimental studies to investigate the double injection strategy for RCCI combustion process. By changing SOI-1 and SOI-2 in separate cases, the effect on the cylinder pressure and combustion phasing is shown. As the first injection was advanced, the combustion phasing is observed to retard. By retarding SOI-2 while keeping SOI-1 constant, the combustion phasing and peak pressure is both seen to have advanced.

Similar to the case for single injection strategy investigated in Chapter-3, not much investigation has been done using an ODT model to study the double injection strategy for RCCI combustion. This study uses an ODT model to investigate the effects of injection strategy for the two injections on the combustion characteristics. Also, the effect of mass split of n-heptane between the two injections on the RCCI combustion characteristics is studied.

#### 4.2 Run Conditions

In order to study the double injection strategy for RCCI combustion, the first two sections in this chapter investigates the effect of the second and first injection timing changes on the combustion process. The third and fourth sections investigates the effect of the second and first injection timings changes on the combustion process for different n-heptane mass splits between the two injections. The common run conditions are provided in Table 4.1.

Table-4.1 Run conditions used for the double injection strategy

| Parameter                         | Value/Range | Units   |
|-----------------------------------|-------------|---------|
| Equivalence Ratio ( $\phi$ )      | 0.3         | -       |
| Compression Ratio (CR)            | 16          | -       |
| Engine RPM                        | 1300        | rev/min |
| First Injection Timing            | 40-80       | CA      |
| Second Injection Timing           | 125-140     | CA      |
| Total injection time              | 5           | CA      |
| Mass split between two injections | -           |         |
| Premixed Ratio (%)                | 60          |         |
| Fuel (iso-octane) Temperature     | 650         | K       |
| Fuel (n-heptane) Temperature      | 850         | K       |
| Injection Velocity                | 1000        | cm/s    |
| Oxidizer Temperature              | 650         | K       |
| Wall type                         | Isothermal  | -       |
| Wall temperature                  | 350         | K       |

## 4.3 Results and Discussion

### 4.3.1 Second Injection Timing

In this section, a double injection strategy for the direct injection fuel is employed. In RCCI process, a low reactivity fuel, in this case iso-octane, is injected as port fuel and it is assumed it forms a homogeneous mixture with air in the cylinder. A higher reactivity fuel, in this case n-heptane, is injected into the cylinder during the compression stroke to form a stratified mixture unique to RCCI combustion process. In this study, the direct injection of the n-heptane fuel is split into two separate injections at different times during the compression stroke. The overall fuel-air ratio is kept constant at 0.0669 and the fuel mass split between the port fuel and the direct injected fuel also is constant for all the runs at 60% to 40% respectively of the total fuel mass. For the first

part of the study, the mass split between the two injections is kept constant at 50:50 ratio of the total mass of the direct injected n-heptane fuel.

In the double injection strategy, the first injection, which is at 40 CA into the compression stroke for all the cases studied, can be termed as the conditioning injection. The higher reactivity fuel (i.e. n-heptane) is being injected into the cylinder, which is used to increase the overall reactivity of the mixture present in the cylinder. The earlier injection timing for the first injection provides a higher mixing time for the n-heptane to form a more reactive mixture with iso-octane and air already present in the cylinder. The second injection of the higher reactivity fuel can be termed as the ignition source. The second injection of n-heptane takes place at a later time into the compression stroke. This reduces the mixing time for the fuel with the existing mixture. Thus, creating a zone of high reactivity mixture of n-heptane, iso-octane and air near the top of the cylinder while the charge becomes leaner downwards in the axial direction of the cylinder. This results in a stratified charge in the cylinder with varying local equivalence ratio. This was observed by Kokjohn et al. [9]. As the cylinder pressure and temperature rise with the compression of the mixture, the high reactivity zone of the fuel-air mixture ignites first and the resulting flame propagates and ignites the other pockets of leaner fuel-air mixture. In the following section, a sweep of the second injection is made between 120 CA and 140 CA into the compression stroke and its effects on the different engine performance parameters is studied.

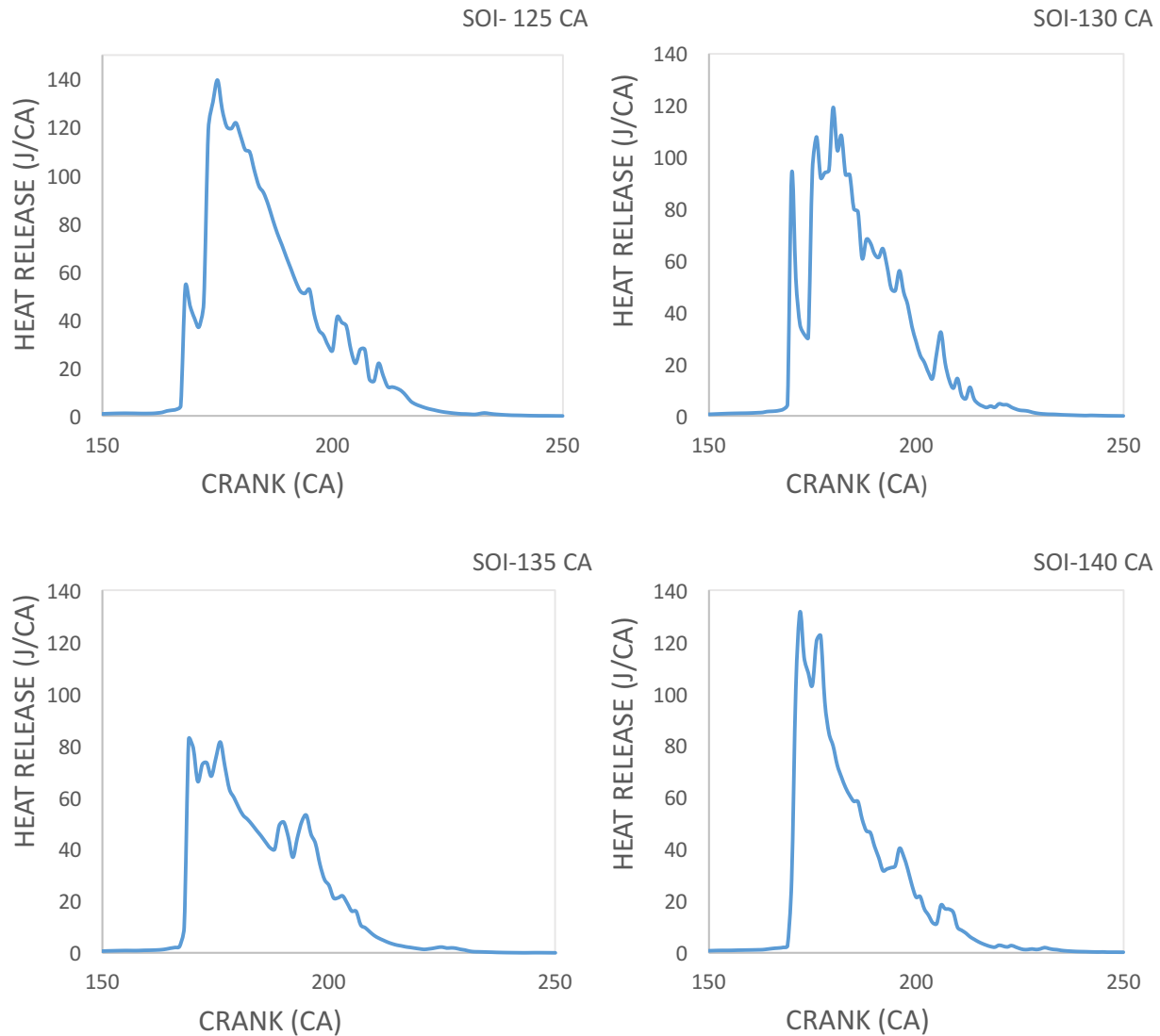
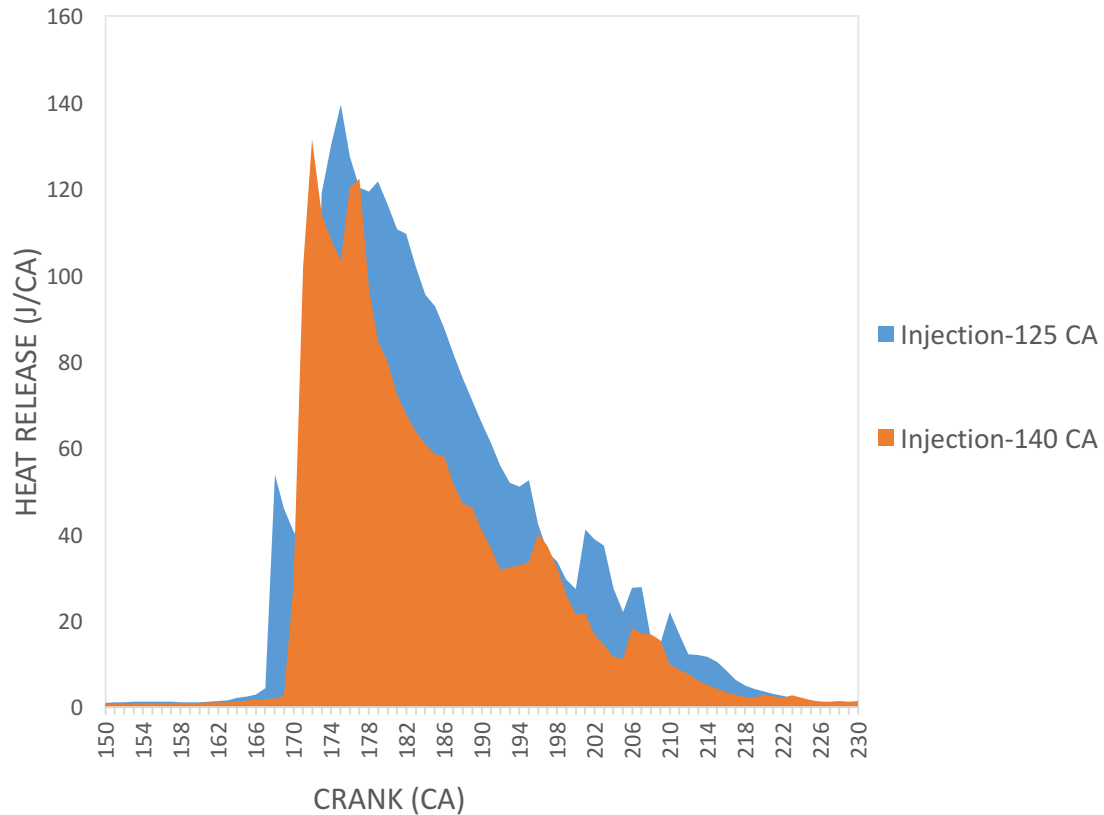


**Figure 4.1** Heat release plots for different second injection timings

Figure 4.1 shows the heat release curves at the different second injection timing. The increase in the pressure and temperature with compression of the charge in the cylinder causes the high reactivity zone of n-heptane, iso-octane and air to ignite towards the top of the cylinder resulting in an initial peak for heat release as clearly exhibited for the case of injection timing of 125 CA. As the flame starts to propagate through the cylinder, it ignites the other pockets of less reactive fuel-air mixture resulting in a much higher heat release. Further heat release is observed as the flame propagates and ignites smaller pockets of fuel and air before being extinguished by

the completion of the reaction during the expansion stroke as observed in the plot for the injection timing of 125 CA. This results in a staged release of heat. However, from the heat release plot for the injection timing of 130 CA, it is observed that the initial peak for heat release due to the combustion of the high reactivity zone is much larger than the case of 125 CA. The primary reason behind it is, with the delay of the second injection timing, the mixing time for the proportion of n-heptane in the second injection decreases. This results in less time for this mass of n-heptane to mix with the pre-existing n-heptane, iso-octane and air. Thus, higher percentage of n-heptane is present towards the top of the cylinder in the high reactivity zone increasing the local equivalence ratio. This results in a much higher heat release and a larger peak as observed in the plot. Also, since the percentage of fuel is less in the leaner parts of the cylinder, the combustion results in a lower heat release for the case of 130 CA than the one for 125 CA.

From the heat release plot for the second injection timing of 140 CA in fig. 4.1, it is observed that the smaller initial peak from the combustion of the high reactivity zone is absent contrary to the cases for 125 CA and 130 CA. This is because, as the second injection timing is delayed further, the mixing time significantly decreases for the n-heptane with the pre-existing charge. Thus, a higher percentage of the mass of n-heptane injected later is present in the high reactivity zone. This results in a very high initial heat release and most the heat release occurs over a much shorter span of time and lacks uniformity compared to the other cases as presented in fig. 4.2 where the heat release for both injection timing of 125 CA and 140 CA is presented as an area plot. This may result in higher cylinder temperatures, which is considered an important factor for NO<sub>x</sub> production, which, is undesirable.



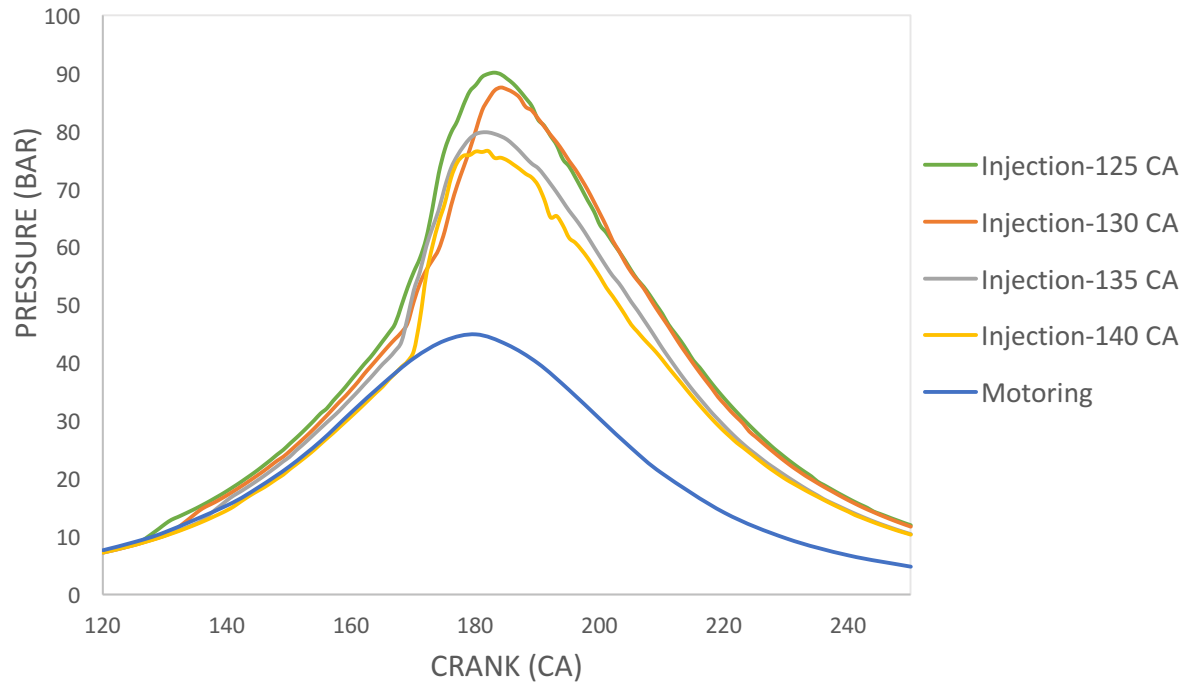
**Figure 4.2** Heat release area plots for SOI-125 CA and SOI-140 CA

Figure 4.3 shows the change in cylinder pressure between the crank angles 120 and 250 for each second injection timing. A motoring curve also is plotted on the same figure to show how the pressures vary from it for the different runs.

It is observed that, for the earlier injection timings i.e. 125 CA and 130 CA, the pressure plots starts to deviate from the motoring curve at a much earlier time. This is because due to the earlier injection, the initial reactions start correspondingly at an earlier timing and the resulting pressure rise and the deviation from the motoring curve is observed. This results in a pressure rise, which is much more uniform and spread over a longer timing. However, for the case for second injection timing at 140 CA, the pressure plot shows a very late deviation from the motoring curve

and a much rapid rise in pressure. The rapid rise of the pressure is undesirable for an engine and may result in engine knocks.

Figure 4.4 shows the maximum pressure achieved for the different second injection timings. A clear trend is observed for the cases that when the injection timing is delayed, the maximum cylinder pressure achieved considerably decreases. The pressure rise in the cylinder is depended on the heat release due to the combustion of the fuel air mixture. Considering that most of the fuel has combusted for all the cases as presented by the plots for the mass fraction of n-heptane and iso-octane in the cylinder at 360 CA at the end of the expansion stroke. Thus, it is evident the pressure rise is also correlated to the uniformity of the heat release. For the injection timings of 125 CA and 130 CA, a staged heat release is observed due to combustion of the fuel air mixture. An earlier injection allows the reactions to start earlier and an initial heat release due to the ignition of the rich zone sets up the staged release of heat. This results in a more uniform rise in pressure from an earlier timing as observed in fig. 4.3. Also, the maximum pressure achieved is much higher for these cases compared to the injection timings of 135 CA and 140 CA. From figure 4.2, it is observed that the heat release at later injection timings is more compact and thus the overall heat release happens in a much shorter time span. Though this causes a rapid rise in pressure compared to the other cases (Fig. 4.3), the maximum pressure achieved is significantly lower as shown in Fig. 4.4. Thus, it can be concluded that for the double injection strategy for RCCI combustion, when the second injection timing is advanced, a more uniform heat release is observed and a higher cylinder pressure is achieved.



**Figure 4.3** Pressure plots for the different second injection timings

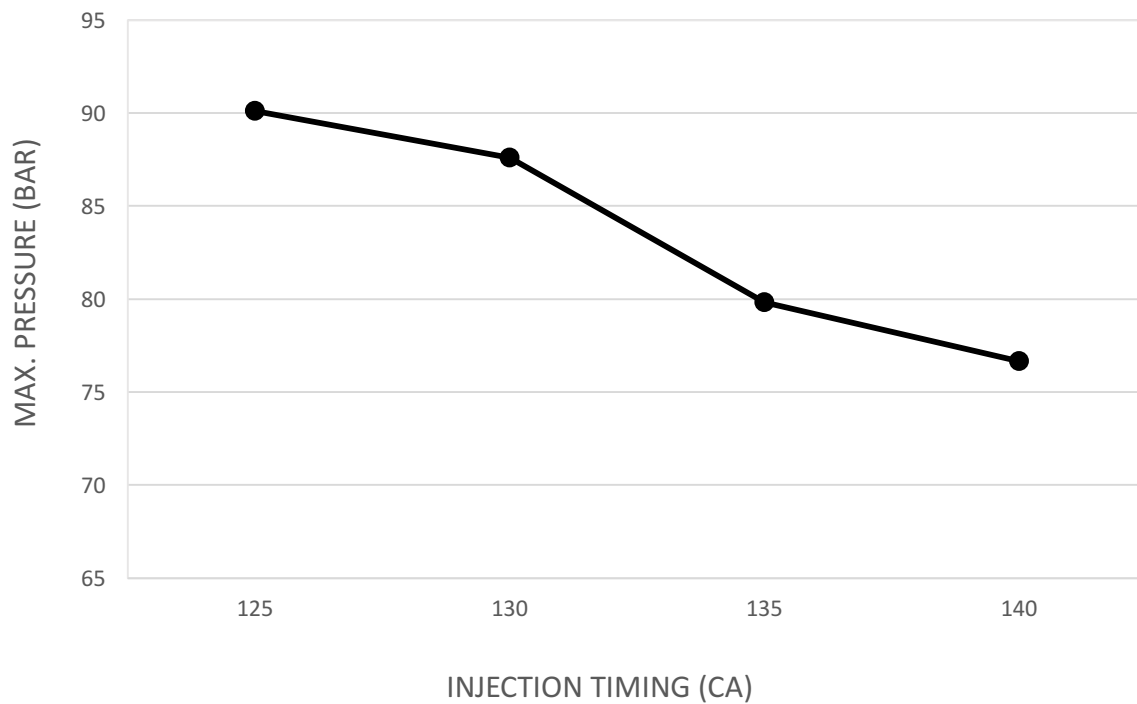


**Figure 4.4** Maximum pressure for the different second injection timings

The ignition timings for the different second injection timings are plotted in Fig. 4.5. The ignition timings are identified by the first rapid rise in temperature observed in the temperature profiles at each crank angle. To demonstrate this, temperature profiles for four different crank angles before, during and after the ignition is provided for injection timing of 125 CA and 130 CA in Figs. 4.6 and 4.7 respectively. The ignition timing for the other cases is identified in the same manner.

It is observed in Fig. 4.5 that the ignition timing does not show any significant correlation with the change in injection timing. As the second injection timing is delayed, the ignition timing does not change much with the change of injection timings nor is any other trend observed. Though, a later injection timing means the mixing time for the fuel mass in the second injection is considerably reduced, and the local equivalence ratio increases in the high reactivity zone; however, that seem to have no impact on the timing of ignition. The fuel mixture ignites when the cylinder pressure and temperature reaches a certain point regardless of the reactivity of the overall mixture. Thus, it can be concluded that for a mass split of 50/50 between the two injections, the ignition timing is not sensitive to the second injection timing. Therefore, the injection timing does not provide much control over the combustion phasing in the RCCI combustion process for a mass split of 50% between each injection.

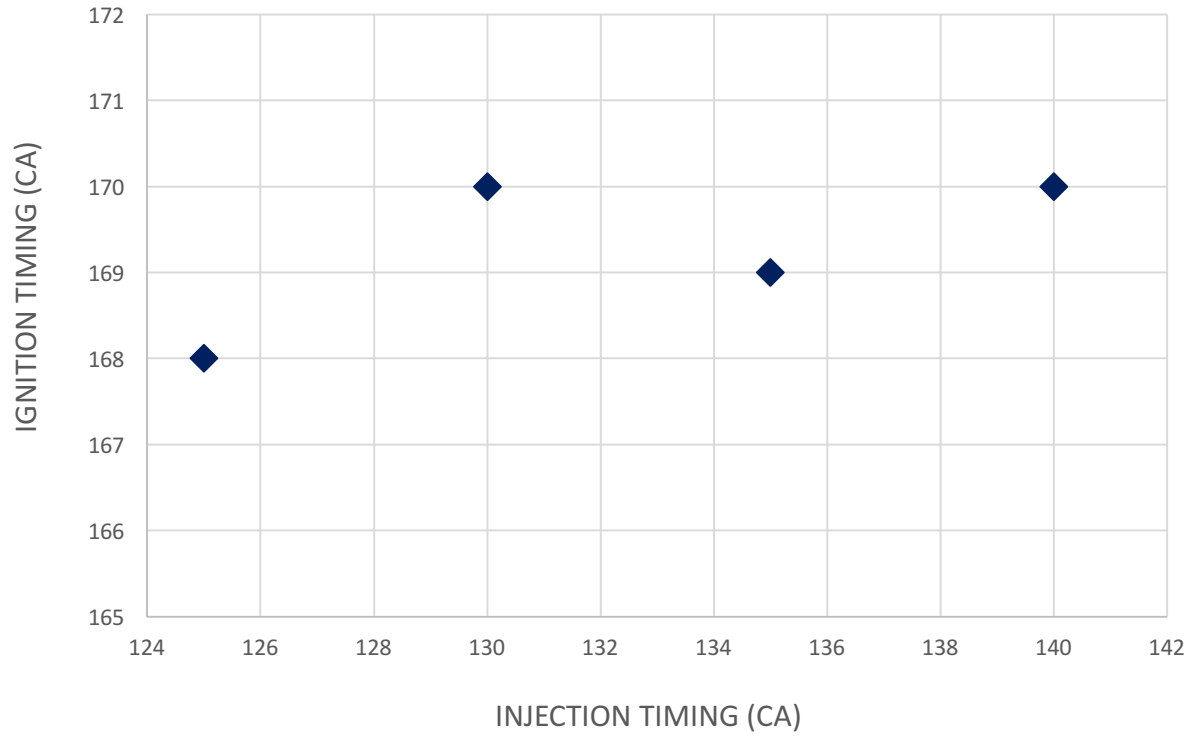


**Figure 4.5** Ignition timings for the different second injection timings

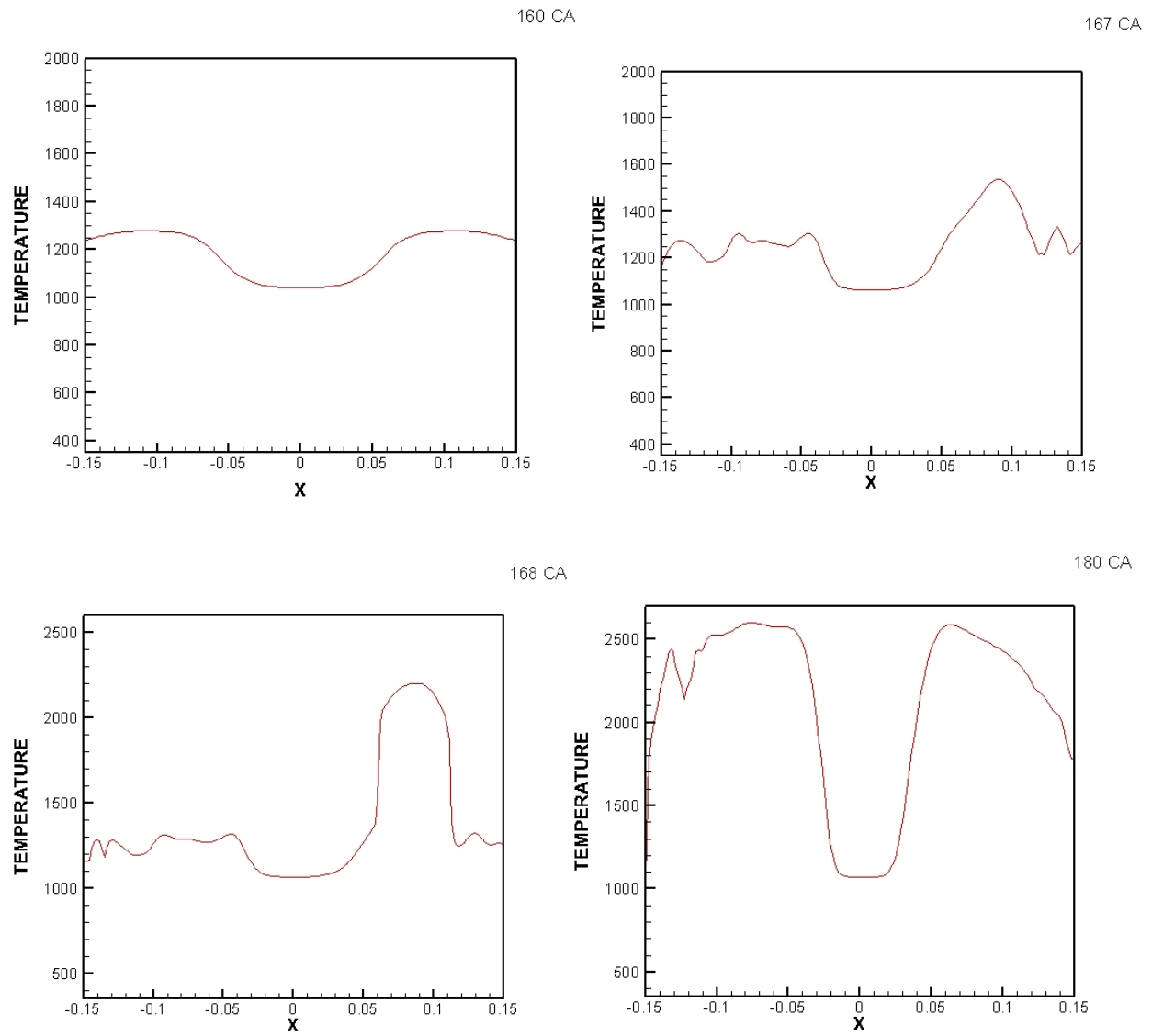
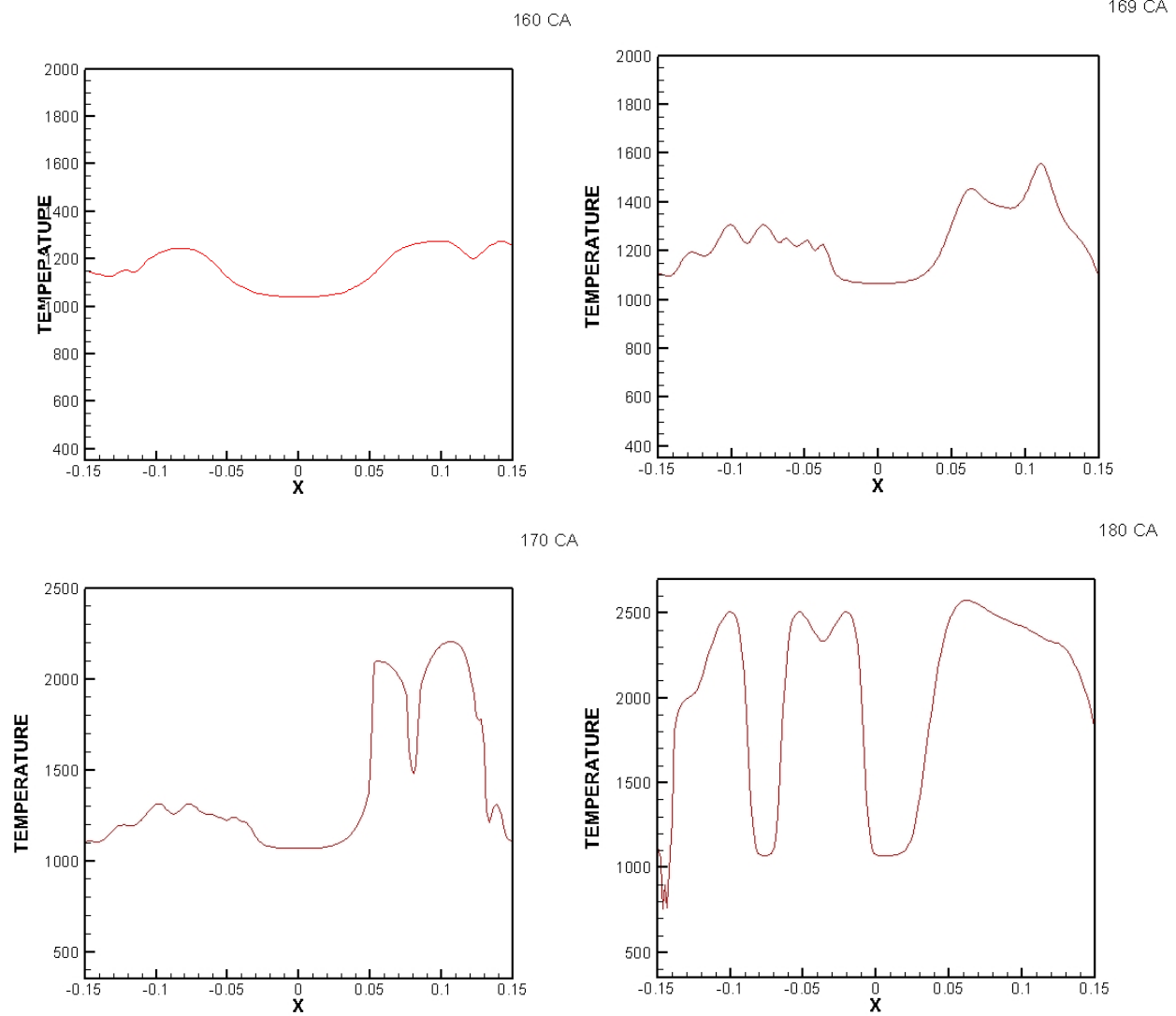


Figure 4.6 Temperature plots for different crank angles for SOI-125 CA



**Figure 4.7** Temperature plots for different crank angles for SOI-130 CA

### 4.3.2 First Injection Timing

In this section, the effect of the first injection timing in a double injection strategy for RCCI combustion is studied. Similar to the previous section, one of the injection timings is kept constant, in this case, the second injection timing at 145 CA into the compression stroke. The fuel/air ratio is kept constant for all the studied cases at 0.0669 and the ratio of direct injected fuel (i.e. n-heptane) for this study is also kept constant at 40% of the total fuel mass. For the following runs, the mass split between the two direct injections is 50% each of the total n-heptane mass injected is similar to the previous section for comparison purposes. For this study, a first injection timing sweep is made between 40 CA to 80 CA into the compression stroke. The heat release plots for the different injection timings is presented in Fig. 4.8.

From the plots for earlier injection timings that is 40 CA and 50 CA, a staged combustion process is observed unlike the later cases. An initial smaller peak for the ignition of the high reactivity zone of fuel air mixture is observed and then a larger peak owing to the ignition and combustion of the leaner pockets of fuel air mixture is observed. For the injection timings of 60 CA and 70 CA, the initial peak is not present. This is because for later injections, the mixing time is much lower, therefore the high reactivity zone of fuel contains a larger mass of fuel. The time difference between the first and second injection is much lower and does not provide enough time for mixing and creating a stratified charge. Therefore, upon ignition, a large heat release peak is observed owing to the pockets of n-heptane-highly reactive mixture. The, due to flame propagation other leaner pockets of fuel-air mixture ignites resulting in smaller peak further into the compression stroke.

For the heat release plot of injection timing of 80 CA, a series of large peaks are observed. Unlike the other cases, where the heat release for the highly reactive zone and the auto ignition of

the leaner fuel air pockets can be identified, the timing of 80 CA does not show such results. At the later injection timing, the mixing time for n-heptane with the iso-octane and air already present in the cylinder is much lower. Also, the timing difference between the first and second injection is much lower compared to the other case. Therefore, the other half of the n-heptane fuel is injected at 145 CA, the lower mixing time does not allow the formation of a stratified mixture with a gradient of local equivalence ratio from higher to lower in the axial direction instead pockets of n-heptane-rich highly reactive mixture is formed. The highly reactive n-heptane has lower resistance to auto ignition and thus instead of ignition due to flame propagation, the pockets explode with the increasing pressure and temperature due to compression. This results in the series of heat release peaks as observed in the plot for 80 CA. The effects of the series of heat release peaks can also be observed on the pressure plot provided in Fig. 4.9. The pressure rise for the injection timing of 80 CA is observed to be not so smooth compared to the other cases. This phenomenon may result in engine knocks, which produces undesirable noise and vibrations in the engine.

Also, it can be observed from the heat release plots in Fig. 4.8, that for the earlier injection timings i.e. 40 CA and 50 CA, a much higher peak of heat release is observed while at later timings, the maximum heat release peaks are much lower. This is because at earlier injection timings, the longer mixing time allows for the formation of a much more uniform mixture of fuel and air where the fuel is surrounded by the air. Thus, when ignition occurs, the flame propagation causes the more uniform mixture to combust simultaneously resulting in a higher heat release. While at later timings, the shorter mixing time may result in pockets of fuel and air, with not much uniformity. Thus, the different pockets may ignite at different times with not much uniformity resulting in a lower heat release peak. The results of this is also observed on the pressure plots presented in Fig. 4.9 where a clear trend in maximum pressure is observed. For the earlier injection timings of 40

CA and 50 CA, a much higher maximum pressure is observed than the later cases. This is because of a more uniform and staged heat release. However, for the cases of 60 CA and 70 CA, the uniformity of the heat release is less and thus the cylinder pressure rise is much lower. This is similar to the results obtained for the second injection timing where an earlier second injection resulted in higher cylinder pressure than later timings.

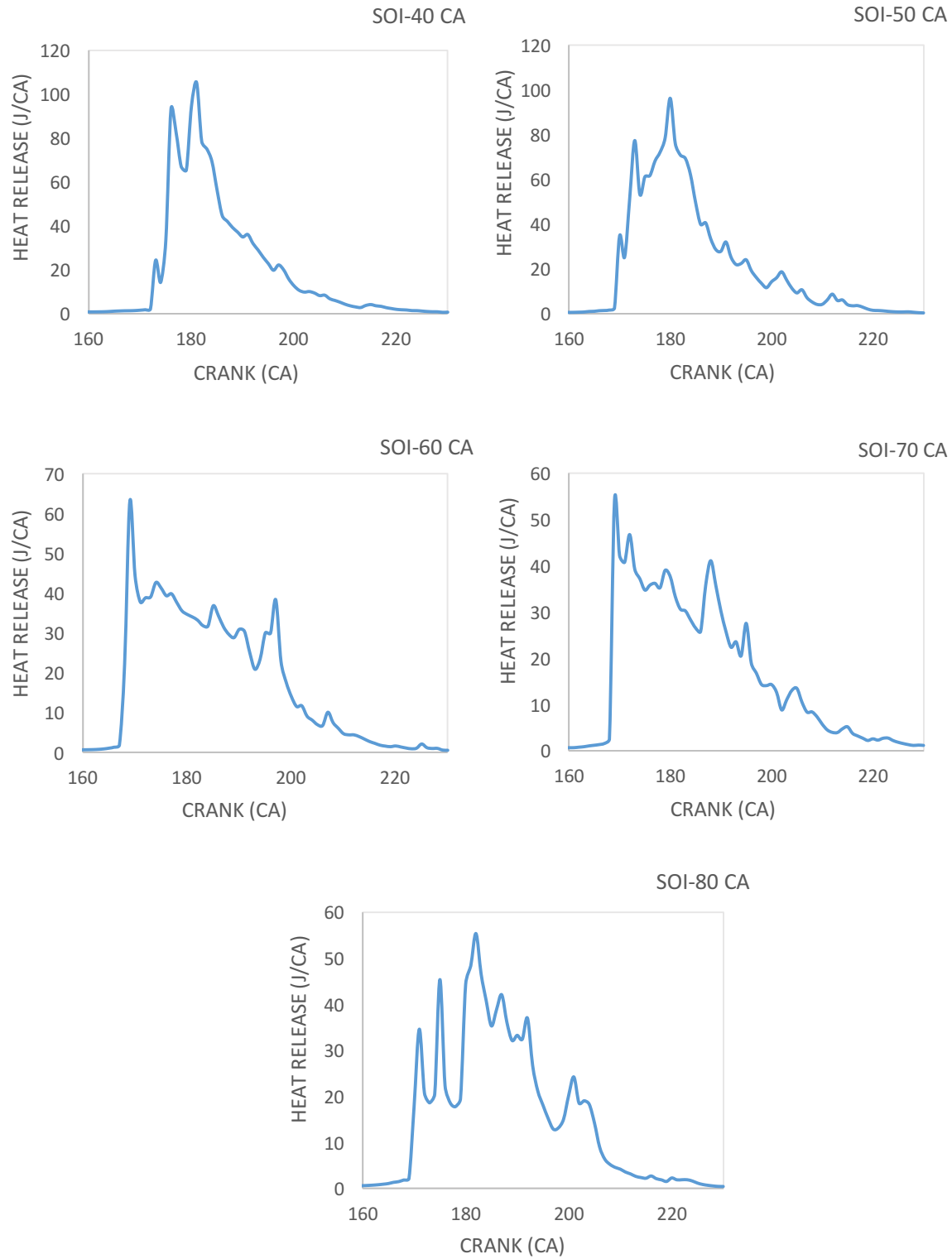


**Figure 4.8** Heat release plots for different first injection timings

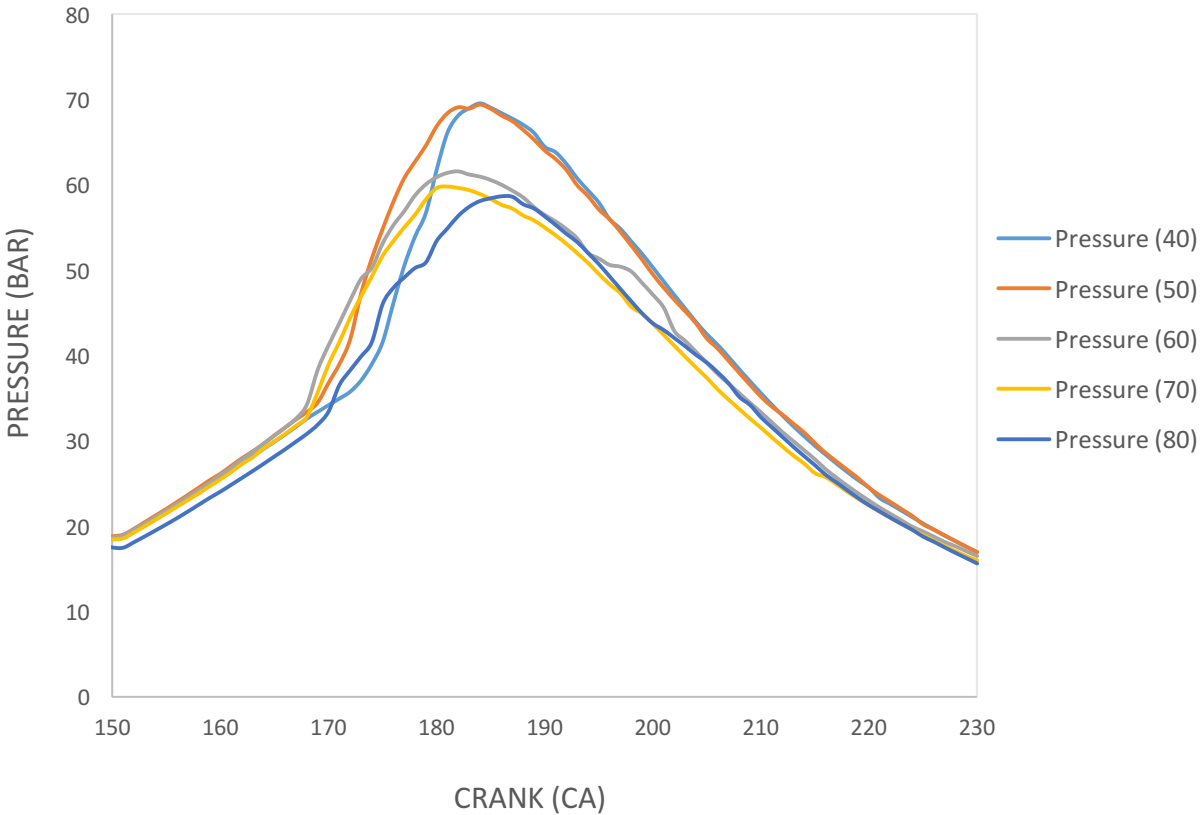


**Figure 4.9** Pressure plots for the different first injection timings

The results provided in Fig. 4.10 are for a 50/50 mass split between the two injections for n-heptane fuel. While the second injection timing is kept constant at 145 CA, a sweep of the first injection timing is made between 30 CA and 80 CA. It can be observed from the plot that there is not much trend or correlation between the ignition timings and the first injection timings. If the ignition timing for the injection at 40 CA is considered an outlier for the data set, the other timings do not follow any trend and the variation between the ignition timings is minimal.

The first injection of n-heptane is responsible for increasing the reactivity of the pre-existing mixture of iso-octane and air and the injection timing determines the mixing time before second injection occurs. However, with a mass split of 50% between the injection, the mass of fuel injected in the first injection does not change the initial reactivity of the mixture to make a

difference for the ignition timing. The change in mixing time with the change in injection timing does not result in the overall change in reactivity before ignition. Thus, the ignition is occurring in the same range for all the timings due to the rise in pressure and temperature due to compression. It can be inferred from the plot that with a mass split of 50% between the two injections, the change in the first injection timing does not provide much control over the ignition timing and combustion phasing.

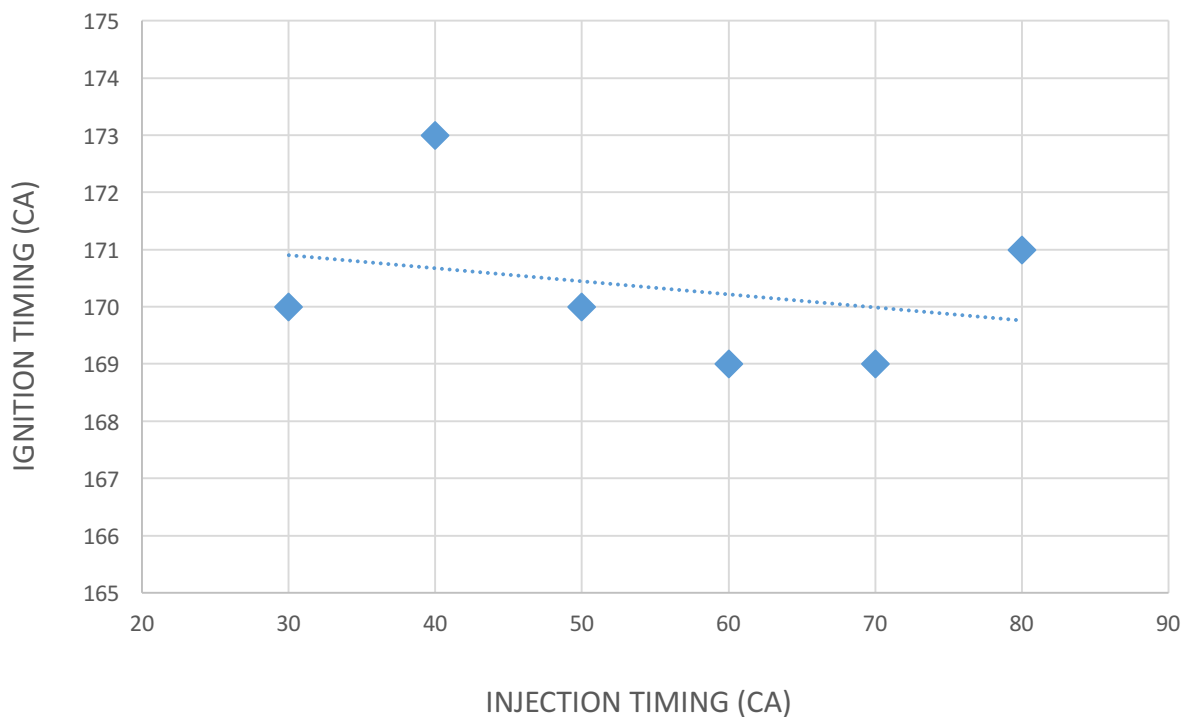


**Figure 4.10** Ignition timings for the different first injection timings

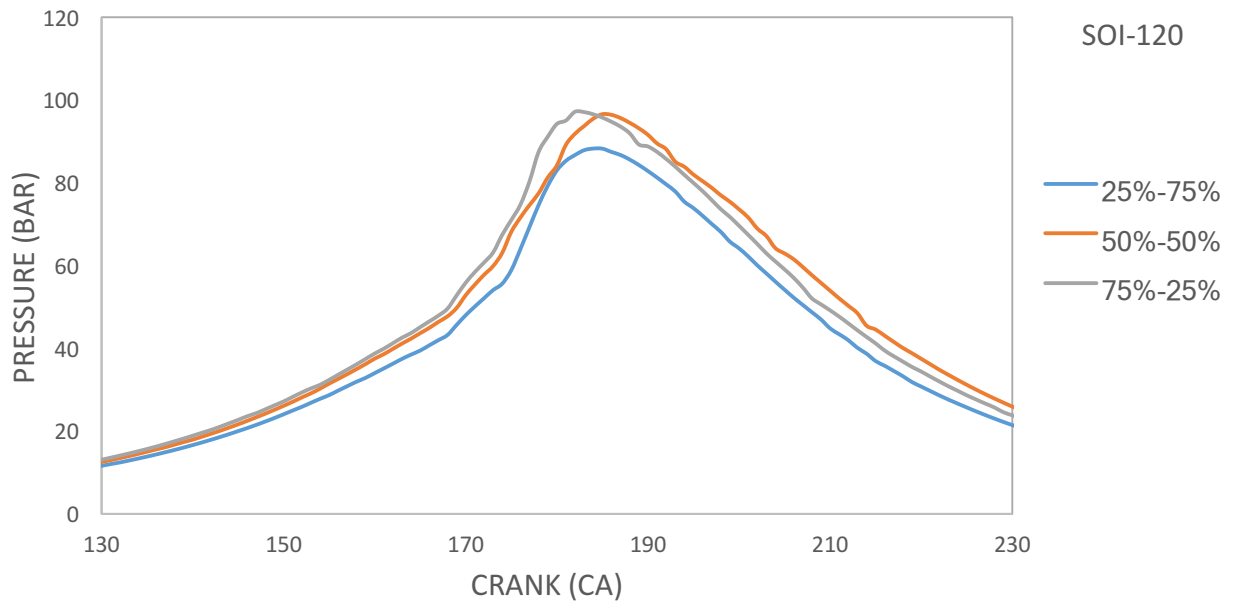
### 4.3.3 Effect of second injection timing for different mass splits

In the previous section 4.3.1, all the findings were based on a mass split of 50%-50% between the two injections of n-heptane fuel. This motivates considerations of other mass splits between the two injections and their impact on the combustion parameters. For this section the first injection timing is kept constant at 40 CA while a sweep of the second injection timing is

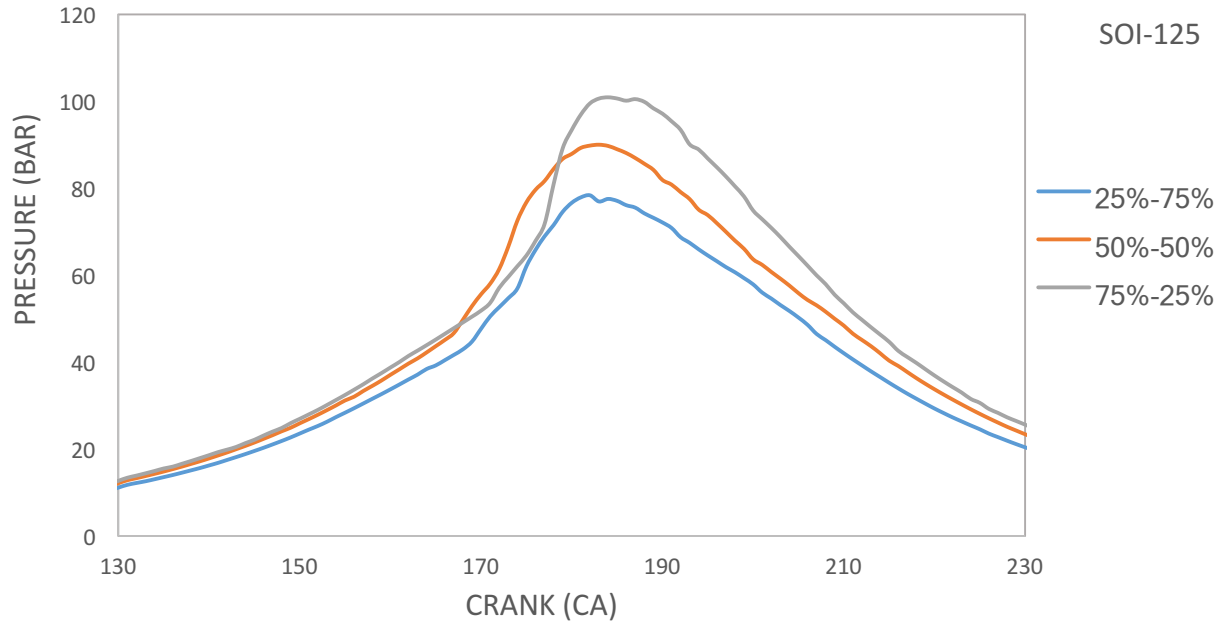
made between 120 CA and 140 CA. For each second injection timing, three cases of mass split of the n-heptane fuel are considered, which are 25%-75%, 50%-50%, and 75%-25% between the two injections respectively.

Figure 4.11 shows the change of cylinder pressure with crank angle for all three cases of mass split at a second injection timing of 120 CA. It is observed that with a higher mass percentage of n-heptane in the first injection that is the case for 75%-25%, the cylinder pressure is observed to increase from the case for 25%-75%. The iso-octane is injected as port fuel and is assumed to form a homogeneous mixture with air before the start of the compression stroke. The higher reactivity n-heptane fuel injected allows the formation of a stratified charge in the cylinder. When the mass of the n-heptane fuel is split between the first and second injection, a higher mass in the first injection allows the n-heptane to form a much more uniform mixture because of the higher mixing time. The smaller percentage of mass injected in the second injection forms the high reactivity zone acting as a source of ignition. The uniformity of the mixture with the higher mixing time, results in a much higher pressure. However, for the case of 25%-75% mass split, higher percentage of the n-heptane is injected in to the cylinder during the second injection that is at 120 CA, therefore, much less time for mixing than the other case. This results in less uniformity in the mixture and a lower resulting pressure.

A similar trend is observed for other second injection timing of 125 CA and 135 CA with a fixed first injection timing of 40 CA. With a higher mass percentage of n-heptane in the first injection, a more homogeneous mixture results in a much higher cylinder pressure than the cases where a higher mass percentage of n-heptane is injected in the second injection. The pressure plots for the different mass percentages of n-heptane at the injection timings of 125 CA, and 135 CA are provided in Figs. 4.12 and 4.13, respectively.



**Figure 4.11** Pressure plots for different mass splits for SOI-120 CA



**Figure 4.12** Pressure plots for different mass splits for SOI-125 CA

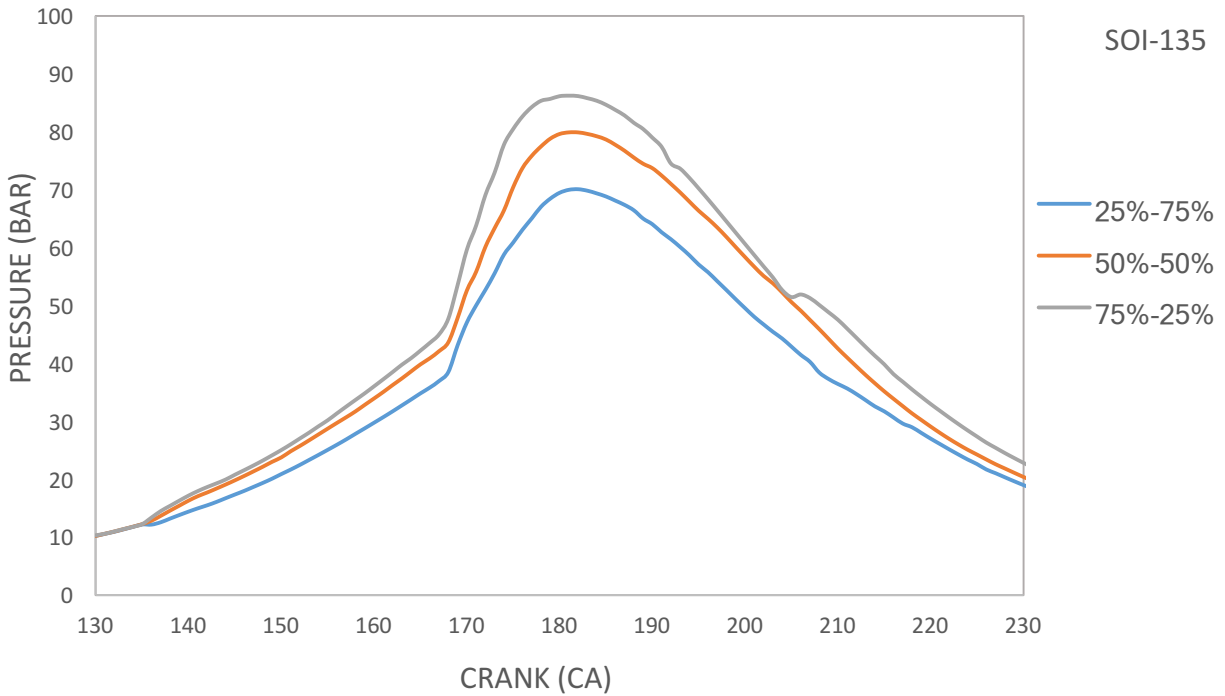


**Figure 4.13** Pressure plots for different mass splits for SOI-135 CA

Figure 4.14 shows the maximum in-cylinder pressure for the different second injection timings between 120 CA and 140 CA into compression stroke and first injection n-heptane mass percentages. The first observation is that at each mass percentage, the maximum cylinder pressure obtained decreases with the delay of the second injection timing. This is because irrespective of the mass split, a later injection means a lower mixing time for the n-heptane fuel injected and thus a less uniform mixture is obtained resulting in lower maximum cylinder pressure. The second observation is that for each injection timing, with increase in first injection mass percentage, the maximum pressure is observed to increase. This is because, a higher mass of n-heptane in the first injection means that it is injected at 40 CA into the compression stroke. This provides enough time for a higher mass of n-heptane to mix with the pre-existing iso-octane and air in the cylinder. A better uniform mixture of n-heptane, iso-octane and air results in a much higher pressure.

However, it is observed that the sensitivity of this increase in pressure with first injection mass percentage depends on the second injection timings. At a lower second injection timing that is 120 CA, the rise in maximum pressure with mass percentage is low compared to the other cases. The reason behind this is that 120 CA is still an earlier timing for injection than the other cases and provides more time for the n-heptane to mix with the iso-octane and air. Therefore, the sensitivity for the pressure rise with mass percentage is less. For the later injection timing cases for example 140 CA, the sensitivity is much higher as the later injection considerably effects the mixing time and a less mass in the second injection would result in a much higher pressure.

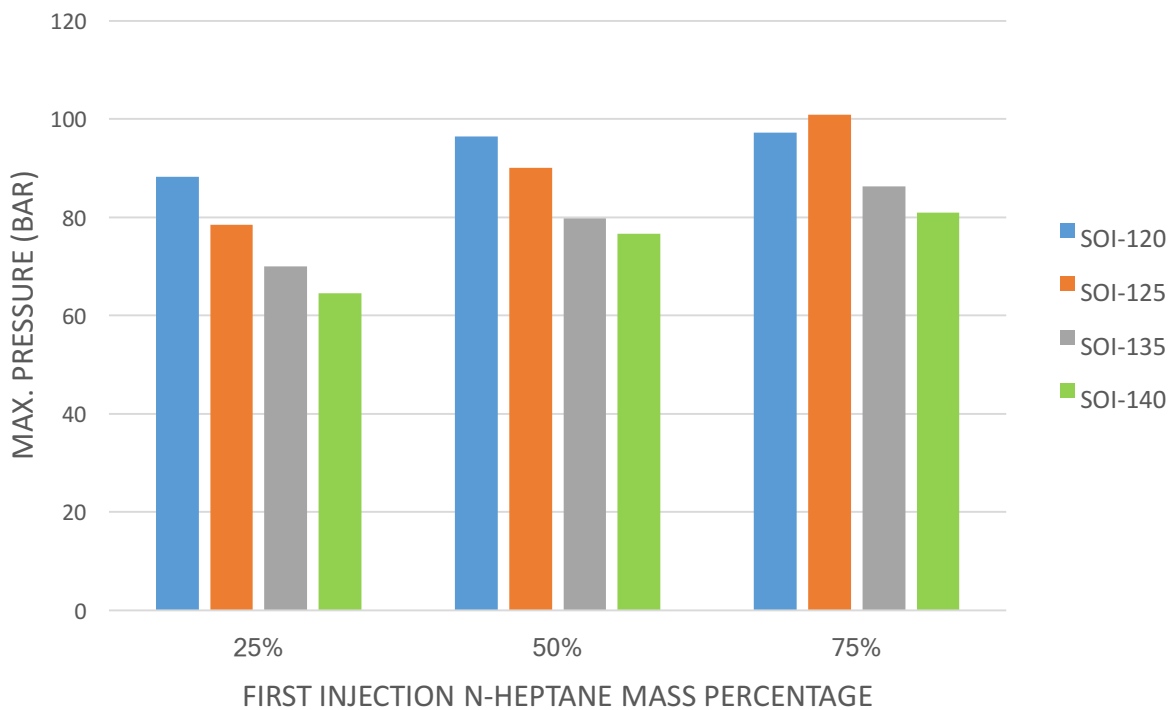


**Figure 4.14** Maximum pressure for different n-heptane mass percentages in first injection

Figure 4.15 shows the heat release plot for the different mass split percentages between the two injections for a second injection timing of 120 CA. The RCCI combustion process is characterized by a staged heat release process. An initial heat release due to the ignition of the rich zone towards the top of the cylinder and auto ignition of the leaner pockets of fuel air mixture due to flame propagation.

For the cases of 50% and 75% of the n-heptane mass in the first injection, a much higher initial heat release is observed. This is due to the fact that a higher mass percentage in the first injection at 40 CA into the compression stroke means more of the n-heptane fuel have a higher mixing time close to a homogeneous mixture resulting in a higher heat release when ignition occurs. For the same reason, higher peaks are observed due to auto ignition of the leaner zones also than the case for only 25% of the mass in the first injection. For the case of 25% of the n-heptane mass in the first injection, most of the heat is observed to be released in bulk in a short period of time than a staged manner. This may result in higher cylinder temperature during that time and, which may result in higher production of NO<sub>x</sub>. Similar phenomenon is observed for the injection timing of 125 CA as presented in Fig. 4.16.

However, for the heat release plots presented in Fig. 4.17 for the injection timing of 135 CA, it is seen that the initial heat release peak as observed for the other timings is absent. This is because, regardless of the mass split percentage, the later injection timing does not provide much mixing time and the mass injected in the second injection does not get sufficient time to mix with the iso-octane and n-heptane. Therefore, instead of a staged process, most of the heat is released in a very short time when the ignition occurs.

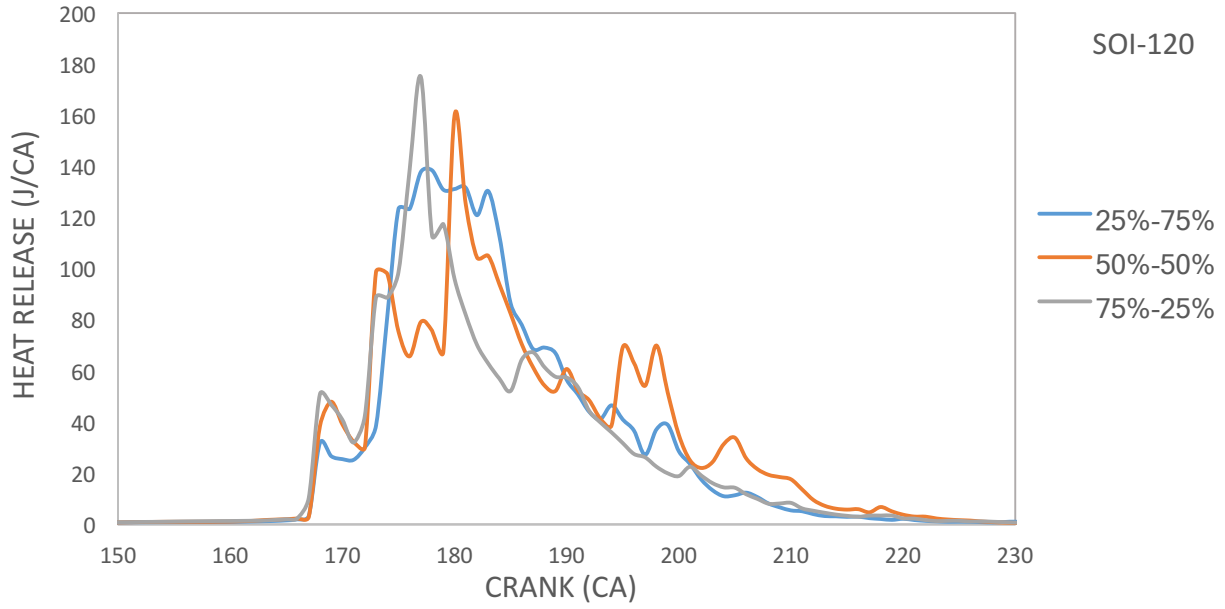


Figure 4.15 Heat release plots for different mass splits for SOI-120 CA

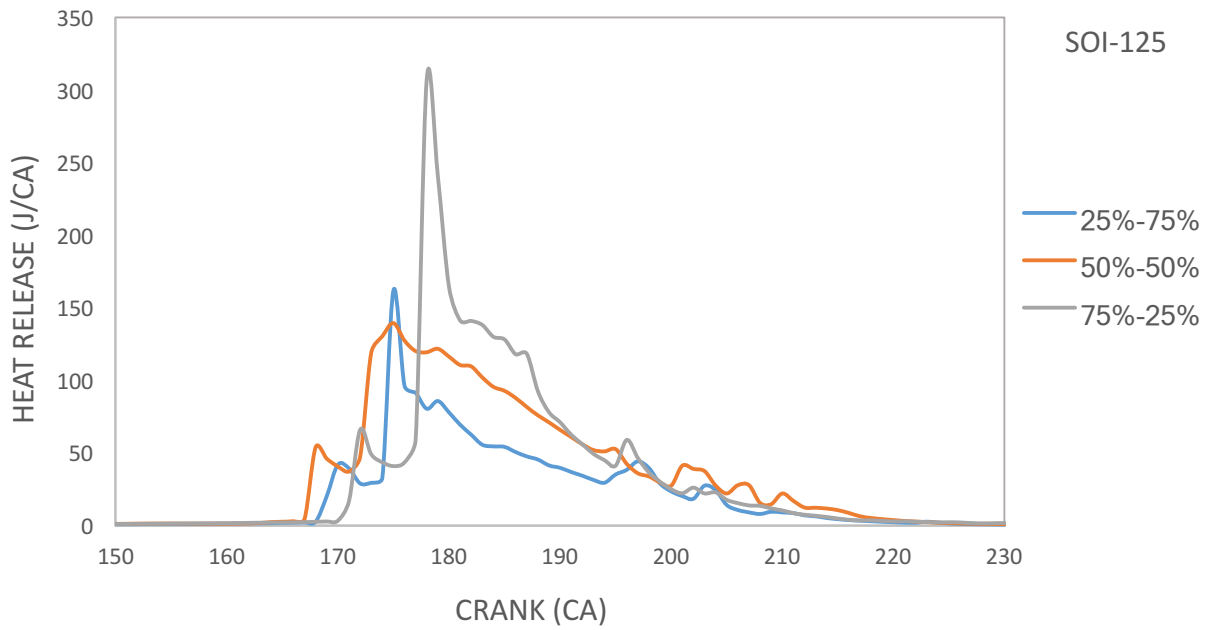
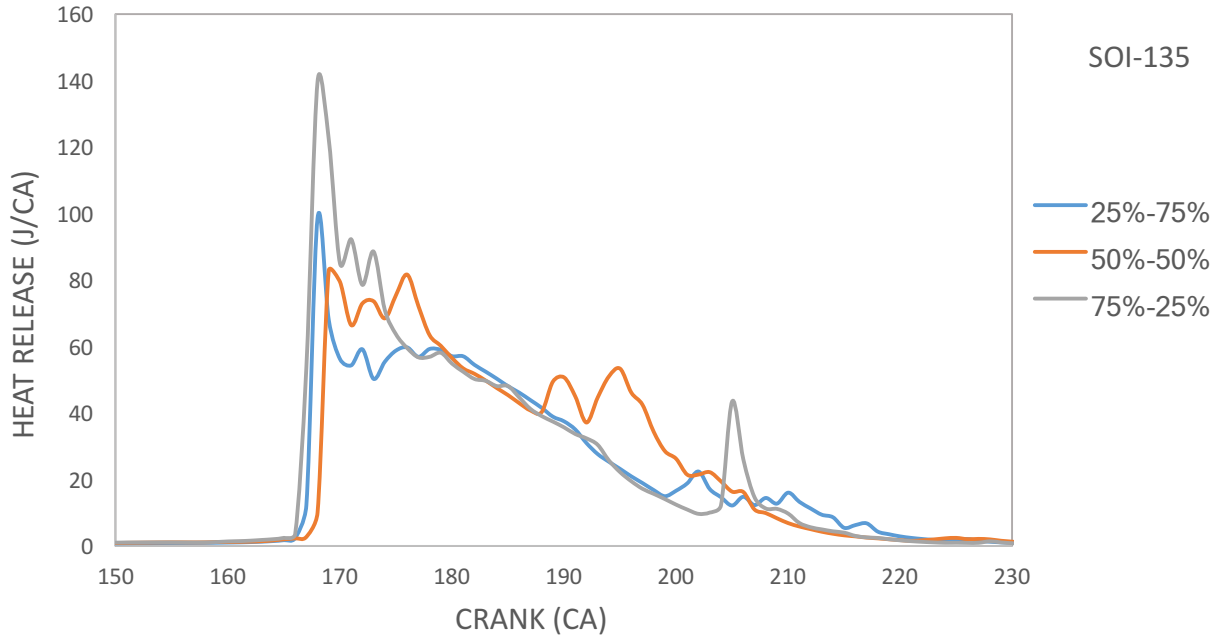


Figure 4.16 Heat release plots for different mass splits for SOI-125 CA



**Figure 4.17** Heat release plots for different mass splits for SOI-135 CA

Figure 4.18 shows the change of the ignition timings with the second injection timing for the different mass split percentages. For the cases of mass percentages of 25% and 50% of the total n-heptane mass in the first injection, it is observed that the ignition timings do not vary that significantly with the delay of the injection timings. Though with the delay of the injection time significantly effects the mixing time, but that seems to not have an effect on the ignition timing for the different cases for mass split considered. The ignition is the result of the increase in pressure and temperature due to compression rather than the reactivity of the mixture. Therefore, it can be concluded that for the cases studied with 25% and 50% of the n-heptane mass in the first injection, do not provide much control over ignition and combustion phasing.

However, for the case of 75% of the n-heptane mass in the first injection, a trend is observed where the ignition timing is delayed with advance in injection timing. Further studies can be conducted to investigate the relationship between injection timing and ignition timing for 75%-25% mass split of n-heptane between the two injections. Similarly, Reitz et al. [19] showed

for a mass split of 73% of total fuel to be gasoline, the injection timing advances for delay in both first and second injection timings.

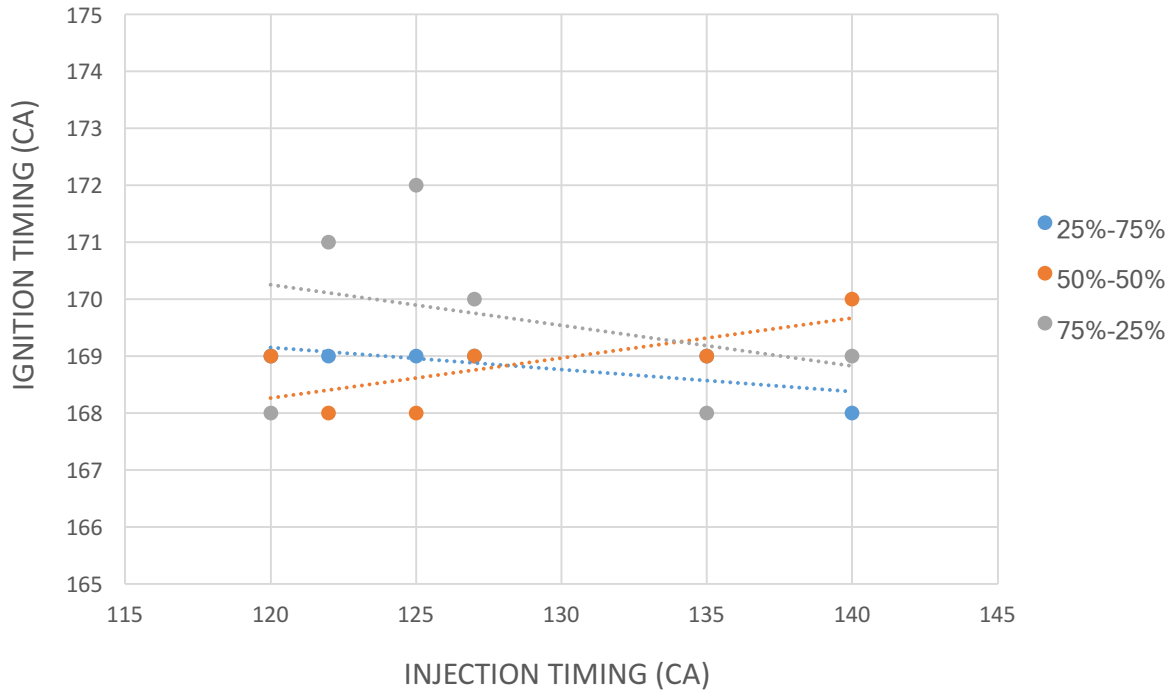
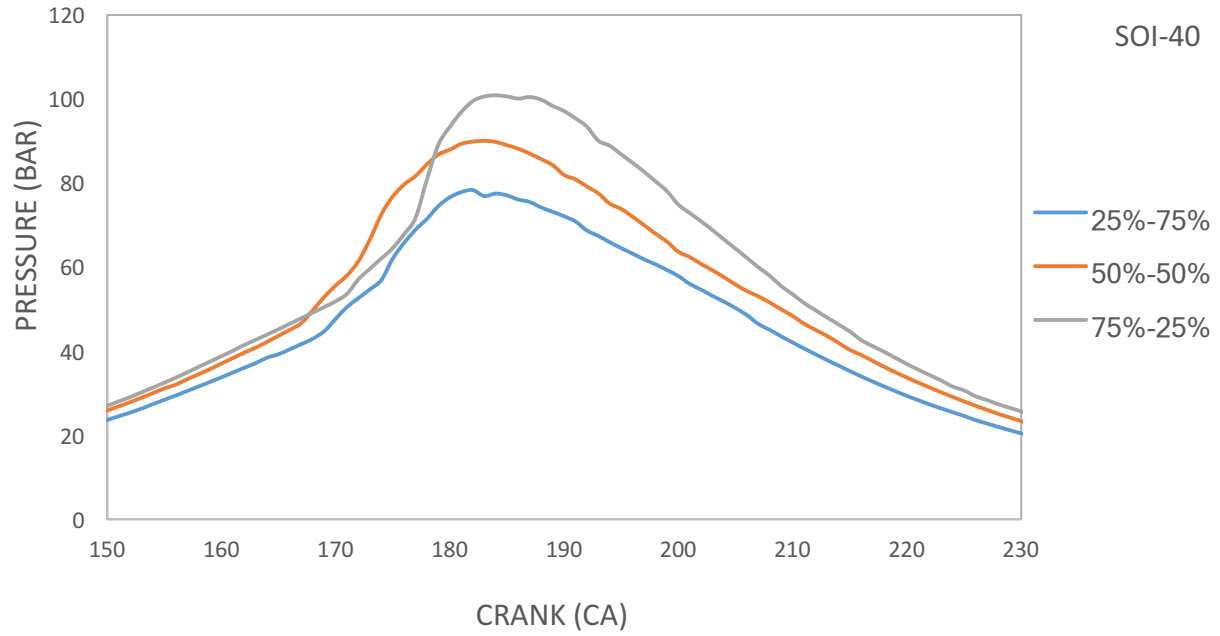


**Figure 4.18** Ignition timings for the different injection timings

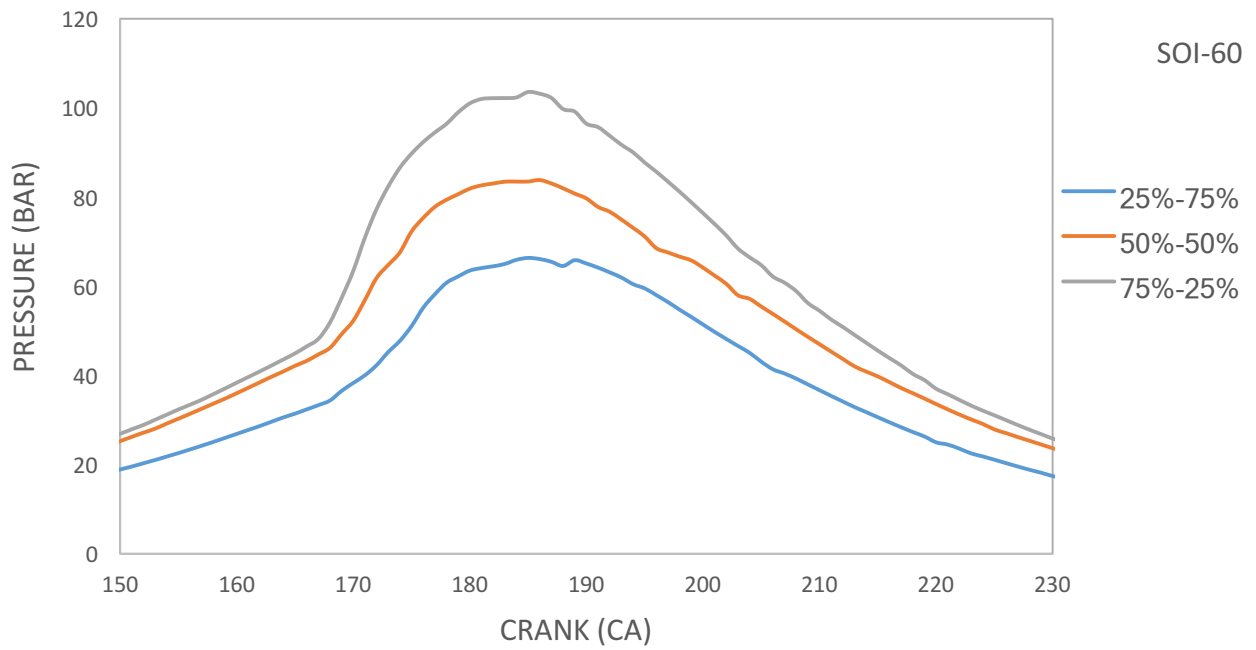
#### 4.3.4 Effect of first injection timing for different mass splits

In this section, the first injection timing is changes and the effects on the combustion parameters are studied for the different mass split between the two injections. The second injection is fixed at 125 CA into the compression stroke for all the cases. The F/A ratio is kept constant at 0.0669 and the premixed ratio also is fixed at 0.6 for the study. Three different cases for mass split is considered, which are 25%-75%, 50%-50% and 75%-25% of the total mass of n-heptane between the two injections respectively.

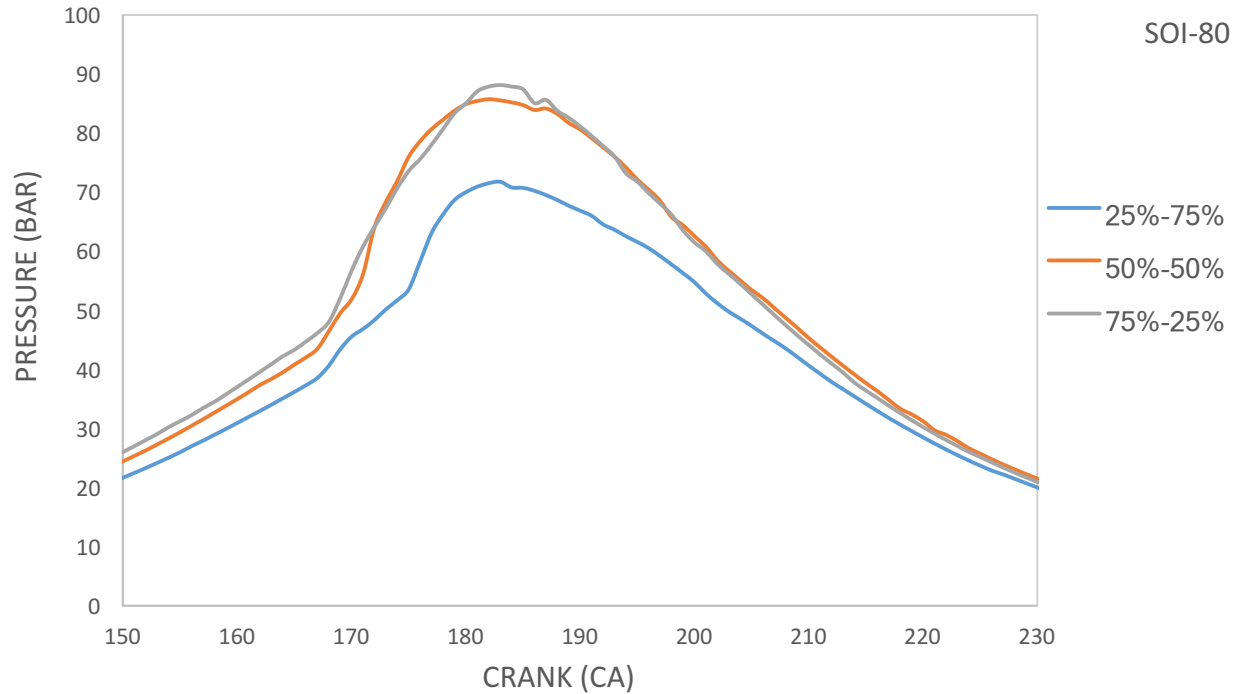
Figure 4.19 shows the change in cylinder pressure for the three mass split percentages for the first injection timing of 40 CA. It is observed from the plots that the pressure rises with the increase in the percentage of mass in the first injection. Similar to the cases for the change in second timing presented in the last section, the rise in pressure is related to the larger portion of the mass being injected at an earlier timing. When the larger portion of mass of n-heptane is injected at an earlier timing in the compression stroke, the mixing time is significantly longer, which results in a much more uniform mixture. Therefore, results in a higher cylinder pressure rise. Similar results are obtained for the first injection timing of 60 CA and 80 CA as observed in Figs. 4.20 and 4.21, respectively.



**Figure 4.19** Pressure plots for different mass splits for SOI-40

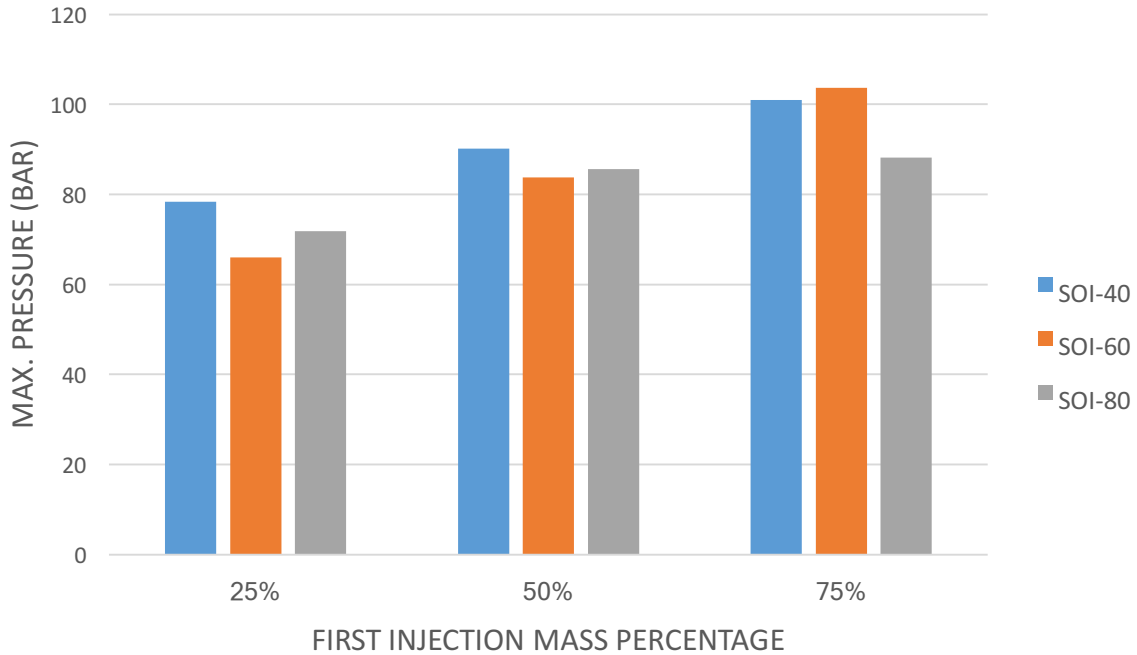


**Figure 4.20** Pressure plots for different mass splits for SOI-60



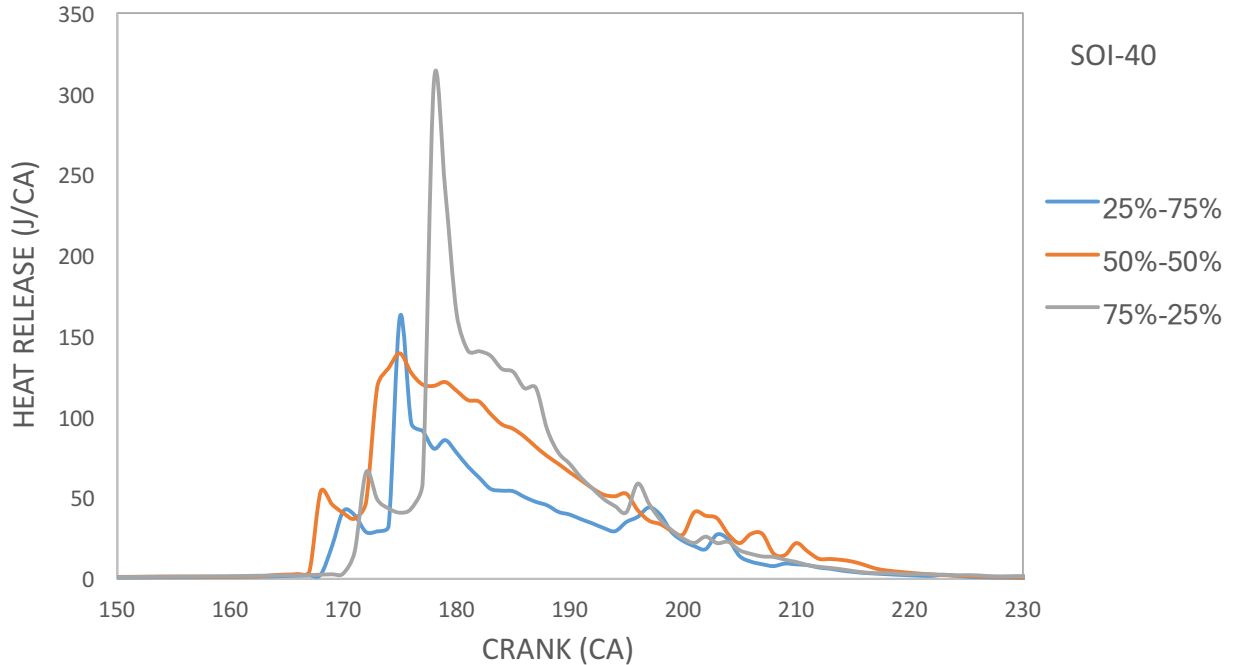
**Figure 4.21** Pressure plots for different mass splits for SOI-80

Figure 4.22 shows the maximum cylinder pressure for the different first injection mass percentage at different first injection timings. It is observed from the figure that as the mass percentage of the n-heptane fuel in the first injection increases, the maximum pressure obtained increases correspondingly. This is a direct consequence of firstly, the mixing time and secondly, the proportion of the n-heptane fuel in the first injection. Therefore, for every n-heptane mass percentage, the pressure decrease with delay of the injection timing, since the mixing time decreases therefore, the mixture lacks uniformity. Also, for every injection timing, the pressure increases with the mass fraction of the n-heptane fuel in the first injection. This is because higher the proportion of n-heptane in the first injection, the higher is the time for it to mix with the pre-existing iso-octane and n-heptane. Therefore, a much more homogeneous mixture is produced, which results in a higher pressure.



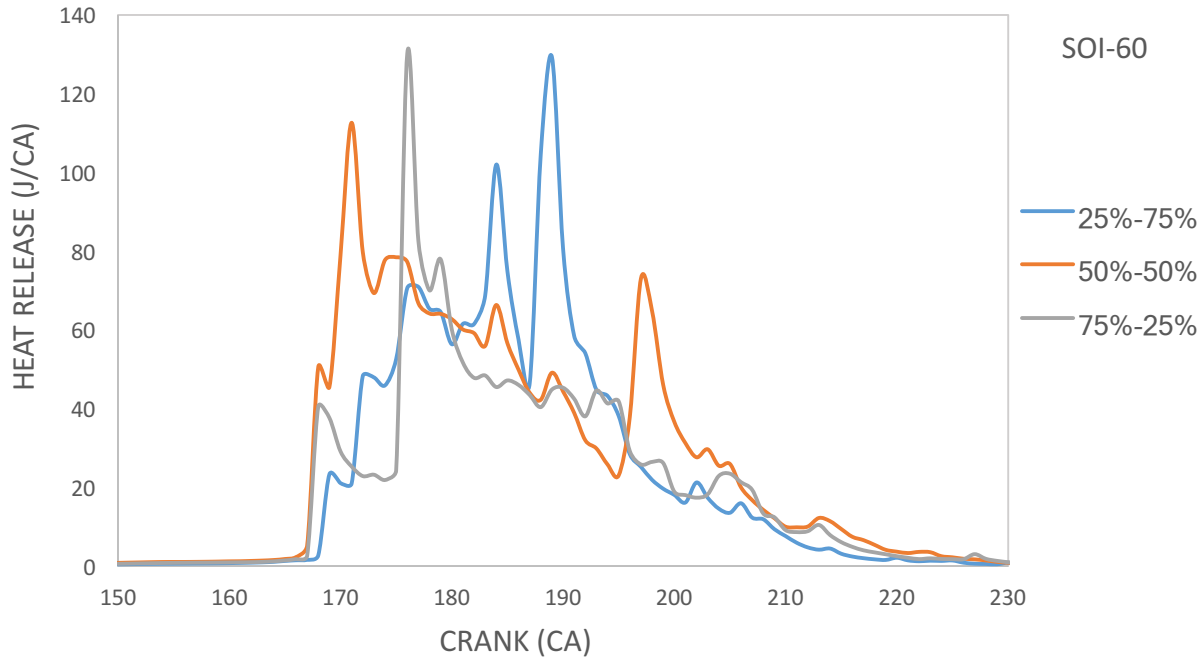
**Figure 4.22** Maximum pressure for different first injection mass percentage

Figure 4.23 shows the heat release plots for the different mass percentages between injections for the first injection timing of 40 CA. A RCCI characteristic staged heat release is observed for all the cases. An initial peak for the combustion of the high reactivity zone close to the top of the cylinder is observed. Then auto ignition of the low reactivity zone due to flame propagation is noticed.



**Figure 4.23** Heat release plots for different mass splits for SOI-40

For the case of the first injection timing at 60 CA in Fig. 4.24, considerable difference in the heat release is observed from the previous case (Fig. 4.23). When 75% of the mass of the total n-heptane mass is injected in the second injection, the heat release is seen to occur in pulses. This is because since most of the mass is injected at a later timing, the mixing time is much lower. Therefore, the mixture lacks uniformity and forms pockets of n-heptane-rich mixture. These pockets combust as the flame propagates and results in these consecutive heat release peaks.



**Figure 4.24** Heat release plots for different mass splits for SOI-60

Figure 4.25 shows the heat release plots show that at higher mass percentages in the first injection, the initial heat release is much higher. This is mainly because of the longer mixture time, which results in a more homogeneous mixture. Therefore, instead of ignition in just the rich zone, an explosion occurs releasing more heat.

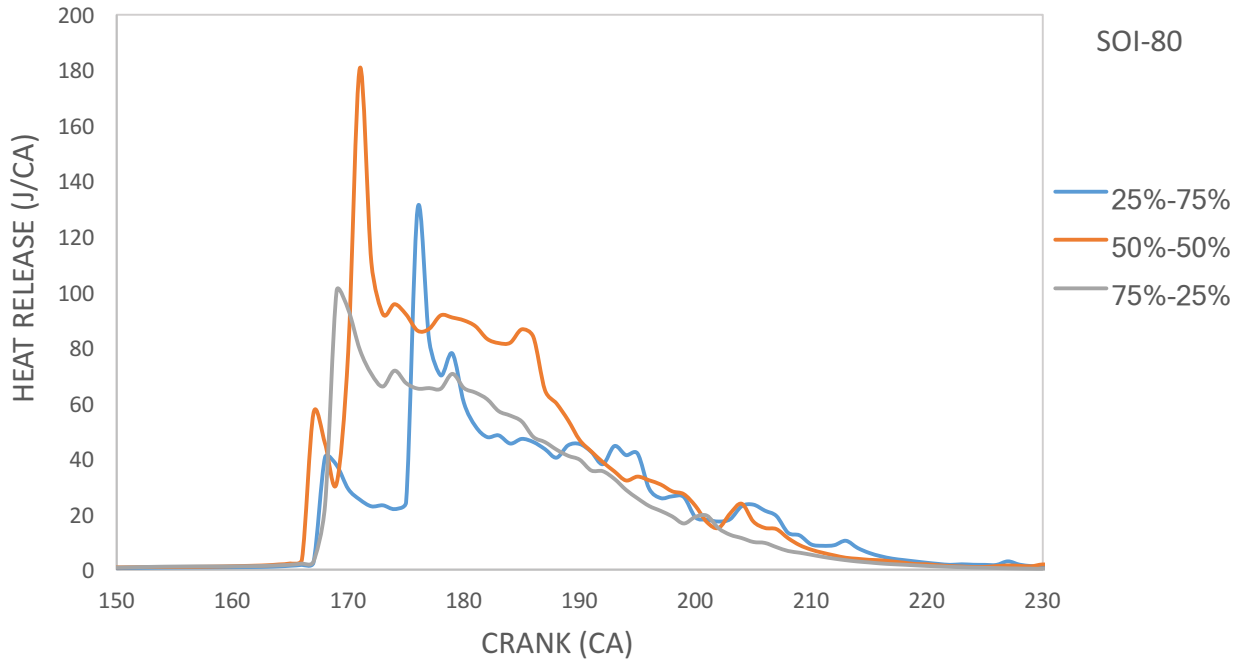


**Figure 4.25** Heat release plots for different mass splits for SOI-80

Figure 4.26 shows the ignition timing for different injection timings and different mass percentages of n-heptane fuel between the two injections. For the mass percentages of 25% and 50% in the first injection, not much change is observed in ignition timings with the injection timings. This is because a large portion of the n-heptane fuel is being injected during the second injection, which is kept fixed at 125 CA. Therefore, with the change of the first injection timing, not much change occurs in reactivity of the mixture. However, the plot for the 75%-25% mass distribution, shows that the ignition timing advances significantly with the delay of the first injection timing. This is a consequence of the change in the mixture reactivity. Since a large proportion the n-heptane is injected earlier during the first injection, a change in the timing, changes the mixture reactivity. Retarding the injection from 40 CA to 60 CA, decreases the mixing time and thus a more reactive mixture is produced with a higher local equivalence ratio, which, makes it prone to ignition. Thus, with delay of injection timing from 40 CA to 60 CA, the ignition timing advances. Therefore, it can be concluded that for a mass split of 75%-25% between the two

injections, the injection timing does provide some control over the combustion phasing, however, for the other cases, no such control is observed.

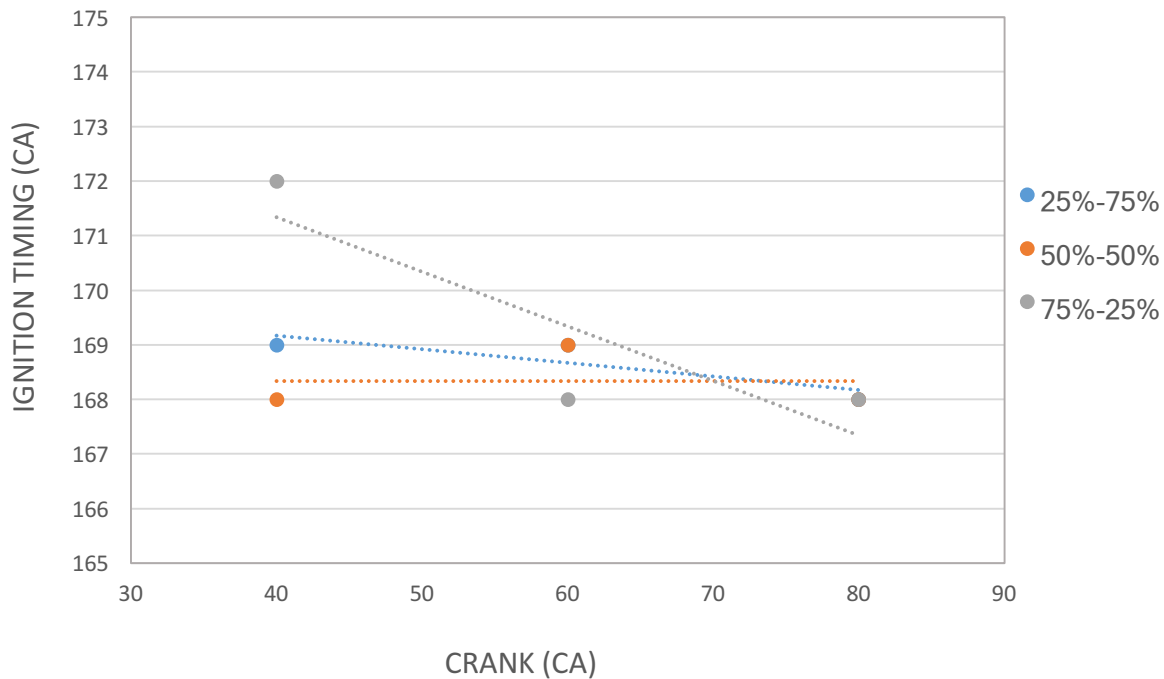


**Figure 4.26** Ignition timing for different injection timings for different mass splits

#### 4.4 Conclusions

The following conclusions can be drawn from the study of the double injection strategy for RCCI combustion process-

1. For the double injection strategy, an advanced second injection timing has shown more uniform heat release compared to a delayed timing. This is beneficial as a lower cylinder temperature rise will occur due to the uniform heat release, which will possibly lead to lower NO<sub>x</sub> production.
2. Higher maximum pressure is achieved with an earlier second injection timing, and also, a smoother pressure rise is observed. For the delayed injection cases, a rapid rise in pressure

is observed, which is a precursor for engine knocking, an undesirable outcome of these injection scenarios.

3. No noticeable relationship is found between the ignition timing and the injection timing and the ignition timing remains fairly constant for all the studied cases for a mass split of 50/50 between the two injections.
4. For the first injection timing sweep, the advanced timings showed uniform heat release and pressure rise. For the case of first injection timing 80 CA, successive heat release peaks are observed which indicates to engine knocking. Therefore, the earlier timings are more suitable for RCCI combustion.
5. Similar to the investigation for the second injection timing sweep, no visible trend is observed for the ignition timing with the first injection timings. Regardless of the injection timing, the ignition seems to occur within a small timing range.
6. For the second injection timing sweep for different n-heptane mass splits between injections, the maximum pressure is achieved for 75% of the total mass of n-heptane injected in the first injection. And the pressure drops as the mass percentage of n-heptane decreases in the first injection for all the second injection timings.
7. No combustion phasing control is observed for the second injection timing sweep with 25% and 50% of the n-heptane mass in the first injection. However, for the case of 75% mass in the first injection, as the injection timing is delayed from 120 CA to 135 CA, the ignition timing is observed to delay and then advance.
8. Similar to the second injection timing sweep, the maximum cylinder pressure is observed for 75% of the n-heptane mass in the first injection regardless of the first injection timing.

However, as the first injection timing is delayed, the sensitivity of the pressure drop is much lower compared to the second injection sweep.

9. For the mass splits of 25% and 50% of n-heptane mass in the first injection, no change in ignition timing is observed for the second injection timing sweep. However, the ignition timing significantly advances with the delay of injection timing from 40 CA to 60 CA into the compression stroke for the case of 75% of the mass in the first injection.

## CHAPTER-5

### SUMMARY AND FUTURE WORK

#### 5.1 Summary

In this study, a stand-alone ODT model is employed to investigate the combustion characteristics of RCCI technique using different strategies. Iso-octane and n-heptane is used as surrogates for gasoline and diesel respectively in this investigation. The iso-octane is injected as the port fuel and the n-heptane is directly injected into the cylinder in single or multiple injections during the compression stroke.

In the first part of the study, the single injection strategy has been investigated. For an equivalence ratio of  $\phi=0.3$ , the injection timing has been changed between 40 CA to 120 CA into the compression ratio and its effects on combustion characteristics is investigated. Then, the equivalence ratio is changed to  $\phi=0.5$ , and the runs are repeated for injection timings 40 CA to 100 CA. A comparative study is presented between the two cases. Finally, a change in the premixed ratio and its effect on RCCI process is shown. In the second part, the double injection strategy is investigated for RCCI process. The first two sections look into the effects of the second and first injection timings between 125-140 CA and 40-80 CA respectively. The latter two sections investigate the effects of different mass splits of n-heptane between the two injections.

In the study using single injection strategy, the later injection timings are observed to release heat more uniformly than the earlier timings, this can act as a deterrent to NO<sub>x</sub> since lower temperature rise will occur in the cylinder. The single injection strategy showed great potential in controlling ignition for both the equivalence ratio,  $\phi=0.3$  and  $\phi=0.5$ . As the injection timing was delayed, the ignition timing is seen to advance. Also, the equivalence ratio and premixed ratio is seen to effect the ignition delay. A higher equivalence ratio caused a delay in the ignition. Also, in

the study for the range of PR 50-90%, a higher premixed ratio resulted in a later ignition compared to lower ratios.

For the study of the double injection strategy, the earlier second injection timings showed more uniform heat release and higher pressure. However, the change in second injection timings showed no control over ignition and combustion phasing. For the first injection timing, later cases like 80 CA showed high heat release in multiple peaks which may be a precursor to engine knocking. Considering heat release and pressure rise, the earlier first injection timings are more suitable for the RCCI operation. However, no combustion phasing control was observed with first injection timing change for a 50/50 mass split between injections. When the mass split of n-heptane was changed to 75% of the total n-heptane mass in the first injection, the process showed more control over the ignition timing for both first and second injection timing sweeps.

## **5.2 Future Work**

A few of the possible directions this work can be extended are-

1. All the studied cases in this investigation is based on one realization, which can be used to understand the phenomenon and explain the trends. However, multiple realizations can be made to understand the cycle-to-cycle variation for each case studied.
2. One of the major advantages of RCCI combustion process over HCCI is that it produces lower NO<sub>x</sub> and soot. A Zel'dovich mechanism for thermal NO<sub>x</sub> and a mechanism for soot production can be incorporated in to the model for prediction of NO<sub>x</sub> and soot production and comparison between the cases.

3. While the study was concerned with understanding the RCCI combustion process and explaining the different trends, the ODT model can be employed to find the optimum points for RCCI operation under different engine operating parameters.
  
4. In this study, iso-octane and n-heptane is used as the port fuel and directly injected fuel. The ODT model can be used to study other combinations of fuel as discussed in Section 1.2, for example a combination of gasoline and ethanol and studying the effect of different percentages of ethanol mixed with gasoline. Also, the single fuel strategy can be studied using the ODT model, where a single fuel is used with combination with a cetane number improver like gasoline and DTBP.

## REFERENCES

1. Johnson, T. V. (2010). Review of Diesel Emissions and Control. *SAE International Journal of Fuels and Lubricants*, 3(1), 16-29. doi: 10.4271/2010-01-0301.
2. Reitz, R. D. <http://www.sae.org/mags/aei/power/8388>; 2010.
3. Manente, V., Johansson, B., & Tunestal, P. (2009). Partially Premixed Combustion at High Load using Gasoline and Ethanol, a Comparison with Diesel. *SAE Technical Paper Series*. doi: 10.4271/2009-01-0944.
4. Hardy, W. L., & Reitz, R. D. (2006). A Study of the Effects of High EGR, High Equivalence Ratio, and Mixing Time on Emissions Levels in a Heavy-Duty Diesel Engine for PCCI Combustion. *SAE Technical Paper Series*. doi: 10.4271/2006-01-0026.
5. Kalghatgi, G. T., Risberg, P., & Angstrom, H. (2007). Partially Pre-Mixed Auto-Ignition of Gasoline to Attain Low Smoke and Low NO<sub>x</sub> at High Load in a Compression Ignition Engine and Comparison with a Diesel Fuel. *SAE Technical Paper Series*. doi: 10.4271/2007-01-0006.
6. Leermakers, C., Luijten, C., Somers, L., Kalghatgi, G., & Albrecht, B. (2011). Experimental Study of Fuel Composition Impact on PCCI Combustion in a Heavy-Duty Diesel Engine. *SAE Technical Paper Series*. doi: 10.4271/2011-01-1351.
7. Office of Energy Efficiency and Renewable Energy, "Homogeneous charge compression ignition (HCCI) technology - a report to the U.S. Congress," tech. rep., U.S. Department of Energy, April 2001.
8. Kokjohn, S. L., Hanson, R. M., Splitter, D. A., & Reitz, R. D. (2011). Fuel reactivity controlled compression ignition (RCCI): A pathway to controlled high-efficiency clean combustion. *International Journal of Engine Research*, 12(3), 209-226. doi:10.1177/1468087411401548
9. Kokjohn, S. L., Hanson, R. M., Splitter, D. A., & Reitz, R. D. (2009). Experiments and Modeling of Dual-Fuel HCCI and PCCI Combustion Using In-Cylinder Fuel Blending. *SAE International Journal of Engines*, 2(2), 24-39. doi:10.4271/2009-01-2647
10. Reitz, R. D., Hanson, R. M., Splitter, D. A., & Kokjohn, S. L. (2010). U.S. Patent No. US9376955B2. Washington, DC: U.S. Patent and Trademark Office.
11. Mikulski, M., & Bekdemir, C. (2017). Understanding the role of low reactivity fuel stratification in a dual fuel RCCI engine – A simulation study. *Applied Energy*, 191, 689-708. doi:10.1016/j.apenergy.2017.01.080

12. Inagaki, K., Fuyuto, T., Nishikawa, K., Nakakita, K. et al. (2006). Dual-Fuel PCI Combustion Controlled by In-Cylinder Stratification of Ignitability. *SAE Technical Paper* 2006-01-0028, 2006, doi: 10.4271/2006-01-0028.
13. Benajes, J., Molina, S., García, A., Belarte, E. and Vanvolsem, M. (2014). An investigation on RCCI combustion in a heavy duty diesel engine using in-cylinder blending of diesel and gasoline fuels. *Applied Thermal Engineering*, 63(1), pp.66-76.
14. Arrègle, J., López, J., García, J., Fenollosa, C. (2003) Development of a zero-dimensional diesel combustion model, part 2: analysis of the transient initial and final diffusion combustion phases, *Appl. Therm. Eng.* 23 (2003) 1319e1331.
15. Pastor, J., López, J., García, J., Pastor, J. (2008) A 1D model for the description of mixing-controlled inert diesel sprays, *Fuel* 87 (2008) 2871e2885.
16. Splitter, D., Wissink, M., DelVescovo, D., and Reitz, R (2013). RCCI Engine Operation Towards 60% Thermal Efficiency. *SAE Technical Paper* 2013-01-0279, 2013, doi: 10.4271/2013-01-0279.
17. Egüz, U., Maes, N.C.J., Leermakers, C.A.J (2013). Predicting auto-ignition characteristics of RCCI combustion using a multi-zone model. *International Journal of Automotive Technology*, 14: 693. doi: 10.1007/s12239-013-0075-2.
18. DelVescovo, D., Kokjohn, S., and Reitz, R (2017). The Effects of Charge Preparation, Fuel Stratification, and Premixed Fuel Chemistry on Reactivity Controlled Compression Ignition (RCCI) Combustion. *SAE Int. J. Engines* 10(4):2017, doi: 10.4271/2017-01-0773.
19. Reitz, R., Duraisamy, G. (2015). Review of high efficiency and clean reactivity controlled compression ignition (RCCI) combustion in internal combustion engines. *Progress in Energy and Combustion Science*, 12-71.
20. Liss W, Thrasher W. Natural gas as a stationary engine and vehicle fuel. *SAE technical paper* 912364; 1991.
21. Napolitano, P., Guido, C., Beatrice, C., and Del Giacomo, N (2017). Application of a Dual Fuel Diesel-CNG Configuration in a Euro 5 Automotive Diesel Engine. *SAE Technical Paper* 2017-01-0769, 2017, doi: 10.4271/2017-01-0769.
22. Nieman, D., Dempsey, A., and Reitz, R., "Heavy-Duty RCCI Operation Using Natural Gas and Diesel," *SAE Int. J. Engines* 5(2):270-285, 2012, doi: 10.4271/2012-01-0379.
23. Walker N.R., Wissink M.L., DelVescovo D.A., Reitz R.D. Natural gas for high load dual-fuel reactivity controlled compression ignition in heavy-duty engines. *Journal of Energy Resources Technology*. 137 (2015) 042202.

24. Doosje, E., Willems, F., and Baert, R., "Experimental Demonstration of RCCI in Heavy-Duty Engines using Diesel and Natural Gas," SAE Technical Paper 2014-01-1318, 2014, doi: 10.4271/2014-01-1318.
25. Kim, K., Kim, H., Kim, B., Lee, K., Lee, K., 2009. Effect of natural gas composition on the performance of a CNG engine. *Oil Gas Sci. Tech.* 64 (2), 199e206.
26. Kakaee, A., Rahnama, P., & Paykani, A. (2015). Influence of fuel composition on combustion and emissions characteristics of natural gas/diesel RCCI engine. *Journal of Natural Gas Science and Engineering*, 25, 58-65. doi:10.1016/j.jngse.2015.04.020
27. Wu, Z., Rutland, C., & Han, Z. (2017). Numerical Study on Controllability of Natural Gas and Diesel Dual Fuel Combustion in a Heavy-Duty Engine. SAE Technical Paper Series. doi:10.4271/2017-01-0756
28. Walker N.R., Chuahy F.D., Reitz R.D. Comparison of Diesel Pilot Ignition (DPI) and Reactivity Controlled Compression Ignition (RCCI) in a Heavy-Duty Engine. ASME 2015 Internal Combustion Engine Division Fall Technical Conference. American Society of Mechanical Engineers 2015. pp. V001T03A16-VT03A16.
29. Qian, Y., Wang, X., Zhu, L., & Lu, X. (2015). Experimental studies on combustion and emissions of RCCI (reactivity controlled compression ignition) with gasoline/n-heptane and ethanol/n-heptane as fuels. *Energy*, 88, 584-594. doi:10.1016/j.energy.2015.05.083
30. Qian, Y., Ouyang, L., Wang, X., Zhu, L., & Lu, X. (2015). Experimental studies on combustion and emissions of RCCI fueled with n-heptane/alcohols fuels. *Fuel*, 162, 239-250. doi:10.1016/j.fuel.2015.09.022
31. Loaiza, J., Sánchez, F., Braga, S., and De Souza, O (2015). Reactivity Controlled Compression Ignition (RCCI) for the Mixture of Diesel Fuel and Hydrous Ethanol in a Rapid Compression Machine. SAE Technical Paper 2015-36-0101, 2015, doi: 10.4271/2015-36-0101.
32. Li, J., Yang, W., An, H., & Zhao, D. (2015). Effects of fuel ratio and injection timing on gasoline/biodiesel fueled RCCI engine: A modeling study. *Applied Energy*, 155, 59-67. doi:10.1016/j.apenergy.2015.05.114
33. Zerrakki, M., Aydin, H. (2016). Analysis of ethanol RCCI application with safflower biodiesel blends in a high load diesel power generator. *Fuel* 184, 248-260
34. Chao MR, Lin TC, Chao HR, Chang FH, Chen CB. Effects of methanol-containing additive on emission characteristics from a heavy-duty diesel engine. *Sci Total Environ* 2001; 279(1-3):167-79.
35. Huang Z, Lu H, Jiang D, Zeng K, Liu B, Zhang J, et al. Combustion characteristics and heat release analysis of a compression ignition engine operating on a diesel/methanol

blend. Proc Inst Mech Eng D: J Automob Eng 2004;218(9):1011–24

36. Li, Y., Jia, M., Liu, Y., & Xie, M. (2013). Numerical study on the combustion and emission characteristics of a methanol/diesel reactivity controlled compression ignition (RCCI) engine. *Applied Energy*, 106, 184-197. doi:10.1016/j.apenergy.2013.01.058
37. Li, Y., Jia, M., Chang, Y., Liu, Y., Xie, M., Wang, T., & Zhou, L. (2014). Parametric study and optimization of a RCCI (reactivity controlled compression ignition) engine fueled with methanol and diesel. *Energy*, 65, 319-332. doi:10.1016/j.energy.2013.11.059
38. Zhou, D., Yang, W., An, H., Li, J., & Shu, C. (2015). A numerical study on RCCI engine fueled by biodiesel/methanol. *Energy Conversion and Management*, 89, 798-807. doi:10.1016/j.enconman.2014.10.054
39. Pan, S., Li, X., Han, W., & Huang, Y. (2017). An experimental investigation on multi-cylinder RCCI engine fueled with 2- butanol/diesel. *Energy Conversion and Management*, 154, 92-101. doi:10.1016/j.enconman.2017.10.047
40. Gross, C. W., & Reitz, R. D. (2016). Transient “Single-Fuel” RCCI Operation with Customized Pistons in a Light-Duty Multicylinder Engine. *Journal of Engineering for Gas Turbines and Power*, 139(3), 032801. doi:10.1115/1.4034445
41. Dempsey, A. B., Curran, S., & Reitz, R. D. (2015). Characterization of Reactivity Controlled Compression Ignition (RCCI) Using Premixed Gasoline and Direct-Injected Gasoline with a Cetane Improver on a Multi-Cylinder Engine. *SAE International Journal of Engines*, 8(2), 859-877. doi:10.4271/2015-01-0855
42. Wang, H., DelVescovo, D., Yao, M., and Reitz, R (2015). Numerical Study of RCCI and HCCI Combustion Processes Using Gasoline, Diesel, iso-Butanol and DTBP Cetane Improver. *SAE Int. J. Engines* 8(2):831-845, 2015, doi: 10.4271/2015-01-0850.
43. Delvescovo, D., Wang, H., Wissink, M., & Reitz, R. D. (2015). Isobutanol as Both Low Reactivity and High Reactivity Fuels with Addition of Di-Tetra Butyl Peroxide (DTBP) in RCCI Combustion. *SAE International Journal of Fuels and Lubricants*, 8(2). doi:10.4271/2015-01-0839
44. Dempsey, A., Walker, N., and Reitz, R (2013). Effect of Piston Bowl Geometry on Dual Fuel Reactivity Controlled Compression Ignition (RCCI) in a Light-Duty Engine Operated with Gasoline/Diesel and Methanol/Diesel. *SAE Int. J. Engines* 6(1):78-100, 2013, doi:10.4271/2013-01-0264
45. Li, J., Yang, W., & Zhou, D. (2016). Modeling study on the effect of piston bowl geometries in a gasoline/biodiesel fueled RCCI engine at high speed. *Energy Conversion and Management*, 112, 359-368. doi:10.1016/j.enconman.2016.01.04.

46. Salahi, M. M., Esfahanian, V., Gharehghani, A., & Mirsalim, M. (2017). Investigating the reactivity controlled compression ignition (RCCI) combustion strategy in a natural gas/diesel fueled engine with a pre-chamber. *Energy Conversion and Management*, 132, 40-53. doi:10.1016/j.enconman.2016.11.019
47. Wang, H., Tong, L., Zheng, Z., and Yao, M (2017). Experimental Study on High-Load Extension of Gasoline/PODE Dual-Fuel RCCI Operation Using Late Intake Valve Closing. *SAE Int. J. Engines* 10(4):2017, doi: 10.4271/2017-01-0754.
48. N. Peters, *Turbulent Combustion*. Cambridge Monographs on Mechanics, Cambridge University Press, 2000.
49. Kerstein A. R (1991). Linear-eddy modelling of turbulent transport. part 6: Microstructure of diffusive scalar mixing fields. *Journal of Fluid Mechanics*, vol. 231, pp. 361–394.
50. Kerstein A.R (1989). Linear-eddy modeling of turbulent transport, part 2: Application to shear layer mixing. *Combustion and Flame*, vol. 75, no. 3-4, pp. 397 – 413.
51. A. R. Kerstein, “One-dimensional turbulence: model formulation and application to homogeneous turbulence, shear flows, and buoyant stratified flows,” *Journal of Fluid Mechanics*, vol. 392, pp. 277–334, 1999.
52. J. C. Hewson and A. R. Kerstein, “Local extinction and reignition in nonpremixed turbulent  $CO/H_2/N_2$  jet flames,” *Combustion Science and Technology*, vol. 174, no. 5, pp. 35 – 66, 2002.
53. S. Zhang and T. Echekeki, “Stochastic modeling of finite-rate chemistry effects in hydrogen-air turbulent jet diffusion flames with helium dilution,” *International Journal of Hydrogen Energy*, vol. 33, no. 23, pp. 7295 – 7306, 2008.
54. T. Echekeki and K. G. Gupta, “Hydrogen autoignition in a turbulent jet with preheated co-flow air,” *International Journal of Hydrogen Energy*, vol. 34, no. 19, pp. 8352 – 8377, 2009.
55. Gowda, B. D., & Echekeki, T. (2012). One-dimensional turbulence simulations of hydrogen-fueled HCCI combustion. *International Journal of Hydrogen Energy*, 37(9), 7912-7924. doi:10.1016/j.ijhydene.2012.02.020.
56. Gowda, B. D., & Echekeki, T. (2012). Complex injection strategies for hydrogen-fueled HCCI engines. *Fuel*, 97, 418-427. doi:10.1016/j.fuel.2012.01.060.
57. T. Echekeki, A. R. Kerstein, T. D. Dreeben, and J.-Y. Chen, “‘One-Dimensional Turbulence’ simulation of turbulent jet diffusion flames: Model formulation and illustrative applications,” *Combustion and Flame*, vol. 125, no. 3, pp. 1083–1105, 2001.

58. W. T. Ashurst and A. R. Kerstein, "One-Dimensional Turbulence: Variable-density formulation and application to mixing layers," *Physics of Fluids*, vol. 17, no. 2, pp. 025107–, 2005.
59. P. N. Brown, G. D. Byrne, and A. C. Hindmarsh, "VODE: A variable coefficient ode solver," *SIAM Journal on Scientific and Statistical Computing*, vol. 10, pp. 1038–1051, 1989.
60. R. J. Kee, J. Warnatz, and J. A. Miller, "A FORTRAN computer code package for the evaluation of gas-phase viscosities, conductivities, and diffusion coefficients," *SANDIA National Laboratories Report No. SAND83-8209*, 1983.
61. R. J. Kee, J. A. Miller, and T. H. Jefferson, "CHEMKIN: A general-purpose, problem independent, transportable, fortran chemical kinetics code package," *SANDIA National Laboratories Report No. SAND83-800*, 1983.
62. M.B. Luong, Z. Luo, T.F. Lu, S.H. Chung, C.S. Yoo, "Direct numerical simulations of the ignition of lean primary reference fuel/air mixtures under HCCI condition," *Combustion and Flame*, Vol. 160 No. 10 pp. 2038-2047, 2013.
63. H.J. Curran, P. Gaffuri, W.J. Pitz, C.K. Westbrook, *Combust. Flame* 129 (2002) 253–280.
64. H.J. Curran, P. Gaffuri, W.J. Pitz, C.K. Westbrook, *Combust. Flame* 114 (1998) 149–177.
65. Y. Huang, C.J. Sung, *Combust. Flame* 139 (2004) 239–351.
66. S. Jerzembeck, N. Peters, P. Pepiot-Desjardins, H. Pitsch, *Combust. Flame* 156 (2009) 292–301.
67. T. Lu, M. Plomer, Z. Luo, S.M. Sarathy, W.J. Pitz, S. Som, D.E. Longman, Directed relation graph with expert knowledge for skeletal mechanism reduction, in: 7th US National Combustion Meeting, Atlanta, GA, 2011, paper#B31.
68. W. Liu, R. Sivaramakrishnan, M.J. Davis, S. Som, D.E. Longman, T. Lu, *Proc. Combust. Inst.* 34 (2013) 401–409
69. T. Lu, C.K. Law, *Combust. Flame* 154 (2008) 153–163.
70. Bhagatwala, Ankit, et al. "Numerical Investigation of Spontaneous Flame Propagation under RCCI Conditions." *Combustion and Flame*, vol. 162, no. 9, 2015, pp. 3412–3426, doi:10.1016/j.combustflame.2015.06.005.

71. Nazemi, M., and M. Shahbakhti. "Modeling and Analysis of Fuel Injection Parameters for Combustion and Performance of an RCCI Engine." *Applied Energy*, vol. 165, 2016, pp. 135–150., doi:10.1016/j.apenergy.2015.11.093.